PSYCHOPHYSICAL INVESTIGATION OF VISUAL FUNCTION IN ALBINISM

A thesis presented to the graduate faculty of New England College of Optometry in partial fulfillment of the requirements for the degree of Master of Science.

Olivia Anna Wynn

May, 2026

PSYCHOPHYSICAL INVESTIGATION OF VISUAL FUNCTION IN ALBINISM

Olivia Anna Wynn

This manuscript has been read and accepted by the
Thesis Committee in satisfaction of the
thesis requirement for the degree of Master of Science

5/14/2026
Date

DocuSigned by:
Nicole Ross
2172A8A6E3CE41E...
Nicole Ross, OD, MSc, FAAO
Graduate Faculty Advisor

DocuSigned by:
Peter Bex
3E92398B601647F...
Peter Bex, PhD
Graduate Faculty Advisor

DocuSigned by:
41B8809FEE92419...
Alexis Malkin, OD
Thesis Committee Member

Signed by:
Jan Skerswetat
86556C5945804DD...
Jan Skerswetat, PhD
Thesis Committee Member

DocuSigned by:
78A8AD972399447...
Thanasis Panorgias, PhD
Thesis Committee Member

5/14/2026
Date

DocuSigned by:
78A8AD972399447...
Thanasis Panorgias, PhD
Director of Graduate Studies

Abstract

PSYCHOPHYSICAL INVESTIGATION OF VISUAL FUNCTION IN ALBINISM

Olivia A. Wynn
New England College of Optometry, 2026

Purpose

Albinism is an inherited condition affecting systemic melanin production and the development of the ocular system. Ocular findings in albinism manifest as varying degrees of refractive error, iris transillumination, nystagmus, fundus hypopigmentation, foveal hypoplasia, and misrouting of temporal retinal fibers at the optic chiasm. Visual acuity and contrast sensitivity have well documented reductions in Persons with Albinism (PwA); however it is unclear how high level visual processing is affected. This thesis explores facets of functional vision through 1) assessing blur tolerance and dioptric defocus using the Angular Indication Measurement (AIM) Low Vision paradigm, 2) understanding face discrimination using the Foraging Interactive D'Prime (FInD) Face paradigm, and 3) assessing emotion recognition with the Genetic paradigm (GA) Emotion program. AIM, FInD, and the Genetic Algorithm are computer-based, generalizable, and self-administered vision tests developed at Northeastern University in Boston, MA.

Methods

AIM Low Vision, FInD Faces, and GA Emotion were first validated for their repeatability in normally sighted individuals enrolled at Northeastern University. These control participants completed the AIM Low Vision algorithm both with and without dioptric blur (+4.00 D), the FInD Face algorithm, and the FInD GA emotion program twice (ie, test and retest). PwA also

completed the AIM Low Vision twice with best correction. Bland Altman analyses were performed to establish repeatable results with minimal bias. AIM Low Vision acuities were also compared to the gold standard Early Treatment Diabetic Retinopathy Study (ETDRS) chart.

To assess blur tolerance in albinism, PwA and their age- and sex-matched controls completed the AIM Low Vision algorithm with 1 through 6 diopters of positive dioptric blur. Linear regressions of their visual acuity performance were fit to assess changes with increased blur. Visual acuity changes and linear regression slopes were compared between groups. To evaluate face discrimination in albinism, PwA and their matched controls completed the FInD Face algorithm with best correction. Controls repeated the algorithm under dioptric blur matched to the acuity of the corresponding PwA. Face discrimination thresholds were then compared across PwA, controls, and blurred controls.

Results

The AIM (coefficient of variation (COV)= 51% in controls and 19% in blurred controls) method revealed increased blur tolerance in PwA with a significant difference in linear regression slope comparison ($p= 0.002$). The FInD Faces (COV = 46%) found no significant difference in upright or inverted discrimination thresholds. Finally, the Genetic Algorithm was established as repeatable (COV = 24% happiness, 19% amusement, 13% anger, and 21% disgust). Further data analysis of emotion perception in PwA is currently underway.

Conclusions

Overall, the paradigms used to test sensitivity in functional vision are novel and repeatable. Blur tolerance is increased in PwA, which should be considered in refractive procedures. Face discrimination also remains intact in PwA. Therefore, the unique pathology of PwA distinguishes them from other low vision groups, and this should be considered in clinical practice.

Acknowledgements

Thank you to my advisor, Dr. Nicole Ross, for your continued support throughout this program. From long days both at the Northeastern and NECO lab to brainstorming zoom calls, your mentorship has been invaluable. I admire you as a clinician scientist. Most importantly, I hope to embody your work ethic and compassion in the years to come.

Next, thank you to Drs. Peter Bex and Jan Skerswetat. Your guidance in the world of psychophysics has opened my eyes to a new perspective of vision science. I have connected with incredible people at the Northeastern Translational Clinical Vision lab through years just how vast vision science can be. Bliss Cui and Drs. Kerri Walter, Samuel Smithers, and Sonisha Nepuane are a few of the great minds I have had the pleasure to work with.

Finally, I would like to thank my committee members Drs. Lexi Malkin and Thanasis Panorgias. The New England College of Optometry has given me an outstanding opportunity to pursue my Master's of Vision Science, and I am grateful for your contributions.

This thesis is in dedication to Norvanna Aja Wynn

TABLE OF CONTENTS

LIST OF FIGURES AND TABLES

TABLES

FIGURES

CHAPTER 1: GENERAL INTRODUCTION

1.1 Ocular and Oculocutaneous Albinism

Albinism, a genetic condition, is prevalent in 1 of 18,000 Americans (Summers, 1996) and 1 in 17,000 patients globally (Kirkwood et al., 2009). Oculocutaneous albinism (OCA) is defined as a presence of dysfunctional melanosomes throughout the body (Tomita et al, 1989; Federico, et al, 2023; Mcham & Fulton, 1992). Persons with Albinism (PwA) often lack pigment in their skin, hair, and eyes depending on the specific gene mutation (Table 1). Ocular albinism (OA) describes melanin dysfunction isolated to the eyes only (Federico, et al, 2023). In both OCA and OA, the melanin cycle's transport of tyrosine (Tomita et al., 1989) impairs eumelanin, pheomelanin, and neuromelanin production (Istrate et al, 2020) causing disruption in the development of the macula and visual pathway (Federico et al, 2023; Kirkwood et al, 2009). The iris, iris stroma, choroid, and retinal pigmented epithelium are most affected by this melanosome deficit (Summers 1996). One genotypic distinction references the tyrosinase activity for the tyrosine transition to 3,4-dihydroxyphenylalanine (DOPA) (Summers, 1996; Grønskov et al, 2007; Tomita et al, 1989) .

Tyrosinase negative, or the OCA1 subtypes, is indicative of a defect that manifests as a complete or partial reduction of pigment (Grønskov et al, 2007; Tomita et al, 1989; King et al, 2003). Incomplete tyrosinase activity has been identified in OCA1B, OCA1MP, OCAITS subtypes. OCA1MP refers to a "minimally pigmented" OCA subtype most apparent in the first few weeks of life before more pigment is gained (Summers, 1996). These individuals typically have visual acuities ranging from 20/50-20/200 (Summers, 1996). OCA1TS is the "temperature sensitive" phenotype where melanin production depends on the atmospheric temperature

(Summers, 1996). Mean visual acuity in these individuals is 20/200 (Summers, 1996). In contrast, tyrosine positive (OCA2) patients are born with some pigment throughout the body and persist to have an abnormal melanin cycle (Summers, 1996; Summers et al, 1991).

Other forms of oculocutaneous albinism, include OCA 3, previously known as "Brown albinism" (Summers, 1996), prevalent primarily in subsaharan African populations, and albinism secondary to other syndromes (i.e., Hermansky- Pudlak Syndrome, Chediak Higashi Syndrome) (Grønskov et al, 2007). Chediak Higashi Syndrome is a systemic disease with prolonged immunocompromise and repeat infections impairing melanin production (Hertle, 2013). Angelman syndrome and Prader-Willi Syndrome are also known to be associated with oculocutaneous albinism, although it is rare for the two to occur together (Federico et al, 2023).

Alternatively, albinism's melanin dysfunction may be restricted to neuroectoderm cells not affecting the neural crest cells (Hertle, 2013), causing ocular only albinism (OA) (Thomas et al, 2023;Summers, 1996). Ocular manifestations of OCA and OA are nystagmus (Neveu, et al, 2009; Abadi, 2002), blonde fundus (Käsmann-Kellner & Seitz, 2007), iris transillumination (Summers et al, 1988), foveal hypoplasia, and irregular decussation of temporal retinal fibers at the optic chiasm (Hertle, 2013; Kirkwood, 2009). The genotypes, phenotype and inheritance patterns of OCA and OA subtypes are summarized in Table 1.

Table 1. Phenotype descriptions detailing inheritance patterns, epidemiology and generalized manifestations of OCA subtypes and OA. Phenotypic presentation is generalized to the extent of hypopigmentation and variations in melanin production postnatal.

Oculocutaneous (OCA) or Ocular only (OA) subtype names	Inheritance pattern	Prevalence	Phenotype
OCA1A (Tyrosinase- negative)	Autosomal recessive inherited complete absence of TYR function (Thomas et al, 2023; Tomita et al, 1989)	1:40,000 of Americans (Grønskov K et al, 2007)	Hair, skin, eyelashes, and irises are all depigmented (Grønskov K et al, 2007; Tomita Y et al, 1989; King RA et al, 2003)
OCA1B (Tyrosinase-negative)	Autosomal recessive inherited reduced function of TYR (Thomas et al, 2023; Grønskov et al, 2007)	1:40,000 of Americans (Grønskov K et al, 2007)	Pigmentation is largely reduced throughout the body, but mild pigmentation may occur. Thus this subtype is referred to as "yellow albinism" (Grønskov K et al, 2007)
OCA2 (Tyrosinase- positive)	Autosomal recessive inherited mutation of the TYR protein 1 gene (Thomas et al, 2023; Summers, 1996; Grønskov et al, 2007)	1:36,000 Americans; most common worldwide, especially in African Americans 1:10,000 (Grønskov et al, 2007)	Skin pigment varies, but these patients often have pigmented hair at birth. A similar "brown OCA" refers to this presentation in African patients Most associated with misrouting of fibers at the chiasm (Summers, 1996; Grønskov et al, 2007)
OCA3	Autosomal recessive (Grønskov et al, 2007)	1:8,500 in African countries (Grønskov et al, 2007)	Hair and skin pigmentation usually presents as reddish or orange in color. It is also known as "brown OCA" due to high demographics in subsaharan Africa (Grønskov et al, 2007)
OCA4	Autosomal recessive (Grønskov et al, 2007)	11% of patients worldwide; 5-8% of Germans and 18% of Japanese populations	Hard to distinguish from OCA1 subtypes (Thomas et al, 2023)

		(Hertle, 2013; Thomas et al, 2023)	
OCA6	Rare SLC24A5 mutation (Thomas MG et al, 2023)	3% of patients worldwide (Thomas MG et al, 2023)	Generalized hypopigmentation of the skin with ability to tan Hair color is variable (Thomas MG et al, 2023)
OCA7	Rare LRMDA gene mutation (Thomas MG et al, 2023)	<1% of patients worldwide (Thomas MG et al, 2023)	Generalized hypopigmentation that may occur with other OCA subtypes
OCA8	Rare inherited DCT, or TYR protein 2, mutation (Thomas MG et al, 2023)	<1% of patients worldwide (Thomas MG et al, 2023)	Mild skin and hair hypopigmentation (Thomas MG et al, 2023)
OA	X-linked recessive inherited GPR143 gene mutation Some cases have been autosomal recessive (Summers, 1996; Thomas et al, 2023)	Not well documented	Ocular hypopigmentation is apparent without affecting the hair and skin- associated with x-linked Few autosomal recessive cases have variable iris transillumination and fundus hypopigmentation (Thomas et al, 2023)
HPS and CHS Related	Autosomal recessive systemic disorders (Summers, 1996)	Not well documented	Generalized hypopigmentation with associated iris transillumination and nystagmus (Summers, 1996)

1.1.1 Visual Acuity & Nystagmus in Albinism

Visual acuity in albinism is known to be impaired, and can vary between 20/30 to 20/400 , and may be associated with specific genotypes and extent of melanin deficiency (Table 2). There is a strong association between nystagmus and reduced visual acuity (Talsma et al., 2023). Largely, the concern is that nystagmus causes image instability and reduces the ability to foveate

(Hertle, 2013), thus reducing acuity (Abadi, 2002). Abadi's comparison of idiopathic nystagmus and nystagmus in albinism showed a significant decrease of acuity in PwA compared to idiopathic nystagmus (Abadi, 2002; Talsma et al., 2023). Nystagmus usually presents in the first 2-6 months of life, but may also be present at birth (Hertle, 2013), and is typically horizontal and pendular in nature (Federico et al., 2023, Gurnani et al., 2025; Abadi, 2002). Much of nystagmus in Albinism has been referred to as periodically alternating nystagmus (Abadi & Pascal, 1994), varying in amplitude and direction (Hertle, 2013). Interestingly, Dysli and Abegg found the reading speed in PwA was unaffected by nystagmus and necessary foveation (Dysli & Abegg, 2016). However, a later study found that reading can be enhanced with magnification in PwA struggling with nystagmus (Christen & Abegg, 2016).

Nystagmus is often accompanied by strabismus and reduced or absent stereopsis (Neveu et al, 2009; Abadi, 2002). Some studies have found a correlation between nystagmus and sensory deficiencies which are known to affect color vision (Neveu M.M, et al, 2009; Skerswetat et al., 2023), contrast sensitivity (Loshin & Browning, 1983; Abadi & Pascal, 1994), motion perception (Shallo-Hoffmann et al., 1998; Neveu M.M, et al, 2009), smooth pursuits, head tilts, and optokinetic nystagmus (Federico et al., 2023; Abadi, 2002; Hoffman et al., 2004). However, it has been argued that image instability assumed of nystagmus does not solely account for decreased reading as magnification can support performance (Abadi, 2002; Christen M & Abegg, 2016). Therefore, the effects of nystagmus are thought to be compounded by foveal hypoplasia (Abadi, 2002; Talsma, et al, 2023).

Correctable visual deficits include refractive error, of which with-the-rule astigmatism (Federico et al., 2023) and hyperopia (Kessel et al., 2023; Yahalom et al., 2012) is the most overwhelming factor often encountered. Those with the OCA1A mutation are known to have the

most reduced acuity (Summers, 1996; Schweigert et al., 2018) corroborated by a high prevalence of significant hyperopia (Schweigert et al., 2018; Yalaholm et al., 2012; Kessel et al., 2023). This is thought to be due to failed emmetropization (Wildsoet, et al., 2000), which has been attributed to nystagmus and foveal hypoplasia (Kessel et al., 2023). Astigmatism is thought to develop as constant nystagmus and squinting alters the corneal topography resulting in a with-the-rule astigmatism (Verkicharla et al., 2007; Grosvenor, 1978). These high levels of hyperopia and astigmatism pose a great risk for amblyopia (Kessel et al., 2023; Thomas et al., 2023) in combination with strabismus (Dobhal et al., 2025; Proudlock et al., 2024). Proudlock et al. details amblyopia as composing approximately 21% of PwA. Of the 61 PwA in the study, 71.8% presented with strabismus and 18% with anisometropia, which are amblyogenic factors (Proudlock et al., 2024).

Table 2. Visual acuity expectations for OCA subtypes and OA. Visual acuity measures are expressed in Snellen and logMAR equivalent at stabilized adult levels.

Oculocutaneous (OCA) or Ocular only (OA)	Average Snellen Visual Acuity

subtype names	
OCA1A	20/200- 20/400 (1.00 - 1.3logMAR) (Summers, 1996; Grønskov et al., 2007)
OCA1B	20/200 (1.3logMAR) (Summers C.G, 1996; Grønskov K et al, 2007)
OCA2	20/70 (~0.6 logMAR) (Grønskov K et al, 2007)
OCA3	Often better VA than the other subtypes as low as 20/20 (0 logMAR) (Summers C.G, 1996)
OCA4	20/60- 20/150 (~0.5-0.9 logMAR) (Summers C.G, 1996)
OA	20/60-20/400 (~0.5-1.3 logMAR) (Summers C.G, 1996)

1.1.2 Iris Transillumination & Blonde Fundus

Albinism is often associated with photophobia and/or glare sensitivity due to iris transillumination, which in turn is highly associated with the degree of fundus hypopigmentation. According to Summers et al, iris transillumination grading is determined by peripheral to diffuse extension of transillumination defects (Table 4) (Summers et al, 1988; Seguy et al, 2023). Fundus hypopigmentation grading metrics were further refined by Kasmann Keller and Seitz on a similar 1 through 4 grading scale. (Table 5) (Käsmann-Kellner & Seitz, 2007; Seguy et al, 2023). Macular pigmentation has its own classifications based on the visibility of the underlying

choroidal vessels. The three categories of grading progress from visibility of choroidal vessels to opacity of the pigment epithelium (Summers et al, 1988; Seo et al, 2007).

Table 3. Description of iris transillumination grading (Summers GC et al, 1988). Classifications are based on clinical description of transillumination extensity.

Grading	Description of Iris Transillumination
1	Punctate peripheral transillumination defects
2	Extensive peripheral transillumination
3	Diffuse peripheral transillumination with visible lens equator
4	Total transillumination to the pupillary rim

Table 4. Description of fundus hypopigmentation grading (Käsmann-Kellner B & Seitz B, 2007).

Grading	Description of Fundus Hypopigmentation
1	Hypopigmentation isolated to peripheral retina
2	Hypopigmentation with peripheral and central extension without macular involvement
3	Diffuse hypopigmentation with limited macular involvement
4	Diffuse hypopigmentation with absence of macular pigment

1.1.3 Foveal Hypoplasia

Foveal hypoplasia is common as a result of the aborted formation of the foveal pit (Proudlock, 2024; Summers, 1996; Talsma, et al, 2023). Normal foveal development begins at the 25th week of gestation; whereas, foveal excavation, the formation of the central pit of the retina, occurs 15-45 months after birth (Thomas et al, 2011). Throughout this process, cones

aggregate perifoveally and develop their spectrum sensitivities (Lee et al, 2018; Bringmann et al, 2022). Failure during the latter process results in irregular cone specialization and excavation of the fovea (Thomas et al, 2011; Proudlock, 2024). The presentation of the macula often resembles a premature retina. There is little differentiation of the outer retina and delineation from the perifoveal avascular zones (Proudlock, 2024). There has been a documented thickening of the ganglion cell layer in the macula that may be apparent upon examination greatly affecting central vision (Summers, 1996; Brücher et al., 2019; Talsma et al., 2023). The most important factors in the budding morphology of the fovea is cone specialization and cone density (Bringmann et al., 2022; Lee et al., 2018). This is primarily driven by the centripetal displacement of Henle's fiber layer (HFL) and the outer nuclear (ONL) into the perifoveal region (Bringmann et al., 2022).

Seo et al, proposed a grading system highlighting four qualities of the fovea using optical coherence tomography (OCT) - foveal hyporeflectivity, choroidal transillumination, tram tract sign, and foveal depression. The tram tract sign here refers to the hyper-reflectivity of the choroidal space layers as a consequence of an irregular foveal pit (Chong et al., 2009). At the inception of this grading system, there was a correlation between visual acuity and these characteristics (Spearman correlation: iris transillumination $P<0.001$, macular transparency $P = 0.014$, and foveal hypoplasia $P = 0.004$). Correlation was stronger for lower visual acuity PwA (20/125-20/200) compared to the better visual acuity (20/100-20/125) group (Seo et al, 2007). However, the pitfalls of this method were highlighted due to its reliance on subjective interpretation and the quality of the photographs in transillumination (Thomas et al., 2011; Chong et al., 2009). Thomas and colleagues (2011) devised a more widely accepted grading model for foveal hypoplasia detailing extrusion of the plexiform layers, formation of the foveal

pit, lengthening of the photoreceptor outer segments, and width of the outer nuclear layer (Thomas et al., 2011) (Table 5).

Foveal hypoplasia is known to be associated with reduced visual acuity (Thomas et al., 2011). Aside from contributions of refractive status and amblyopia, this anatomical difference is an important associated factor in best corrected visual acuity (Thomas et al., 2011). Thomas et al found grade 1 hypoplasia was associated with mean visual acuity of 0.2 logMAR; whereas, grades 2-4 were associated with mean visual acuity measures of 0.44, 0.6, and 0.78 logMAR respectively. Most PwA in the study presented with grade 3 hypoplasia (Thomas et al., 2011), which is consistent with previous general reports of visual acuity ranges in albinism (0.4-1.3 logMAR) (Summers, 1996). Specifically the irregularity of the outer nuclear layer (ONL) widening increases suspicion for arrested cone photoreceptor development. Additionally, there has been a question of foveal hypoplasia being the driving factor for failed emmetropization in albinism, but current data does not support this theory (Kessel et al., 2023). Talsma et al, hypothesizes increased (grade 4) foveal hypoplasia increased the magnitude of peduncular and jerk nystagmus (Talsma et al., 2023). Generally, visual perception such as depth perception, contrast sensitivity, and color vision are thought to be affected (Hoffman et al., 2001; Skerswetat et al., 2023).

Table 5. Foveal hypoplasia grading scale. Grading is based on the displacement of henle's fibers out of the foveal zone (extrusion of the plexiform layer), formation of the fit, lengthening of the outer segment (OS), and widening of the outer nuclear layer (ONL), and integrity of the IS (inner segment)/OS junction (Thomas MG et al, 2011).

Foveal Hypoplasia Grading Scale	Description of Clinical Presentation
1	- Absent extrusion of the plexiform layers - Shallow foveal pit - OS lengthening - ONL widening
2	- Absent extrusion of the plexiform layers - Absent foveal pit - OS lengthening - ONL widening
3	- Absent extrusion of the plexiform layers - Shallow foveal pit - Irregular OS lengthening - ONL widening
4	- Absent extrusion of the plexiform layers - Shallow foveal pit - Irregular OS lengthening - Irregular ONL widening
Atypical	- Absent extrusion of the plexiform layers - Shallow foveal pit - Disrupted IS/OS junction

1.1.4 Decussation of Retinal Fibers at the Chiasm

The neurological visual pathway anatomy is affected in albinism. The post-retinal processes that interpret input from the visual system are organized into two hemispheres. Normally, each hemisphere is a combination of contralateral fibers from the nasal retina and ipsilateral temporal retinal fibers (Ather et al., 2019). The decussation of fibers is described by the vertical meridian

of the retina striking through the fovea, separating temporal and nasal fibers. The delineation of fibers is most obvious in the isolation of crossing nasal fibers at the optic chiasm (Hoffmann et al., 2005; Guillery et al., 1975). In albinism, this organization is disrupted as the decussation line is shifted temporally causing both nasal and temporal retinal fibers to cross at the chiasm (Hoffmann et al., 2005; Neveu et al., 2009). Similarly, the spatial configuration of the retinal vasculature is altered without apparent consequences (Ehrenberg et al., 2013).

Visually evoked potentials (VEPs) have been used as an outcome measure to confirm irregular decussation of retinal fibers (Hoffman, et al 2001, 2005). Such studies have been used to pinpoint the new decussation lines and their variability amongst PwA, and have found variability between individuals but also between OCA and OA genotypes. Hoffman et al. found, in PwA, of whom were primarily identified as OCA1, there was a 5.9-12.1 degree shift in the line of decussation. The few PwA who identified as OA had less than a 5 degree shift (Hoffman et al., 2005).

This misrouting of fibers then affects the subsequent projection to the calcarine fissure (Neveu, et al, 2009; Hupfeld et al, 2006). A consequence of irregular fiber projection could be disorganization in the visual cortex, which can cause fundamental field changes (Hoffman et al, 2001; Hoffman et al, 2007; Guillery et al, 1975). It has been suggested visual fields in PwA may have marginally reduced sensitivity nasally (Hoffman et al, 2007) not influenced by the amount of misrouted fibers (Neveu M.M, et al, 2009). It has been suggested that the crossing ratio of temporal fibers may influence visual acuity (Schmitz B et al, 2004) contribute to an overall depression of the visual field (Hoffman et al, 2007).

Changes to the visual field organization are important for detecting neurological insults (Schmitz et al., 2004; Hupfeld et al, 2006; Neveu, et al, 2009). Visual fields are a representation

of flow of visual information from the retina to the visual cortex. In PwA, Schmitz et al. found there was a visual field dominance. Contralateral hemispheres, representative of crossed fibers, were more prominent in PwA without statistical significance. This was also evident in the organization of the lateral geniculate nuclei (LGN) and visual cortex on fMRI (functional magnetic resonance imaging) (Schmitz B et al, 2004). Downstream from the LGN and visual cortex, global motion is processed in the medial temporal (MT) and medial superior temporal (MST) regions of the brain (Nishida S, et al, 2018; Neveu M.M, et al, 2009). Skerswetat et al., found while low level processing of visual acuity and contrast sensitivity were reduced, global motion had normal sensitivity (Skwerswetat et al., 2023). Implications for high level visual processing - faces (Logan et al., 2022; Grill-Spector K, 2017) and objects (Haque et al., 2018; Barton, 2022, Cao et al., 2021) - are not well understood in PwA.

In few studies, global motion has been reduced in PwA, but there is no definitive connection to the decussation of fibers opposed to nystagmus or reduced acuity (Hupfeld D, et al, 2006, Neveu M.M, et al, 2009).

1.1.5 Aims

Given the unique pathology associated with albinism, the expectations for vision function may differ from other low vision patient populations. Particularly when evaluating the dichotomy of visual function and functional vision, or everyday use of vision, (Benett et al., 2020) we must explore if there is a distinction in PwA. From a retinal perspective, foveal hypoplasia has been identified as the primary cause for concern for visual acuity. However, contributions of the chiasmal misrouting to functional vision is not well understood. Visual acuity and contrast sensitivity are considered to be first-order, low-level visual functions.

Supranuclear processing of color, motion, objects, and face are mid and high-level visual functions beyond V1. Previously, studies conducted have found mid-level processing, such as global motion coherence , to remain unaffected in PwA (Skerswetat et al., 2023). The aim of this thesis is to further explore the dichotomy of visual function and functional vision of low and high-level visual processes. The high-level processes explored in PwA are the following:

1. **Test-retest repeatability for Angular Indication Measurement (AIM) with modification for low vision patients (AIM Low Vision) was explored**. A Bland Altman analysis was used to assess test-retest repeatability for the AIM Low Vision algorithm in both normally sighted individuals and PwA. Visual acuity measures were also compared to ETDRS visual acuity. Our broad research question, is the AIM Low Vision algorithm a valid visual acuity alternative to ETDRS acuity? (Chapter 1)
2. **The assessment of blur tolerance in Persons with Albinism (PwA) compared to literature.** The AIM low vision acuity algorithm was applied to evaluate changes in logMAR acuity with dioptric defocus. This change in visual acuity as a function of dioptric blur in PwA was compared to normally sighted individuals. Here, our research question is, are PwA able to tolerate more dioptric defocus with mild effects on visual acuity? (Chapter 2)
3. **The Foraging Interactive D'Prime (FInD) algorithm was introduced as a new method to explore face discrimination**. A Bland Altman analysis was used to assess test-retest repeatability in normally sighted individuals. Here our research question is if FInD Faces provides acceptable test-retest repeatability to assess face discrimination, especially in low vision patients? (Chapter 3)

4. **Given the extensive information of the retinal manifestation in albinism and the budding research on the misrouting at the chiasm, does this affect face processing in albinism?** Face discrimination threshold comparisons were analyzed between PwA, controls, and blurred controls. (Chapter 4)
5. **An alternate form of the FInD algorithm was introduced with a modification for emotion recognition.** This version integrated a genetic algorithm to assess emotion recognition. A Bland Altman analysis was used to assess performance in normally sighted individuals. Here the research question is if the genetic algorithm provides a repeatable assessment of emotion discrimination that can be used in PwA. (Chapter 5)

1.2 Dioptric Blur Perception

Blur perception refers to the subjective experience of the optical defocus (Walker MG, et al, 2017). Fundamentally, this relies on optical blur refers to the quality of the retinal image relating to media opacities and refractive error. As established by Jacobs et al, blur perception is defined on an anatomical level as +/- 0.18 diopters (D) (Jacobs RJ, et al, 1989). Optical defocus then is processed eliciting a neural acknowledgement of blur (Vera Diaz et al, 2017). This concept has influenced the use of 0.25 D steps in both optical correction in normally sighted individuals (Taneri et al, 2020). In low vision refractions, lens presentation is guided by the Just Noticeable Difference (JND), or just-detectable blur (Borish, 2006). The JND is influenced by acuity and pupil diameter (Green et al, 1980). Therefore, the inverse relationship between acuity and depth of defocus (Green et al, 1980) suggests lower sensitivity to dioptric defocus in low vision patients (Decarlo & Woo, 2006). In clinical practice, the JND is calculated based on the minimum angle of resolution divided by 100 (Decarlo & Woo, 2006; Legge et al., 1989).

Therefore, a normally sighted individual, correctable to 0.0 logMAR, is presumed to appreciate a difference of +/- 0.25 diopter (Taneri et al, 2020); however an individual with an acuity of 0.7 logMAR, would have a JND of +/- 1 diopter.

Optimized visual acuity is important given its influence on contrast sensitivity and stereopsis. It has been well documented that contrast sensitivity is more sensitive to visual deficits (Kiser et al., 2005; Xiong et al., 2020; Blackhurst et al., 1989). Hoosen et al. demonstrated that 1 diopter of blur reduced visual acuity by 0.02logMAR but decreased contrast sensitivity by more than 15%. Similarly, stereoacuity was reduced by three times for 3-5 diopters (Hoosen et al, 2020). This highlights the importance of impact of blur perception on visual acuity compared to other low level processing. In everyday life, this manifests as struggles with face discrimination (Sunness & Annan, 2010), reading (Kestenbaum, 1956; Leat & Woodhouse, 1993), and quality of life (Fenwick et al., 2025). Therefore, the relationship between blur perception yielding accurate visual correction in low vision patients is crucial. However, the mode of vision loss in low vision patients is important. For example, some patients with scotomas and central retinal pathology do not report as much visual gain with spectacle correction (Sunness & Annan, 2010). Therefore, blur perception is perceived as less sensitive with visual correction.

Based on the foveal hypoplasia in albinism, we hypothesized the perception of blur may be impaired in PwA. The aborted development of the fovea (Brigmann A, et al, 2022; Thomas et al, 2011) and lack of specialization of cones (Bringmann et al., 2022; Lee et al., 2018) may compromise the perception of blur. In the current state of albinism research, the correlation between foveal hypoplasia and acuity is not well correlated. Factorial amblyopia and nystagmus are used to bridge the gap in reduced acuity (Thomas et al., 2011; Proudlock et al., 2024). The contribution of the misrouted retinal fibers at the optic chiasm is also not well understood.

Perhaps, if there is irregularity in organization of the visual cortex (V1), this could also alter blur perception. Anderson et al found spectacle correction significantly improves visual acuity in clinical settings (Anderson et al., 2004). Anecdotally, however, some PwA with high refractive error report subjective minimal change in vision with or without correction. In general, blur perception has been assessed in low vision patients, but it has not considered the albinism pathology not encountered in other low vision patients. This thesis aims to clarify sensitivity to blur in PwA.

1.3 Face Discrimination

Facial processing is processed in the fusiform face area (Logan et al., 2022; Grill-Spector K, 2017), occipital cortex, and superior temporal sulcus of the brain (Barton et al., 2021). Deficits in face processing are generally recognized as prosopagnosia, or face blindness (Barton et al., 2021). Alternatively, there is mild deterioration in face discrimination with age and memory (Logan et al., 2017,2022). Prosopagnosia originates from lesions in the occipital cortex and anterior temporal cortex (Barton et al., 2021), or it may present in congenital forms (Logan et al., 2022). Electrophysiology studies using functional magnetic resonance imaging (fMRI) have shown this originates from improper integration of face processing in the aforementioned neural regions ((Logan et al., 2022; Grill-Spector K, 2017). Given the social importance of face discrimination (Dalmaso M et al, 2025; Klauke S et al, 2023; Avery SN et al, 2016; Barton JJS et al, 2021), reductions in this area affect daily function and quality of life (Wang SW et al, 2008; Lane J et al, 2008; Klauke S et al, 2023).

Reductions of face discrimination in low vision patients have been well documented. This is largely due to the reduced sensitivity to high spatial frequency facial features (Peli E et al., 1994;

Fox & Bindemann, 2020) and low luminance environments (Venugopal D et al., 2023; Bullimore & Bailey, 1991). Again, this results from the reduction in visual acuity and contrast sensitivity (Sunness & Annan, 2010; Tejeria et al., 2002). Studies in face discrimination amongst low vision patients have primarily explored AMD and advanced glaucoma (Barnes CS et al., 2011; Venugopal D et al; Tejeria et al., 2002). Minute changes in the middle and low spatial frequency components have been generally reduced in these groups (Logan et al, 2020; Tejeria et al, 2002). Sensitivity significantly decreases for internal features such as lips, eyes, and nose; this is opposed to external features of face shape and hairline (Logan et al., 2022; Jeantet et al., 2018)) with age and logMAR visual acuity (Logan et al., 2017,2022). Especially in cases of central retinal pathology, the image quality of high spatial frequency (Tian et al., 2018; Jeantet et al., 2018) components is compromised.This results from the disrupted parvocellular visual input (Jeantet et al., 2018).

1.3.2 Inverse Face Effects

The face inversion effect (FIE) is a naturally occurring disruption of face discrimination (Bossi et al., 2024; Gerlach et al., 2023; Tian F, et al, 2022) . The effect refers to the decline in face recognition performance when a face is presented upright versus inverted (Gerlach et al., 2023; Tian F, et al, 2022). The fusiform face area becomes accustomed to upright face presentations in the infancy (Gerlach et al., 2023; Bossion et al, 1999; Goffaux et al., 2015; Dobkins & Harms, 2014). The organization of high spatial frequency facial features (ie, eyes, nose, and mouth) is crucial to recognize stimuli as faces (Dobkins & Harms, 2014). Electrocephalography (EEG) has demonstrated there is a latency of neural processing in the FIE (Bossi et al., 2024). Additionally, EEG signals N170 and P1 (Itier & Taylor, 2004; Bossion et al, 1999) have presented higher

amplitudes in the FIE suggesting increased processing demand (Bossi et al., 2024). According to Gerlach et al, the FIE decreased face discrimination by 15-18% (Gerlach et al., 2023). Similarly processed perception of human figures (Bossi et al.,2024) and objects is also decreased to a lesser degree (Gerlach et al., 2023).

Considering the decline in upright face discrimination in low vision patients (Peli E et al., 1994; Fox & Bindemann, 2020), it is expected performance would decrease portionally to controls. As Balas et al concludes, blur decreases image quality in face perception, but the FIE is maintained (Balas et al, 2019). Therefore, an intact FIE alludes to the integrity of the face processing system. This thesis hypothesized PwA would have an atypical FIE, or no change in upright to inverted performance, due to misrouting of fibers at the chiasm (Hoffmann et al., 2005; Guillery et al., 1975) and possible disorganization of the visual cortex.

CHAPTER 2: TEST REPEATABILITY OF A NOVEL ACUITY MEASURE FOR LOW VISION PATIENTS: LOW VISION ANGULAR INDICATION MEASUREMENT (AIM) ACUITY

2.1 Introduction

Visual acuity is an important clinical measure to monitor ocular disease progression, assess best corrected visual potential, trial frame refraction, and to prescribe visual assistive equipment magnification (i.e., low vision devices) (Phan et al., 2021; Van der Zee et al., 2025; Holz FG et al., 2016). The ETDRS acuity chart, based on Bailey-Lovie principles, has become the standard for use in clinical trials due to its logarithmic letter size progression (Bailey, 2012; Chaikitmongkol et al., 2018; Bailey & Lovie, 1976). This chart offers uniform log scaled spacing, and high test-retest repeatability (Bailey & Lovie, 1976; Sanchez-Gonzalez et al., 2021). The Letter by letter logMAR scoring methods used in ETDRS have shown approximately +/- 0.11-0.25 logMAR test-restest variation with ETDRS in normally sighted individuals (Dunbar et al., 2022; Barrio et al., 2015; Manny et al., 2003). In contrast, the widely used Snellen acuity charts have many shortcomings. Line scoring of Snellen acuity has yield repeatability of +/- 0.11 logMAR equivalent; whereas, the letter by letter scoring is much more variable (+/- 0.2logMAR)(Vesely P & Synek K, 2012). A full Snellen acuity chart, not accounting for modifications of an electronic chart, is limited to 1.3 logMAR, or 20/400 (Kaiser PK 2009). Moreover, there is more test-retest variability in vision acuity measures between 20/200-20/400 compared to ETDRS. Whereas the ETDRS chart is able to assess visual acuities up to 1.6logMAR, or 20/800 (Wang T et al, 2021). Thus, Snellen is unable to adequately assess visual

acuity in low vision patients without testing at closer distance, which is not the intention of Snellen. Furthermore, the ETDRS chart uses the Sloan letters system, which avoids legibility bias as letters A,J, and L, for example, are more easily recognized than others (Arditi A & Cagenello R, 1993).

Test-retest variability of visual acuity has been established to be higher for low vision patients compared to normally sighted individuals (Patel PJ et al, 2008; Kiser AK et al, 2003; Blackhurst DW & Maguire, 1989). Patel et al, found increased variation in ETDRS measures in advanced stages of Age Related Macular Degeneration (AMD) (Patel PJ et al, 2008). Those in the early stages of the disease wavered in a mean of 9 letters (0.18 logMAR) between measures while late stage individuals varied in approximately 17 letters (0.34 logMAR)(Patel PJ et al, 2008). Similarly, Kiser et al found variability of acuity in a mixed low vision group to be 11 ETDRS letters, (0.22 logMAR) (Kiser AK et al, 2005). Additionally, visual acuity is not as sensitive to disease progression compared to contrast sensitivity (Kiser AK et al, 2005; Xiong YZ et al, 2020).This study included a variety of low vision patients including participants with retinitis pigmentosa, macular disease, optic nerve disease, and other retinal diseases prompting legally blind visual status (Kiser AK et al, 2005). However, other low vision etiologies such as albinism have not been included in these studies. It is theorized that ETDRS chart test-retest variability in low vision patients may be in part due to factors such as: to crowding effects, presence of scotomas, and eccentric viewing. As a result of this variability the “minimum clinically important difference” (MCID) in acuity has been recognized as more than 0.3 logMAR, or 15 letters (Joussen AM et al, 2007; Kniestedt C & Stamper RL, 2003; Rosser DA et al, 2003; ETDRS Group, 1991; Age-Related Eye Disease Study Research Group, 2001). The MCID is a

reference for acuity loss or gain (Joussen AM et al, 2007; Kniestedt C & Stamper RL, 2003; ETDRS Group, 1991; Age-Related Eye Disease Study Research Group, 2001).

These are reasons why ETDRS acuity has become the gold standard for low vision patients and clinical research (Wang T et al, 2021; Hazel CA & Elliott DB, 2002; Sanchez-Gonzalez MC et al, 2021). However, despite the advantages of the ETDRS chart, it has still not been widely adopted in clinical practice, and many studies are still using electronic or projector-based Snellen charts. Additionally, Kaiser suggests there is ambiguity in letter by letter scoring by examiners and more time required of ETDRS (Kaiser PK, 2009). Perhaps other reasons for not incorporating ETDRS into clinical practice are letter crowding, variable lighting, and reduced legibility with time. For these reasons, in addition to literacy reasons, people have explored the Landolt C paradigm.

The Landolt C method is often used in place of ETDRS for populations that are unfamiliar with Roman letters used in ETDRS's SLOAN letters (Chaikitmongkol V et al, 2018; Treacy MP et al, 2015). This acuity method has been particularly successful in childhood amblyopia (Lai YH et al, 2021; Chaudhry N et al, 2025). Specifically for amblyopes, a discrepancy of approximately 0.4 logMAR has been reported between ETDRS and Landolt C, with reported lower scores for Landolt C (Lai YH et al, 2021). Repeatability between the two methods has been well established. One study suggested Landolt C and ETDRS (with Sloan letters) had comparable acuity test-retest repeatability in both normally sighted individuals and low vision patients (Chaikitmongkol V et al, 2018). Landolt C presented repeatability of 0.73 in controls and 0.91 in individuals with acuity between 20/125-20/200; whereas ETDRS had repeatability coefficients of 0.7 and 0.93 respectively (Chaikitmongkol V et al, 2018). Additionally, agreement between the two methods was high across different retinal disease groups (0.72 in normals, 0.95 in the

cataract group, 0.99 in the AMD group, and 0.96 in the diabetic macular edema group) (Chaikitmongkol V et al, 2018). Recorded acuities were also lower with Landolt C across all groups. Similarly, Kuo et al suggests Landolt C measures are more repeatable for maculopathy patients with reduced acuity in patients, or other low vision patients with central vision loss (Kuo HK et al 2011). This study expressed a 4 line (0.4logMAR) difference, or limits of agreement, in patients with acuity worse than 20/200, or 2.0 logMAR (Kuo HK et al 2011).

In regard to methodology, Landolt C is often performed as a 4 alternative forced choice task of equal difficulty (with the participants indicate one of four orientations for the gap in the "C" - up, down, left, right), limiting variations in responses compared to ETDRS (Koenig S et al, 2014; Ferris FL & Bailey IL, 1996). Generally, Landolt C charts require direction indication toward one quadrant of 360 degrees; whereas, ETDRS offers 10 different Roman letter optotypes with varying difficulty (Koenig S et al, 2014; Bailey IL & Lovie JE). However, the use of the "C" optotype dispels letter bias that may be present in ETDRS charts (Koenig S et al, 2014; Ruamviboonsuk P et al, 2003). Additionally, ETDRS charts have previously reported to acquire faster measures (Fenwisk EK et al, 2025; Chaikitmongkol V et al, 2018). Koenig et al found ETDRS testing was 1.5 time faster than Landolt C. That study showed ETDRS acuity required approximately 54 seconds in normally sighted individuals while Landolt C took 83 seconds (Koenig S et al, 2014). This difference is influenced by the termination rule, which depends on either majority-correct responses or letter-by-letter scoring. (Elliott DB, 2016; Ferris FL & Bailey IL, 1996). Thus, there is a need for more reliable tests that are easy to administer and suitable for self-testing in modern clinical practice.

The Angular Indication Measurement (AIM) is a novel method for visual acuity testing (Neupane S et al, 2024, 2025; Skerswetat J et al, 2024). AIM allows for a self-administered

computerized version of visual acuity testing. The method requires participants to judge the orientation of a chart composed of C optotypes at various sizes, similar to Landolt C acuity charts (Ruamviboonsuk P et al, 2003; Koenig S et al, 2014) Presented orientations are randomized and adapt to performance in subsequent charts. This method eliminates termination rules (Elliott DB, 2016; Arditi A & Cagenello R, 1993) used in both Snellen and EDTRS by way of the staircase thresholding method (Neupane S et al, 2024). In AIM, a psychometric function is fit to the error between the true and reported orientation of each C as a function of its size. This adaptive psychophysical function is used to select stimulus sizes on successive charts and to generate an estimate of threshold visual acuity in a stepwise fashion. The psychometric function also offers insight into the deterioration of performance, shown by the slope of the function. Previously, the repeatability of AIM outcomes have been established amongst normally sighted individuals (Skerswetat J et al, 2024). It is our intention to implement this program in participants with low vision, including albinism, macular degeneration, and other macular diseases. We therefore modified the algorithm to measure low vision acuities. This new version offers a self-administered analysis of vision that can be used remotely to monitor vision in low vision patients.

Our aim is to validate and explore test-retest repeatability of the modified version of AIM for use in both control and low vision patients. AIM could repeatable and clinically valid results in an efficient manner in both populations. Both through the demonstration of the acuity measures and the time administered for the test, we present this as a valid alternative for acuity testing. Additionally, analyzing the psychometric function parameters may better allow us to understand changes in rate of performance with larger and smaller optotypes.

2.2 Methods

2.2.1 Control Participants

48 Northeastern University students aged 18-24 were recruited February to September 2024. Participants were consented and pertinent ocular and medical histories were recorded. Inclusion criteria were defined as students with vision correctable to 20/20, or 0.0 logMAR, and no history of ocular disease. Binocular vision testing (i.e., cover testing and stereoacuity) were conducted to confirm normal binocular status. Participants were instructed to report diplopia or eyestrain during testing. Both autorefraction and loose lens refraction were performed by a proficient optometry student (author OW) to confirm refractive status. The test order for tasks was assigned using block randomization through the Robust Randomization App developed by the Center for Biostatistics at the Icahn School of Medicine at Mount Sinai and the excel "Randarray" function.

Participants completed both ETDRS acuity and the Low Vision AIM Acuity paradigm. Following clinical refraction, acuity was measured both with best correction and 4 diopters of effective blur to simulate reduced acuity. The program was completed at 1 meter; therefore, 5 diopters was added to the manifest to achieve 4 diopters of effective blur.

2.2.2 Albinism Group Participants

A separate group of 8 Persons with Albinism (PwA) was also recruited from the Janet L. LaBreck Center for Low Vision Rehabilitation at the NECO Center for Eye Care. Inclusion was restricted to participants with albinism, excluding any additional confounding conditions The Mini-Mental State Examination was completed before testing to confirm adequate cognitive

status. ETDRS acuity was reported and a loose lens refraction was performed in these participants. Participants completed the Low Vision AIM algorithm twice with best correction. Testing was performed amongst other psychophysical testing and was randomized accordingly.

2.2.3 Angular Indication Measurement (AIM) Paradigm

The Low Vision AIM Acuity program required participants to identify the orientation of the gap in "C" optotypes. Responses were made by clicking a mouse cursor along a ring surrounding each optotype where they see a gap. There was no time limit and participants were able alter their responses an unlimited number of times (Figure 1). The program started with a single 4.0 logMAR optotype (20/20,000 or 6/6,000) and adapted to the participant's performance in subsequent charts according to the calculated angular error.

To accommodate low-vision patients and reduce photophobia, optotypes are shown in black on a gray background with sufficient contrast. All optotypes are logarithmically shaped to standardize crowding. The gaps of the optotypes were 20% of the line width. Orientations were randomly selected for each presentation. A forced-choice response structure was used to advance the program, substituting the standard termination rule with a staircase approach. Opposed to the traditional Landolt C acuity, all directions of the 360 degree orientation ring were tested with AIM acuity instead of only the four quadrants (Ruamviboonsuk P et al, 2003).

Responses were considered correct if the gap orientation was identified within 22.5° of its true position. (Figure 2). Error reports were recorded according to the guess angle, optotype size and noise. Therefore sensitivity is reported for each response (Figure 3) altering optotype sizes to be closer to threshold in subsequent charts. In total, 32 optotypes are displayed.

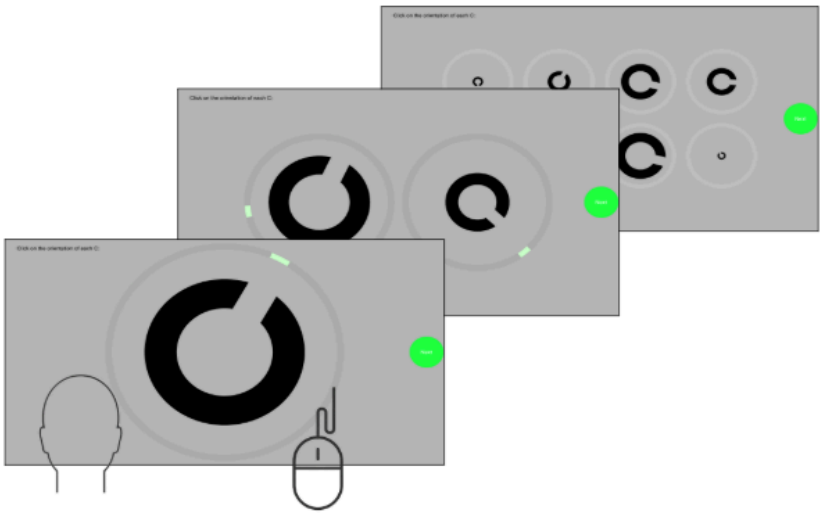

Figure 1. Example for the first three charts of the adaptive AIM algorithm. Optotypes are adjusted on a logarithmic scale based on performance on previous charts. A psychometric function is fit to performance over 32 presented optotypes.

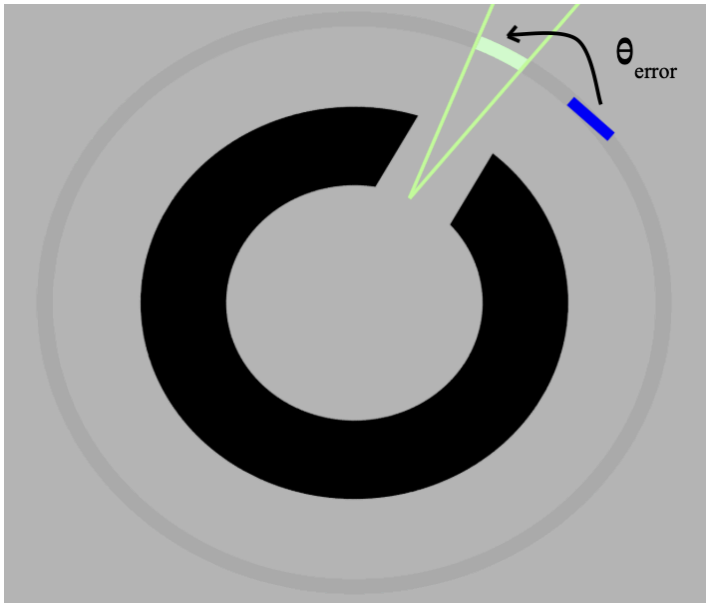

Figure 2. Example of response selection and and demonstrated angular error (θ_{error}). The reference point for no error is indicated by the midpoint of the gap in the optotype. An indication with minimal error is represented by the green bar along the correspondence ring while the blue bar is an incorrect response more than 22.5° from the correct selection.

$$\theta_t = (\theta_{error} + (\theta_{guess} - \theta_{error}))(0.5\text{-}0.5)(\mathrm{erf}(s\text{-}\ t/\sqrt{2}y))$$

Figure 3. The equation used in Low Vision AIM to calculate the threshold angle includes the error from the correct response including selections within 22.5° (θ_{error}) and guesses (θ_{guess})(Neupane S et al, 2024, 2025; Skerswetat J et al, 2024).

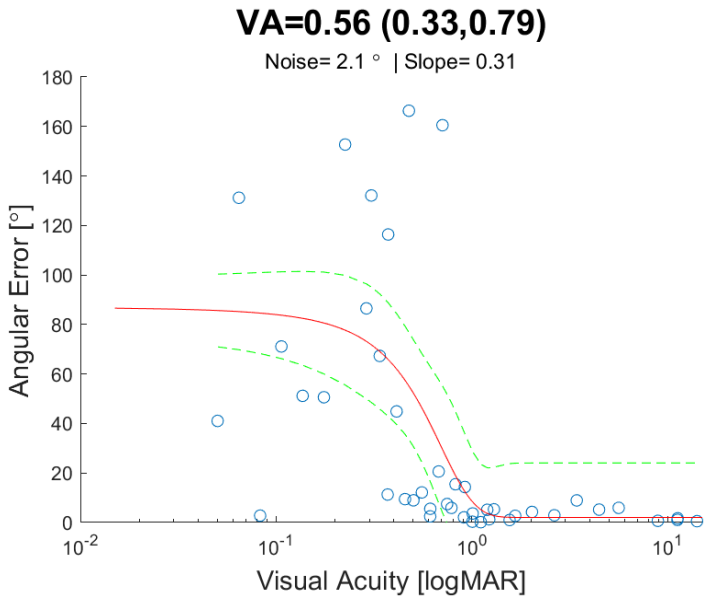

Figure 4: Example of AIM Low Vision psychometric function output. The angular error report is plotted as a psychometric function. The midpoint represented the threshold acuity of the participant. Beyond the midpoint to the lower plateau of the curve is the range of stimulus detectability improvement (ROSDI), which shows performance 0.05 logMAR beyond threshold.

2.2.4 Equipment Details

A 32-inch 60 Hz LG HD 4K monitor system was used. Pixel resolution was sustained at 3840 x 2160. Programming for the Low Vision AIM acuity program was generated in Matlab (MathWorks, R2021a) using the Psychophysics Toolbox.

2.2.5 Statistical Analysis

Statistical analyses were performed using Matlab toolbox (Version 2020b) and RStudio. A Bland Altman analysis (95% confidence) was deployed for comparison of the original test trial and the retest. A two tailed t-test was used to justify the application of a Bland Altman. Output values of the Bland Altman were expressed as slope, p-value (α= 0.5), correlation of variance and correlation of repeatability. Acuity was expressed as the minimum angle of resolution (MAR) to clarify acuity without influence of logarithmic changes. Additionally, a sample t-test and Bland Altman were performed for Low Vision AIM and ETDRS acuities.

2.3 Results

2.3.1 Participant Demographics

All participants were correctable to 0.0logMAR in each eye. A loose lens refraction by an experienced optometry student was performed on all participants. Additionally, stereo acuity and a cover tests were performed to rule out amblyopic pathology.

Table 6. Demographics of control study participants for Low Vision AIM test-retest repeatability protocol

Demographics	Participants
Age (mean)	20.0 ± 3.3
ETDRS Visual Acuity (logMAR)	-0.22 ± 0.08
Randot 3 Stereoacuity (Arcseconds)	78.78 ± 111.78
Sex, n=48 (%)	
Male	17 (35.4)
Female	31 (64.6)

Table 7. Demographics and visual measures for PwA for Low Vision AIM test-retest repeatability protocol

Demographics	Participants
Age (mean)	48.88 +/- 22.8
ETDRS Visual Acuity (logMAR)	0.74 +/-0.17
Pelli Robson Contrast Sensitivity (logCS)	1.44 +/- 0.38
Stereoacuity	No subjects presented with stereo
Sex, n=8 (%)	
Male	6 (75)
Female	2 (25)

Table 8. Race and ethnicity demographics for PwA.

	Race/ethnicity, n (%)
White	6 (75)
Black or African American	2 (25)
Hispanic or Latino	1 (12.5)

Table 9. Race and ethnicity demographics for control participants.

	Race/ethnicity, n (%)
White	22 (45.8)
Black or African American	6 (12.5)
Asian	14 (29.2)
Hispanic or Latino	7 (14.6)
More than one race	5 (10.4)
Prefer not to say	1 (2.1)

2.3.2 Test-Retest Reliability with Best Corrected Acuity

A Bland Altman (Giavarina D, 2015) was used to analyze test-retest variability of acuity performance. A two tailed t-test was applied prior to the Bland Altman confirmed no statistical significance between trials (p=0.824). Habitual correction yielded a mean acuity of +0.06 logMAR using the AIM algorithm. Between the first and second trials the coefficient of variation was 51% while the coefficient of reliability was 6%. Participants displayed 0.002 bias with no

significant difference between the performances (p =1.0). Limits of agreement were +/- 0.06 logMAR.

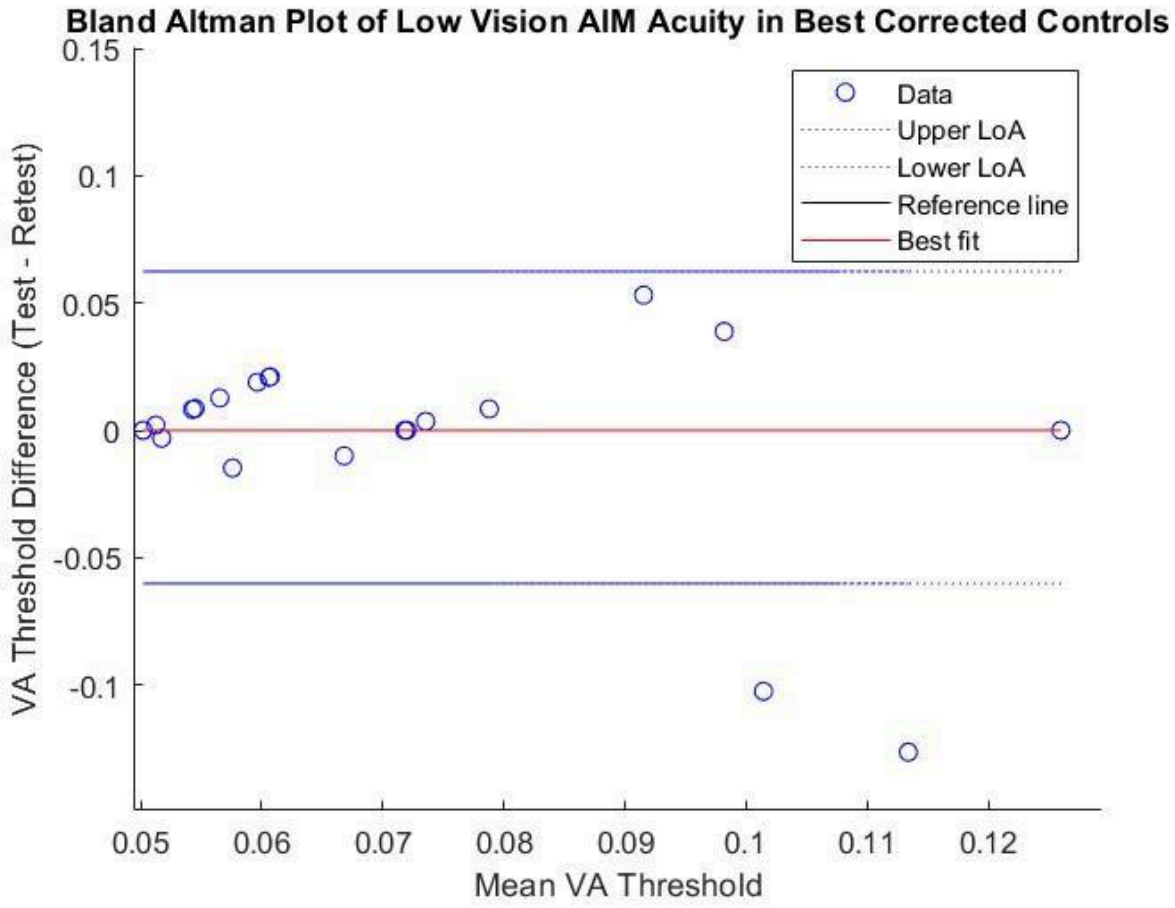

Figure 5. Bland Altman plot of acuity threshold repeatability of AIM Low Vision in best corrected controls. The red line represents the best fit function of average threshold and the difference between test and retest. Limits of agreement were narrow at - 0.06 (lower limit; bottom blue line) and 0.06 logMAR (upper limit; top blue line). Bias (red line) was reported as 0.2% and the coefficient of variation was 51%.

2.3.3 Test-Retest Reliability with Dioptric Defocus

The confirmatory two tailed t-test performed prior to Bland Altman was statistically non-significant (p= 0.4338). The limits of agreement in the Bland Altman showed differences as

much as -0.1847 to 0.2670 logMAR. The negative values here denote deviation from the test and retest acuity, not the true logMAR acuity.

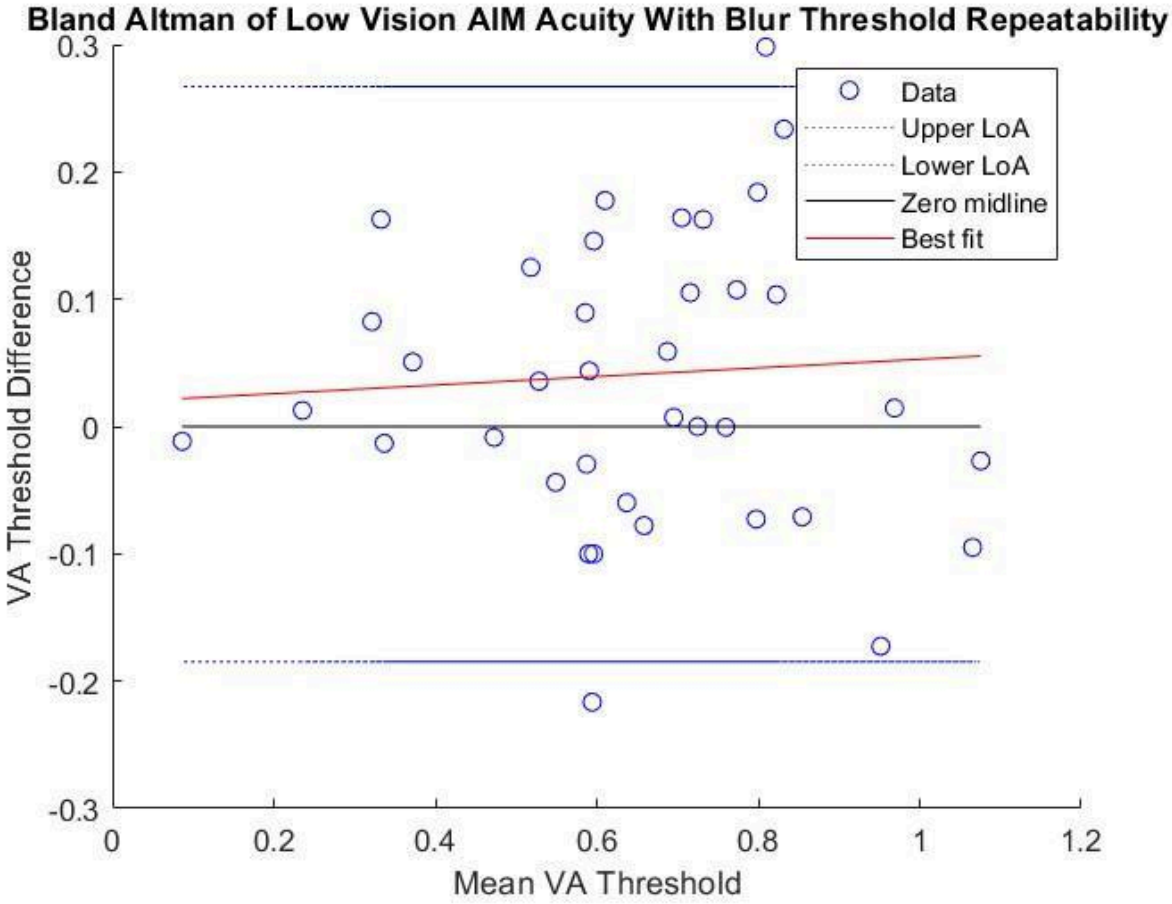

Figure 6. Bland Altman plot of acuity thresholds in controls with +4.00 diopters of blur. Performance differences between test and retest (red best fit) ranged from -0.1847 (lower limit of agreement; bottom blue line) to 0.2670 logMAR (upper limit of agreement; top blue line). The black line presents a model of no difference, or zero, between tests. Bias was limited to 6% and the coefficient of variation was reported as 19%.

2.3.4 Low Vision AIM Repeatability in Persons with Albinism

The mean difference between first and second retest measures was not significant (p= 0.9525). Variation for this group was 28.89%. The limits of agreement were -0.297 to 0.325 MAR, or approximately +/- 0.2 logMAR.

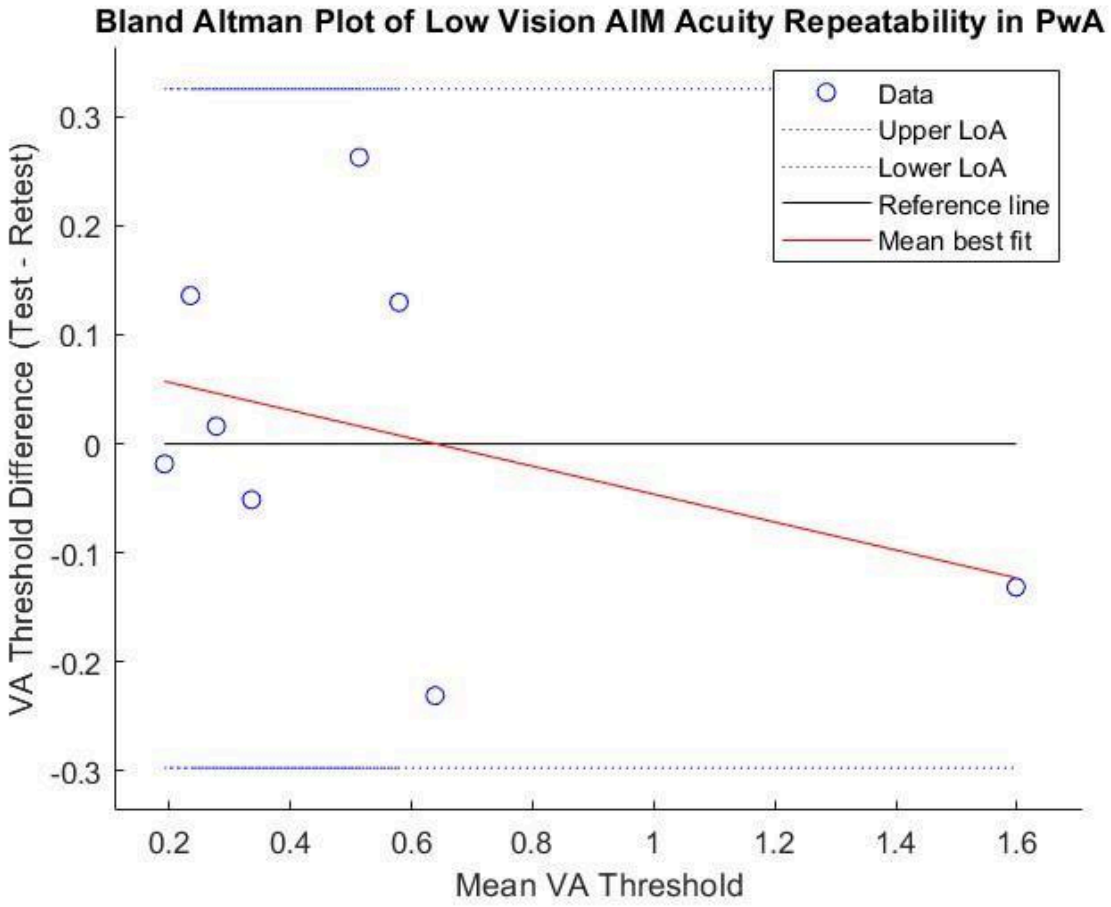

Figure 7. Bland Altman plot of repeatability of acuity threshold in PwA. The mean visual acuity threshold was derived from the AIM Low Vision outputs for both tests and retest. The y axis represents the difference between thresholds. Plotted data is confined to the upper (0.325 MAR) and lower (-0.297 MAR) limits of agreement (+/- 0.2 logMAR)

2.3.5 Low Vision AIM & EDTRS Acuity Comparison

A sample t-test and Bland Altman analysis were performed to evaluate the difference between mean acuity performances with habitual correction and dioptric blur. The sample t.test for dioptrically blurred acuity difference was statistically significant ($p < 0.001$). Similar results were found for best corrected acuity ($p < 0.0001$). For blurred acuity, the limits of agreement showed clinically significant differences of -0.1195 to 0.4199 MAR, which favors AIM as the better logMAR acuity. Acuities were best corrected performance displayed limits agreement of -0.1136 to +0.1087 MAR differences, which is not clinically significant ($p<0.001$).

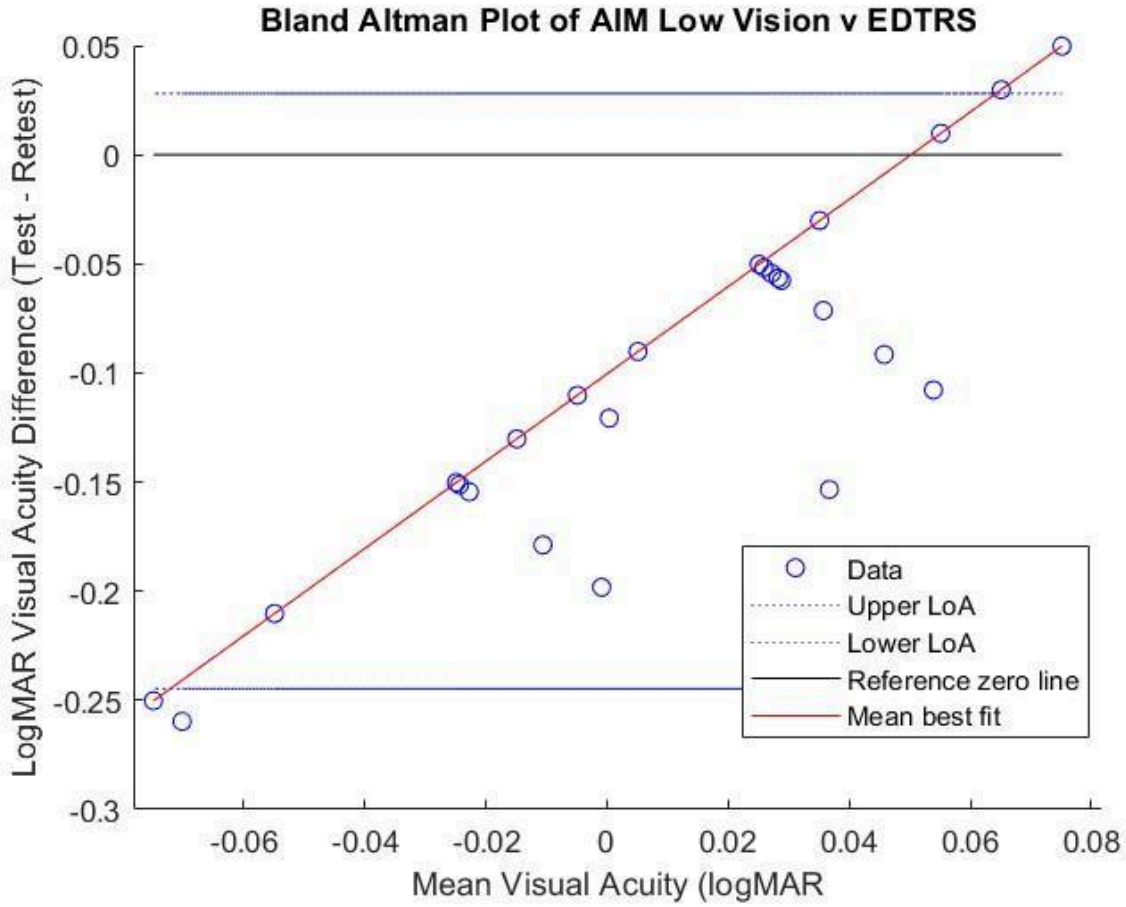

Figure 8. Bland Altman compared mean AIM Low Vision and ETDRS acuity. Bias and coefficient of repeatability were calculated at 11% and 25% respectively ($p<0.000$). The coefficient of variation was reported as 19.01%

2.3.4 Testing Duration

Between tests and retests with best correction, participants completed the AIM algorithm in 139 seconds on average. Acuity with +4.00 diopters of blur was completed in 107 seconds on average amongst controls and 186 seconds in PwA. ETDRS acuity duration was not recorded. These recorded times included initial instructions of the AIM algorithm.

2.4 Discussion & Conclusion

This study serves as proof of concept for a modified version of the original AIM Visual Acuity paradigm. The repeatable results suggest AIM Low Vision is suitable for high reductions of acuity up to +4.0 logMAR. Variability in acuity has previously been reported with the widely used ETDRS chart, remaining within non-clinically significant limits of two lines(0.2logMAR). The AIM algorithm offers narrower limits of agreement compared to this standard with variability within a line (< 0.1logMAR).

The advantages of the AIM algorithm over the EDTRS chart include its ability to assess visual quality across 360 degrees, deterioration of performance, self administration and swift assessment of suprathreshold stimulus. The use of "C' optotypes avoids the ambiguity of letter presentation. Snellen letters are more likely to pose ambiguity, Sloan letters in the EDTRS chart exhibit a similar issue with letters "C,O, and D" (McAnany JJ, et al, 2011). (Ruamviboonsuk P et al 2003 & Koenig S et al 2014). AIM Low Vision, using Landolt C, focuses more on resolution of the gap instead of letter recognition; therefore, participants must focus more on the details of the optotype. The error report allows for analysis of response patterns and accuracy of the gap's identification. The psychometric function output then allows for analysis of the breakdown in performance with smaller optotype presentation. These features are not offered in the letter by letter scoring of ETDRS acuity. The results from this group also display discrepancies between acuity reports of ETDRS and AIM. AIM Low Vision acuity with best correction have test-retest differences that are likely related to constraints of the optotypes display. However test-retest differences with dioptric blur can be attributed to methodological differences seen in Landolt C comparisons.

As previously discussed, ETDRS has been documented to be faster than Landolt C in normally sighted individuals (Koenig S et al., 2014; Pang et al., 2020). In low vision patients, ETDRS visual acuity takes approximately 280 seconds to administer (Hepler et al., 2023). Although testing in best corrected controls in this study was slower than other studies which documented ~54 secs for ETDRS, both blurred control trials and PwA trials performed were faster than previous studies with low vision groups. Hepler et al., assumes approximately 280 secs for acuity testing (Hepler et al., 2023), which is corroborated by other studies (Camparini et al, 2001; Pang et al., 2020). This testing time is notably higher than the 107 secs (blurred controls) and 186 (PwA) found in this study.

As previous studies have suggested, Landolt C may be more sensitive to acuity deficits compared to ETDRS (Kuo H.K, et al , 2011). The results of this study are in agreement with these findings using +4.00 diopters of blur. Therefore, the combination of the minimum error report, psychometric function analysis, and fourier spectra formation of the optotypes provide an accurate assessment of visual stasis. Again, visual acuity is used to closely track changes in the visual system, especially in retinal conditions.

2.4.2 Limitations

As AIM Low Vision allows for optotypes as large as +4.0logMAR, the parameters are constrained to no smaller than 0.0502 logMAR. Since the participants of the study were correctable to 0 logMAR, and often better, the AIM Low Vision acuity does not agree with the entering ETDRS acuity due to these constraints. However, it should be acknowledged the reported visual acuities were reproducible from the test to retest.

2.4.3 Future Directions

Further testing in other low vision groups (eg, AMD, advanced glaucoma, Stargardt's, etc.) will be explored to assess differences in performance from normally sighted controls. AIM Low Vision was only tested in individuals with albinism during an ongoing study. However, the intention is for Low Vision AIM-VA to be used in all low vision patients including macular disease, advanced glaucoma, retinal dystrophies, etc..

CHAPTER 3: EXPLORATION OF DIOPTRIC BLUR TOLERANCE IN ALBINISM

3.1 Introduction

Optical defocus is particularly important when prescribing spectacles, evaluating low vision devices, and surgical outcomes affecting refractive status (Holz et al., 2016 ; Phan et al., 2021; Van der Zee et al., 2025; Holz et al., 2016). Clinical refractions are known to improve acuity in 11% of low vision patients with a two more with visual acuities worse than 20/40 (0.3 logMAR) (Sunness & Annan, 2010; Cheng & Woo, 2021). Sunness and Annan reported patients with Age Related Macular Degeneration (AMD), diabetic retinopathy, advanced glaucoma, and retinal dystrophies reported a visual acuity gain of 3-4 lines (0.31-0.4 logMAR) (Sunness & Annan, 2010; Guo et al., 2020). Particularly in the AMD group, eccentric viewing seems to improve in the worse with optimized correction (Sunness & Annan, 2010). Although clinical refractions do not directly treat ocular pathology, it remains important to optimize the remaining visual vision in low vision patients (Guo et al., 2020); thus improving quality of life (Van Nispen et al., 2020; Osley et al., 2007). Maximizing refractive correction influences reading (Kestenbaum, 1956), magnification prescribing, and face discrimination (Sunness & Annan, 2010), and mobility (Elliot & Chapman, 2010; Marron & Bailey, 1982). Optimal refractive correction manifests as expanding one's field of view, adjusting ergonomics (ie, view distance), and blunt nystagmus amplitudes (Tsai et al., 2020; Bolduc, 1992). However, some patients with central retinal pathology do not report as much visual gain with spectacle correction. For example, those with central scotomas have reported no change in their visual status with glasses (Sunness & Annan, 2010) citing benefit of glasses with certain disease presentation.

The ability to detect retinal defocus and blur has been well studied (Wang & Ciuffreda, 2005; Jacobs et al., 1989). Principles established through retinal sensitivity to blur have influenced

refraction protocols. It is well established that decreased acuities are accompanied by low sensitivity to defocus (Legge et al., 1989; Cheng & Woo, 2021). Therefore, entering acuity and the just noticeable difference have been applied (Decarlo & Woo, 2006; Legge et al., 1989). Leat et al. inferred that individuals with low vision depend more on low spatial frequency cues during reading, which may contribute to increased blur tolerance. (Leat & Woodhouse, 1993). However, some studies suggest dioptric sensitivity cannot be predicted based on acuity (Cheng & Woo, 2021).

Persons with Albinism (PwA) represent a subgroup of the low vision population with unique ocular pathology. This condition arises from dysfunctional melanosomes (Tomita et al, 1989; Federico, et al, 2023; Mcham & Fulton, 1992) resulting in high refractive error (Federico et al., 2023; Kessel et al., 2023; Yahalom et al., 2012), nystagmus (Neveu et al, 2009; Abadi, 2002), iris transillumination, fundus hypopigmentation (Summers et al, 1988; Seo et al, 2007), foveal hypoplasia (Proudlock, 2024; Summers, 1996), and misrouting of retinal fibers at the optic chiasm (Summers, 1996). These visual consequences have been well documented along with the marked reduction of visual acuity and contrast sensitivity (Federico, et al, 2023; Mcham & Fulton, 1992; Summers, 1996), but implications of clinical procedures (i.e., refractions) have not been explored. Again, we understand blur tolerance is expected in acquired and progressive retinal conditions (Vera Diaz et al, 2017). However, the contribution of foveal hypoplasia, nystagmus and possible irregularities in downstream processing to the visual cortex to blur perception are not well understood. This study aimed to compare the range of objective acuity measures with induced dioptric defocus between normally sighted controls and PwA. Acuity measures were achieved using the Angular Indication Measurement (AIM) algorithm

(Skerswetat et al). Investigating this comparison seeks to clarify refractive procedures for albinism, improving clinical outcomes.

3.2 Methods

3.2.1 Patient recruitment

Twenty PwA were recruited from the Janet L. LaBreck Center for Low Vision Rehabilitation at the NECO Center for Eye Care in Boston, Massachusetts. Included participants presented with no other ocular pathology aside from albinism. All participants received an eye exam within the year prior. Participants were age- and sex-matched for analysis. The electronic records of the last exam were reviewed for noted pathology and ocular alignment (nystagmus). Before psychophysical tests were applied a Mini Mental State Examination for cognitive status was administered and demographics were recorded. Additionally, basic acuities were acquired with ETDRS at both distance and near (logMAR), and so were Pelli Robson contrast sensitivity (logCS), and MNread (threshold and critical print size). A loose lens refraction was performed by an experienced optometrist on all participants.

3.2.2 Visual stimulus

A 32-inch 60 Hz LG HD 4K monitor system was used. Pixel resolution was sustained at 3840 x 2160. The default mouse size was 4.98 mm for controls and enlarged to 8 mm for PwA. Programming for the tasks was generated in Matlab (MathWorks, R2021a) using the Psychophysics Toolbox (Pelli et al & Brainard et al). The Angular Indication Measurement

(AIM) algorithm was used to assess visual acuity (Skwerswetat et al). The AIM Low Vision algorithm used in this study is self administered and adapts to participants' responses throughout 32 trials. Participants were instructed to indicate the position of the gap in a "C" optotype along a 360 degree response ring (Figure 9). Each response reported an error of angle. Through subsequent presentations a psychometric curve is fit (Figure 10). Thresholds are derived from the midpoint of the psychometric curve, representing an acuity with correct indications 50% of the time (Figure 11). Performance noise and the slope from the highest to lowest point of the psychometric function were reported.

All testing was performed at 1 meter with the appropriate correction from the aforementioned refraction and near power as needed. Participants first completed the program without blur. Then, in randomized fashion, the program was again completed with 1, 2, 3, 4, 5, 6 in plus dioptric blur. Minus blur was not used to avoid over accommodation. Participants were instructed to avoid squinting as to discourage a pinhole effect.

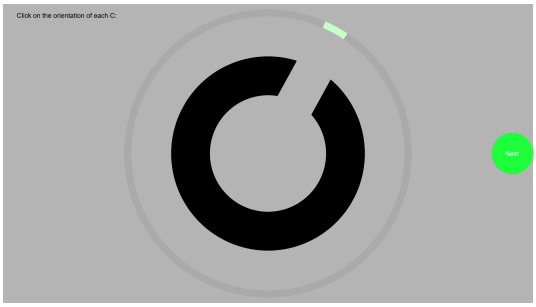

Figure 9. Illustration of AIM Low Vision task. Participants were instructed to identify the orientation of the gap in the "C" optotype by clicking. Each response reported an error value, the difference between the patient selection and centered orientation.

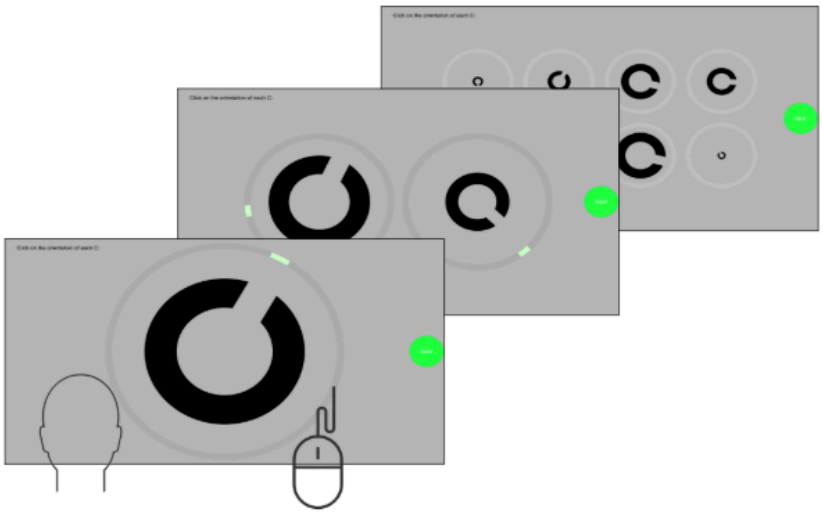

Figure 10. Illustration of subsequent charts in the AIM Low Vision tasks. While adapting to previous error reports, the participants are presented with progressively smaller optotypes reaching threshold.

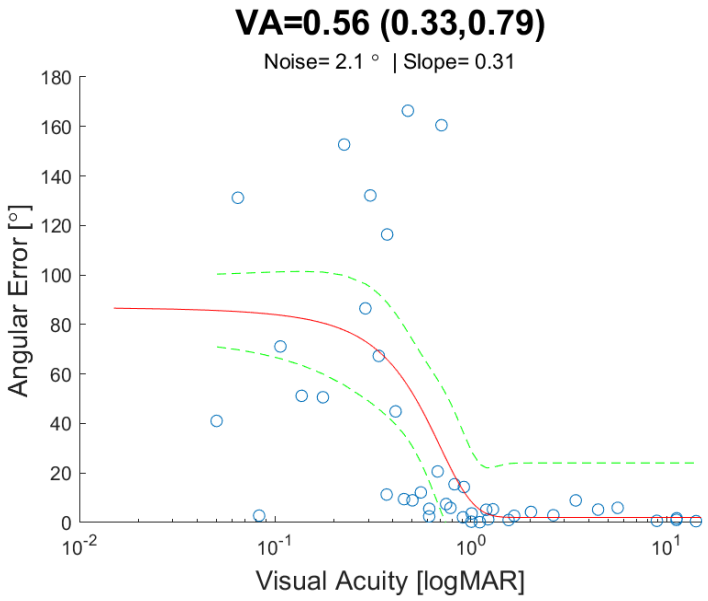

Figure 11. Example of psychometric function output. The angular error report is plotted as a psychometric function. The midpoint represented the threshold acuity of the participant. Beyond the midpoint represents the threshold acuity of 0.05 logMAR.

3.2.3 Data Analysis

A linear mixed regression model was used to assess differences in performance between blur levels. Then, a linear regression analysis was fit over acuity performed at each level of blur for individual participants (Figure 12). Individual linear regression fits remain appropriate as the majority of participants in each group followed a linear pattern in visual acuity (Appendix A). The slope taken from each linear regression was then applied to a Wilcox Rank Sum comparison between PwA and control performance. Additionally, a separate Linear Mixed Model was performed for acuity comparison between groups for each level of blur.

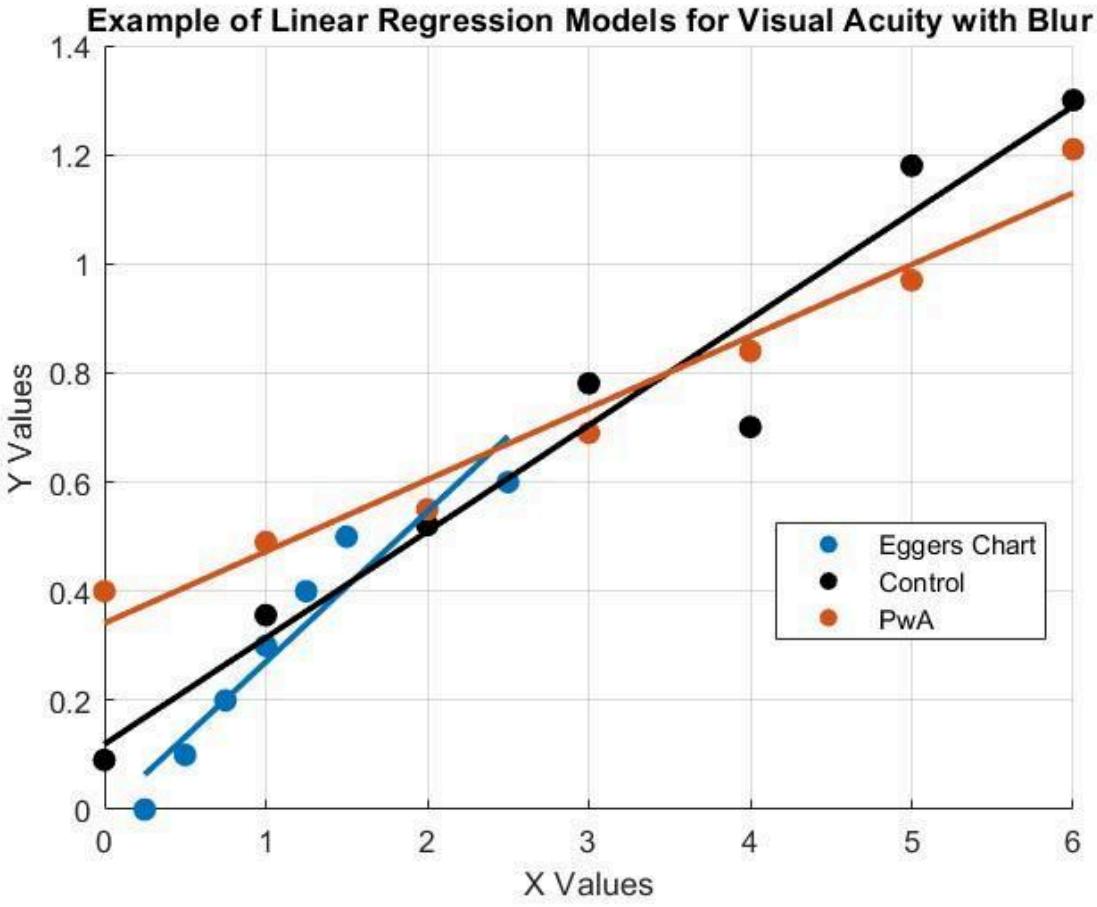

Figure 12. Linear regression model for effective blur visual acuity in AIM Low Vision for one PwA and control participant. The blue line represents suspected defocus accounted for according to Egger's Chart (This only refers to 0.25-2.5 D of blur). The black line presents performance of a reliable control detailing visual acuity from 1-6 D of blur (1D steps). The red line represents a reliable PwA participant's performance from 1-6D of blur. The slope of these linear regression lines were used in analysis of change of visual acuity with increasing blur. A larger slope suggests more sensitivity to blur.

3.3 Results

3.3.1 Participants age and acuity distribution

Twenty PwA and age- and sex-matched participants (8 females per group) presented with a mean age of 40 +/- 21 years in the albinism group and 34 +/- 19 years in the control

group (p= 0.36) (Table 12). Entering clinical measures (distance acuity, near acuity, and contrast sensitivity) in the better eye were significantly different between the groups (Table 13). All of the participants in the albinism group displayed varying levels of nystagmus. Participants were allowed to complete the AIM Low Vision algorithm at their null point.

Table 10. Race and ethnicity demographics for PwA.

	Race/ethnicity, n (%) **of 20
White	11 (65)
Black or African American	6 (30)
Hispanic or Latino	2 (10)
Prefer not to say	1 (5)

Table 11. Demographics of participants from the Albinism group and their age matched controls (+/- 5 years).

Demographics	Persons with Albinism (p=20)	Matched Controls
Mean Age (SD) years	40.9 (± 21.4)	34.7 (± 19.0)
Sex, n (%)		
Male	7 (35)	7 (35)
Female	13 (65)	13 (65)

Table 12. Comparison of entering clinical measures between the Albinism and Control groups.

	Albinism Group Mean (SD)	Control Group Mean (SD)	P Value from student t-test
Distance ETDRS VA in the better eye (logMAR)	+0.73 (± 0.25)	-0.03 (± 0.15)	p< 0.0001
Near Lighthouse VA in the better eye (logMAR)	+0.62 (± 0.27)	-0.01 (± 0.18)	p<0.0001
Pelli Robson contrast sensitivity in the better eye (logCS)	1.4 (± 0.33)	1.7 (± 0.39)	p= 0.03
MNRead Critical print size (logMAR)	+0.70 (± 0.29)	+0.03 (± 0.18)	p<0.0001

3.3.2 ETDRS Acuity Versus AIM Low Vision Acuity

Entering acuity between groups was significantly different for ETDRS ($p<0.001$) and AIM Low Vision ($p=0.005$). Otherwise, there was good agreement between ETDRS acuity and AIM Low Vision (controls $p=0.125$; PwA $p=1.0$).

3.3.3 Linear Mixed Regression Model of Acuity Comparison

A linear mixed regression model was applied to the acuity data between groups. Figure 13 displays the spread of data for each level of blur. This method was used opposed to a repeated measures ANOVA as the data was not normally distributed. Between groups there was a significant difference in acuity with best correction ($p=0.03$) and 1 diopter of blur ($p=0.0247$) (Figure 13). Within-group comparisons showed more frequent deviations of acuity across the different blur levels (Table 14). In particular, the albinism group had a significant difference in acuity from best corrected to +6 diopters of defocus ($p < 0.0001$) with an acuity mean difference of 0.5820 logMAR. Similarly, controls also presented a significant difference in performance ($p <0.0001$) with an acuity mean difference of 0.8863 logMAR.

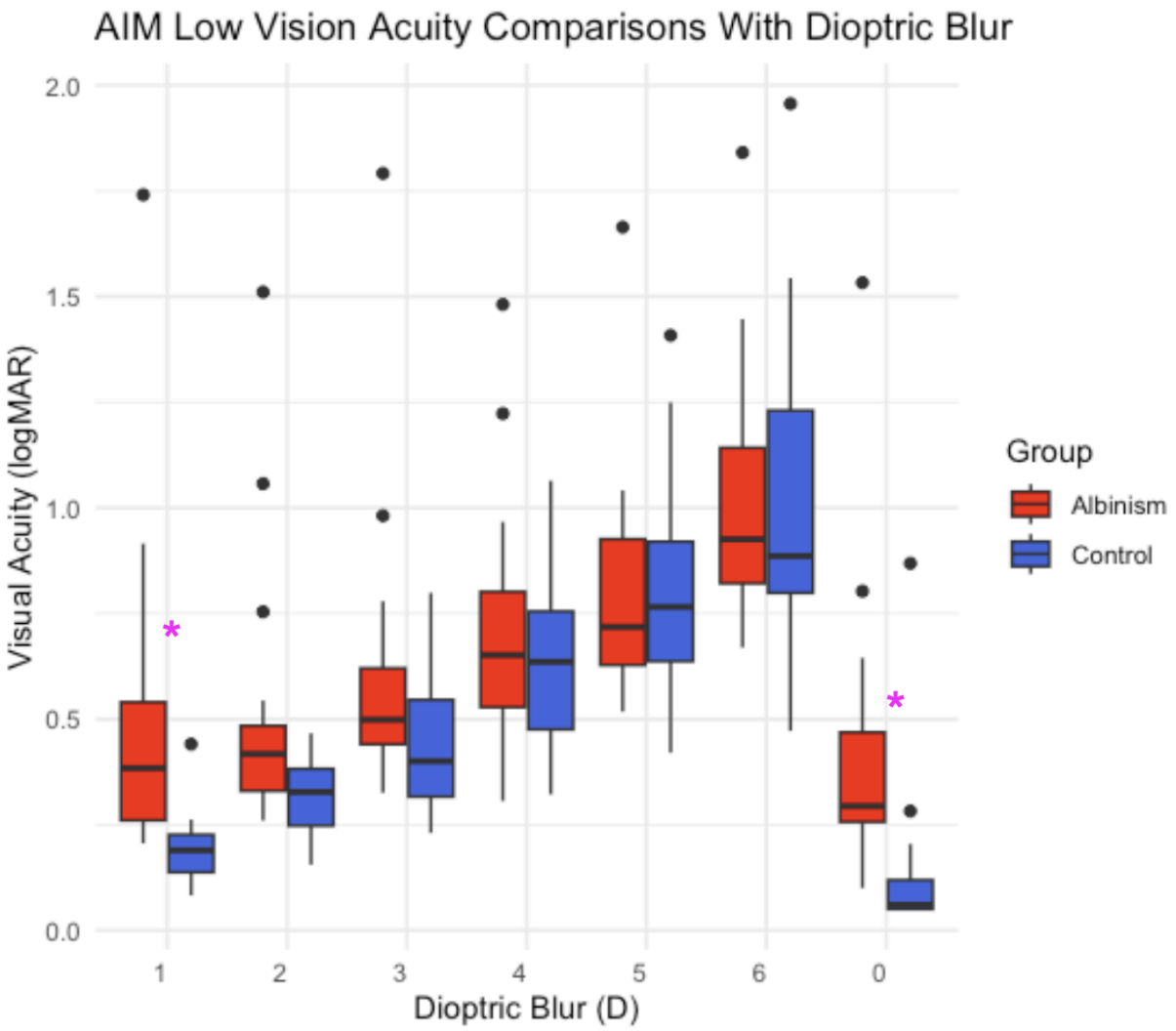

Figure 13. Boxplot of visual acuity at each level of dioptric blur for controls (blue) and PwA (red). The best correction is denoted as 0 diopters of blur. The "*" represents significantly different performance bet groups with best correction(p= 0.0314) and 1 diopter of blur (p=0.0247). Performance with 2 diopters (p=0.6324), 3 diopters (p=0.7330), 4 diopters (p=1.0), 5 diopters (p= 1.0), and 6 diopters (p=1.0) were not significant.

Table 13. Linear mixed regression model results comparing acuity with best correction (BCVA) and dioptric blur. Denotation of "*" *are statistically significant* while "" are *clinically significant*, or >0.2logMAR difference.**

	Albinism Group		Control Group	
Dioptric Blur Comparison (D)	P-value (***α***= 0.05)	Estimated Deviation (logMAR)	P-value (***α***= 0.05)	Estimated Deviation (logMAR)
BCVA to 1D	0.9839	0.0530	0.9639	0.0622
BCVA to 2D	0.9203	0.0736	0.0487*	0.1953
BCVA to 3D	0.0891	0.1805	0.0001*	0.3112**
BCVA to 4D	0.0006*	0.2782**	<0.0001*	0.5075**
BCVA to 5D	<0.0001*	0.3779**	<0.0001*	0.6811**
BCVA to 6D	<0.0001*	0.5820**	<0.0001*	0.8863
1D to 2D	0.9999	0.0206	0.3971	0.1331
1D to 3D	0.4514	0.1275	0.0034*	0.2490**
1D to 4D	0.0120*	0.2252	<0.0001*	0.4453**
1D to 5D	<0.0001*	0.3249	<0.0001*	0.6189**
1D to 6D	<0.0001*	0.5291	<0.0001*	0.8241**
2D to 3D	0.6618	1.632	0.5703	0.1159
2D to 4D	0.0324*	0.2046	0.001*	0.3122**
2D to 5D	0.0001*	0.3043	<0.0001*	0.4858**
2D to 6D	<0.0001*	0.5084	<0.0001*	0.6909**
3D to 4D	0.7499	0.0977	0.0467	0.1963
3D to 5D	0.0445	0.1974	<0.0001*	-0.3699**
3D to 6D	<0.0001*	0.4015	<0.0001*	0.5751**
4D to 5D	0.7314	0.0997	0.1157	0.1736
4D to 6D	0.0001*	0.3038	<0.0001*	0.3788**
5D to 6D	0.0331*	0.2041	0.0316	0.2051**

3.3.4 Slope Comparison Analysis

A Wilcoxon Sign Rank test was applied to the slope of acuity performance between groups. Slope values were acquired by fitting each participant with a linear regression model to assess change in performance. The Wilcoxon Rank Sum test revealed a significant difference between groups (p= 0.0023)(Figure 14). Additionally, visual acuity as a function of the linear regression slope had weak correlation in both the controls (p=0.14) and PwA (p=0.38)(Figure 15).

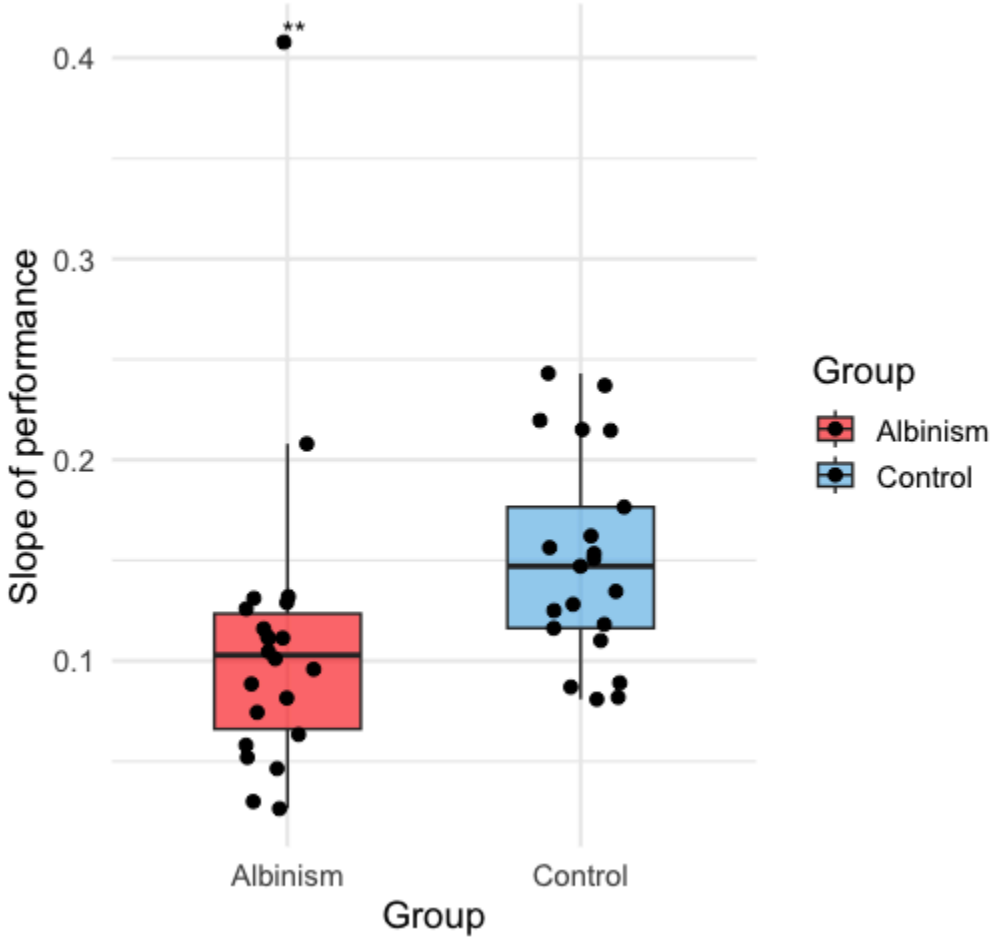

Figure 14. Linear regression slope comparison between the albinism group (red, mean= 0.1) and the control group (blue, mean= 0.16) (p= 0.0023). The slopes were extrapolated from the performance of each subject across 0 to plus 6 diopters of blur. A linear regression

model was fit according to the Low Vision AIM acuity measurement. A Wilcoxon Sum Test was used to compare the slopes between the albinism and control group to access discrepancies in performance with increased blur.

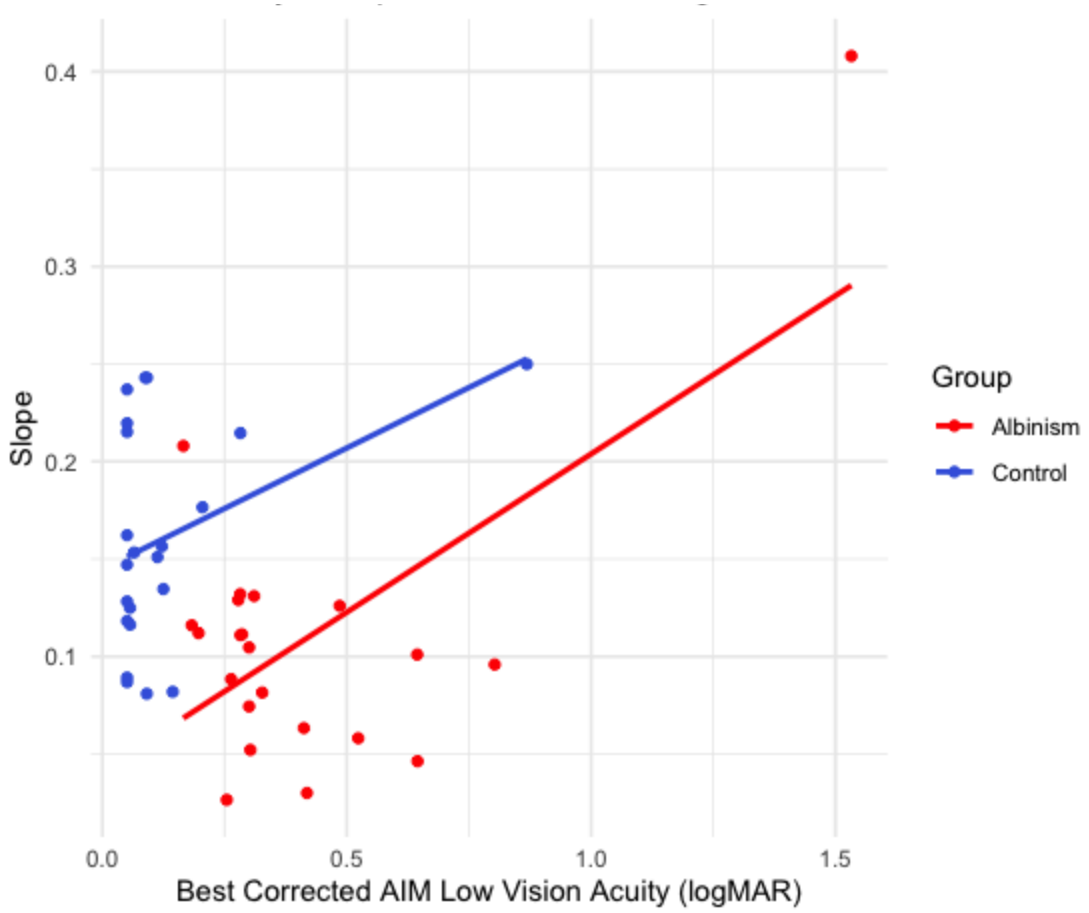

Figure 15. Comparison of visual acuity and individual linear regression slopes. Shallower slopes represent less sensitivity to blur. The Pearson R-squared for these plots are 0.14 for Controls (blue) and 0.38 for PwA (red) suggesting weak correlation.

3.3.5 Minimum Error Comparison

The minimum error report was extracted from each psychometric function of the participants at the various levels of blur. A Wilcox sign test revealed a significant difference in best corrected performance compared to maximum blur in the albinism group (p= 0.0001) and controls (p= 0.0001) (Table 14). A Wilcox sum rank comparison between groups was

significantly different with best corrected acuity ($p < 0.0001$) but not with maximum blur ($p = 0.5428$).

Table 14. Comparison of the minimum error report from the output psychometric slopes of best correction (BCVA) and dioptric blur (D) performance. Denotation of "*" are statistically significant.

	Albinism Group	Control Group
Dioptric Blur Comparison (D)	P-value (***α***= 0.05)	P-value (***α***= 0.05)
BCVA to 1D	0.9999	0.9996
BCVA to 2D	0.9976	0.1520
BCVA to 3D	0.2543	0.0003*
BCVA to 4D	0.0024*	<0.0001*
BCVA to 5D	<0.0001*	<0.0001*
BCVA to 6D	<0.0001*	<0.0001*
1D to 2D	1.0	0.7461
1D to 3D	0.7984	0.0129*
1D to 4D	0.0428*	<0.0001*
1D to 5D	0.0001*	<0.0001*
1D to 6D	<0.0001*	<0.0001*
2D to 3D	0.9361	0.8878
2D to 4D	0.1058	0.0003
2D to 5D	0.0005*	<0.0001*
2D to 6D	<0.0001*	<0.0001*
3D to 4D	0.9682	0.1464
3D to 5D	0.1405	<0.0001*
3D to 6D	<0.0001*	<0.0001*
4D to 5D	0.9625	0.3146
4D to 6D	0.0005*	<0.0001*
5D to 6D	0.1079	0.1035

3.3.6 Psychometric Function Slope Comparison

An applied Wilcox signed rank test to compare the slope of the psychometric functions with best corrected AIM to maximum dioptric blur (6 diopters) performance. The albinism group revealed a borderline significant difference between conditions ($p=0.045$). Similar analysis in the control group was also significant ($p<0.000$) (Table 15). A Wilcox sum rank test showed a significant difference in slope performance with best correction ($p=0.007$); however, slopes with 6 diopters of blur were not statistically different ($p=0.839$).

Table 15. Comparison of the slope from the output psychometric slopes of best correction (BCVA) and dioptric blur (D) performance. Denotation of "*" are statistically significant

	Albinism Group	Control Group
Dioptric Blur Comparison (D)	P-value (***α***= 0.05)	P-value (***α***= 0.05)
BCVA to 1D	0.9999	0.9996
BCVA to 2D	0.9203	0.1520
BCVA to 3D	<0.0001*	0.0003
BCVA to 4D	0.0024*	<0.0001*
BCVA to 5D	<0.0001*	<0.0001*
BCVA to 6D	<0.0001*	<0.0001*
1D to 2D	1.0	0.7461
1D to 3D	0.7984	0.0129*
1D to 4D	0.0428*	<0.0001*
1D to 5D	0.0001	<0.0001*
1D to 6D	<0.0001*	<0.0001*
2D to 3D	0.9361	0.8878
2D to 4D	0.1058	0.0003*
2D to 5D	0.0005*	<0.0001*
2D to 6D	<0.0001*	<0.0001*
3D to 4D	0.9682	0.1464
3D to 5D	0.1405	<0.0001*
3D to 6D	<0.0001*	<0.0001*
4D to 5D	0.9625	0.3146
4D to 6D	0.0005*	<0.0001*
5D to 6D	0.1079	0.1035

3.4 Discussion

The findings of this study suggests increased blur tolerance demonstrated by significantly shallower changes in visual acuity to dioptric blur in PwA. The mean acuity for PwA included in the study was 0.73 logMAR, or approximately 20/100 Snellen acuity. By convention these individuals would be presented with +/- 0.5 diopters, or a JND of 1 diopter. However, PwA shallow change of acuity with dioptric blur, or slope, suggest larger defocus is needed achieve previously published visual acuity expectations (eg. Egger's or JND rule) (Legge et al, 1989; Decarlo & Woo, 2006).

Low vision refractions rely heavily on acuity as a starting point for refraction (Legge et al, 1989). The application of the Just Noticeable Difference (JND) suggests patients need a larger dioptric difference in lens presentation as logMAR acuity increases (Legge et al, 1989; Decarlo & Woo, 2006). All of the PwA in this study were refracted according to this practice. However, low vision refraction procedures are generalized for all reduced acuity patients. The results of this study questions this standard appliance. The slope analysis comparison between the groups is the main factor that calls this into question. The PwA had a significant shallower slope in performance across blur levels. This means the change in performance from best corrected visual acuity to +6 diopters of defocus yielded a much smaller change in acuity. The results suggest PwA have a higher tolerance for blur compared to other individuals with reduced acuity. Thus, presentations of lenses of higher dioptric differences deviating from standard practice may be indicated.

The contribution of foveal hypoplasia and chiasmal misrouting to blur tolerance in albinism is unknown. Perhaps, there are implications for refractive methodology in PwA compared to other

low vision patients. Particularly when comparing albinism to acquired macular diseases (i.e., Age Related Macular Degeneration), the etiology of central vision loss is fundamentally different (Holz et al., 2016). Foveal hypoplasia has been significantly correlated with visual acuity (Talsma et al., 2023). Another factor to consider is nystagmus. All of the participants in this study had nystagmus, either horizontal or pendular, with moderate to high amplitude and frequency. Additionally, although it is not well studied, misrouting of fibers at the optic chiasm may influence image processing.

3.5 Limitations

The parameters of the AIM algorithm restrict acuity measurements to 4.0logMAR. Although none of the participants exceeded this acuity with best correction, one participant had an entering acuity of 1.48logMAR. Prior to assessing AIM performance, we confirmed the patient was able to see a 2.4logMAR ETDRS letter. AIM acuity for this patient did not exceed 4.0logMAR, however these parameters limited exploration of other participants with severely reduced acuity.

CHAPTER 3: EXPLORATION OF FACE DISCRIMINATION USING FORAGING INDICATION D'PRIME ALGORITHM

3. 1 Introduction

Face perception is a fundamental component of daily human interaction (Dalmaso et al, 2025; Klauke et al, 2023; Avery et al, 2016). Face perception includes both identity recognition and perception of emotion. Face discrimination is a component of face perception that allows us to differentiate identities (Avery et al, 2016; Barton et al, 2021). Most importantly, face perception provides a better understanding of social implications resulting from deficits in the visual system (Klauke et al, 2023). As the neural processing of face perception is extensive and the knowledge surrounding it is ever evolving (Dalrymple et al, 2011; Duchaine et al, 2006; De Renzi et al, 1991), proper analysis of this system is needed.

Face discrimination is especially important for patients with congenital or progressive vision loss. Although face discrimination capabilities have been documented to change with age (Barnes et al, 2011) they are also associated with young low vision patients (Klauke et al, 2023). Deficits in face discrimination have already been well documented in low vision patients, specifically Age Related Macular Degeneration (AMD) and glaucoma (Barnes et al, 2011; Venugopal et al); however, emerging data for Retinitis Pigmentosa (RP) has yielded similar conclusions (Klauke et al, 2023). There is a strong correlation between visual acuity (and contrast sensitivity to a lesser degree) with face discrimination performance. Tejeria et al. found there was a moderate correlation between distance visual acuity and face recognition in AMD ($r= -0.69$). Contrast sensitivity, however, did not have a strong correlation ($r= +0.37$) (Tejeria et al., 2002). Similarly, Logan et al, found patients with dry and wet AMD patients discriminated faces 1.76 and 1.73 times poorer, respectively, compared to normally sighted controls (Logan et al.,

2020). Previous studies have outlined difficulties with low spatial frequency face aspects (Peli E et al, 1994) and struggles in low luminance environments (Venugopal et al, 2023; Bullimore et al, 1991). Both of these issues may be related to reductions in contrast sensitivity (Kiser AK et al, 2005; Xiong YZ et al, 2020).

When assessing face discrimination clinically in low vision patients, however, we often leave these visual-social behaviors under-addressed (Wang et al, 2008). Previous psychosocial studies have shown that deficits in these areas can cause individuals with visual impairments to withdraw from others or mask their struggles (Wang et al, 2008; Lane et al, 2008). This is especially true for children with low vision as they present a higher risk of anxiety and depression (Klauke et al, 2023; Bakhla et al, 2023). The deficits can be detrimental to an individual's quality of life (Wang et al, 2008; Lane et al, 2008; Klauke et al, 2023). As Bullimore and colleagues highlight, patients do not normally report reduced contrast sensitivity or acuity. Their complaints may manifest as impairments of everyday visual activities such as face viewing (Bullimore et al, 1991). Therefore, there is a need for a clinical application for face discrimination, resulting in better vision rehabilitation practices to accommodate daily visual tasks.

Traditionally, behavioral assessments such as the Benton Facial Recognition Test (BFRT) (Benton & Van Allen, 1968), Cambridge Face Memory Test (CFMT), and Glasgow Face Matching Test (GFMT) have been used to distinguish patients with face perception deficits (Duchaine & Nakayama 2006) (Table 18). They have been used in patients on the Autism spectrum, specifically with Asperger's Syndrome, and those with prosopagnosia (Duchaine et al, 2006). Many face discrimination tests have been critiqued for their superficial cues, such as hair, race, and gender components (Duchaine et al, 2006). This emphasizes the difference between holistic

face processing and perception of specific facial features (i.e., the mouth, nose, eyebrows, etc.) (Duchaine et al, 2006). The holistic approach to testing face processing has been established as the best way to identify face discrimination deficits (DeGutis et al, 2013; Taubert et al, 2011). This approach details first order perception as recognizing a face compared to an object; then second order processing differentiates features. While the BFRT and GFMT best captures this principle, the reliability of results using limited face stimuli requires further evaluation. Finally, all of these tests face challenges in how accurately their stimuli replicate the reliability of faces encountered in everyday life. Faces are observed at several different angles with variable lighting. None of these methods have yet perfected a viable way to include this in their stimuli.

Table 16. Description of most common face discrimination tests and their repeatability correlation analysis.

Test Name	Task Description	Correlation values (repeatability value, study size)	Possible pitfalls
BFRT	**Feature Matching:** Participants are to match face stimuli to one of six comparative faces (Benton AL & Van Allen MW, 1968; Miranda de Vasconcelos et al, 2026). In the original format there are 22 available stimuli (Lanca M, 2003). The test faces vary in position and lighting to discriminate features (Benton AL & Van Allen MW, 1968; Duchaine BC et al, 2006).	r=0.735, n=78 (Murray E, et al, 2022) Normal participants are expected to achieve approximately 76% accuracy (Rossion B & Michel C, 2018).	Repeatability of this test has been questioned as those with identified prosopagnosia have reported normal results (Miranda de Vasconcelos et al, 2026; Duchaine BC et al, 2006). This lapse in definitive results has been attributed to compensatory methods of those with prosopagnosia (Murray E, et al, 2022; Miranda de Vasconcelos et al, 2026; Rossion B & Michel C, 2018).
GRMT	**Identity Discrimination:** Participants are presented with 40 unfamiliar face pairs from which they are to select faces of the same identity (Burton AM, et al, 2010).	r= 0.81, n=300 Normal participants have been expected to have approximately 89% accuracy (62-100%) (Burton AM, et al, 2010)	Face stimuli are usually face fronting only, thus limiting variability (Burton AM, et al, 2010) Ceiling effect in normals reduces the appearance of variability in normals (Fysh MC, 2018)
CFMT	**Memory based recognition:** Participants are tasked with selecting a previously displayed face stimuli from a group of six stimuli (Duchaine BC et al, 2006)	r= 0.69, n=31 (Duchaine BC et al, 2006)	The combined effort of face memory and face perception may confound the results. Poor performance may be due to not remembering a face opposed to differentiating it among a group. Similar lighting with matched face pictures can be an external cue (Wilmer et al, 2010).

The Foraging Interactive D' Prime (FInD) Face model is a computer-based, generalizable, and self-administered vision test used to assess face discrimination (Bex and Skwerswetat 2021; Walter and Bex, 2025; Walter et al, 2025). FInD has been used in other visual assessments (i.e., contrast sensitivity, color vision, and motion detection), but the model has not been formally validated for face discrimination (Neupane et al 2024; Bex and Skwerswetat 2021). This new model is able to distinguish 199 parameters of texture and shape of face stimuli according to the Basel Face model (Gerig et al, 2018). The Basel Face Model provides a vast amount of facial parameter combinations and reduces lighting or gender cues. It may expose systematic differences in face perception and allow us to better understand compensatory methods. The FInD paradigm seeks to establish a new method of face discrimination testing that is not limited to forced-choice methods and provides insight into specific differences in face space.

The aim of this study was to present an alternative form of face discrimination analysis. The FInD Faces model offers quantitative analysis of face discrimination that is self administered. This chapter explores the reliability and specifically, test-retest repeatability of the FInD Faces paradigm.

3.2 Methods

3.2.1 Participant Recruitment

Twenty students enrolled at Northeastern University aged 18-24 were recruited from February to September 2024. All participants consented through the university's Institutional Review Board (IRB). Pertinent ocular and medical history were obtained through a survey prior

to testing. Inclusion criteria required normal binocular status and no history of ocular disease. Two of the participants were excluded in data analysis due to admitted fatigue and loss of attention to the program. ETDRS visual acuity was reported and a refraction was performed by a proficient optometry student (author OW). Binocularity was confirmed with cover test and stereoacuity.

3.2.2 Visual Stimulus: Set Up

A 32-inch 60 Hz LG HD 4K monitor system was used. Testing was conducted 66 cm from the display screen. The FInD algorithm was configured in Matlab (MathWorks, R2021a) using the Psychophysics Toolbox (Pelli et al, 1997; Brainard et al, 1997). The order of testing was randomized through the Center for Biostatistics at the Icahn School of Medicine at Mount Sinai's Robust Randomization app and the excel "random array" function.

3.2.3 Foraging Indication D'Prime Paradigm

This study utilized the FInD paradigm in conjunction with the Basel Face Model (Walter K et al, 2025). Previously used in this patient population, the FInD algorithm uses an adaptive threshold method similar to the AIM algorithm (Neupane S et al, 2022). Other versions of the algorithm were used to assess contrast sensitivity, motion perception, and color vision. This version of the FInD paradigm incorporates the Basel Face Model, which originates from photographs of human faces generated as digital images that are easily manipulated (Walker et al, 2018; Gerig et al, 2018). Generated faces are composed of 199 structure and texture parameters in the face space (Walter et al, 2025). Each digital face presentation subtends 4.9

degrees to coincide with face sizes that are typical for social interactions. Thresholds are determined based on the D' prime formulate calculated for each presented chart. Probability of reselecting a specified euclidean difference in faces is determined and influences the stepwise method of future charts. The objective of the FInD algorithm is to have fewer stimuli at high suprathreshold deviations in favor of more analysis around the threshold.

In this version of the test, participants were instructed to identify computerized face pairs that were perceived as "different people." Face pairs are presented for 70 trials, subtending 4.9 degrees to coincide with face sizes that are typical for social interactions. Participants completed the program twice and performance was analyzed with a Bland Altman.

Again, the FInD Face paradigm adapted to selections made in the previous charts influences future charts to increase in subjective homogeneity closer to threshold. For example, *Figure 16* shows two vastly different faces. Ideally, participants would select this face pair as an extreme. A probability of reselection is calculated per the D'prime equation for each selected face pair. A psychometric function was fitted with the euclidean difference of face pairs and their D'prime probability (Figure 2) (Walter K et al, 2025). The threshold was defined as the midpoint of the psychometric function. Additionally, slope and false alarm rates were reported.

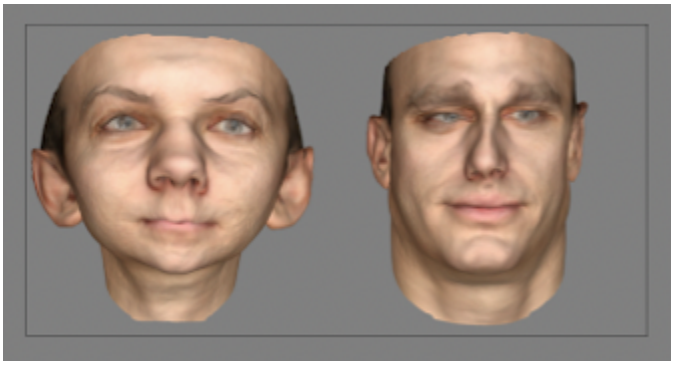

Figure 16. Example of face pair selection. This would be a correct response such that it would be plotted on a psychometric function based on the euclidean difference in face space between presentations.

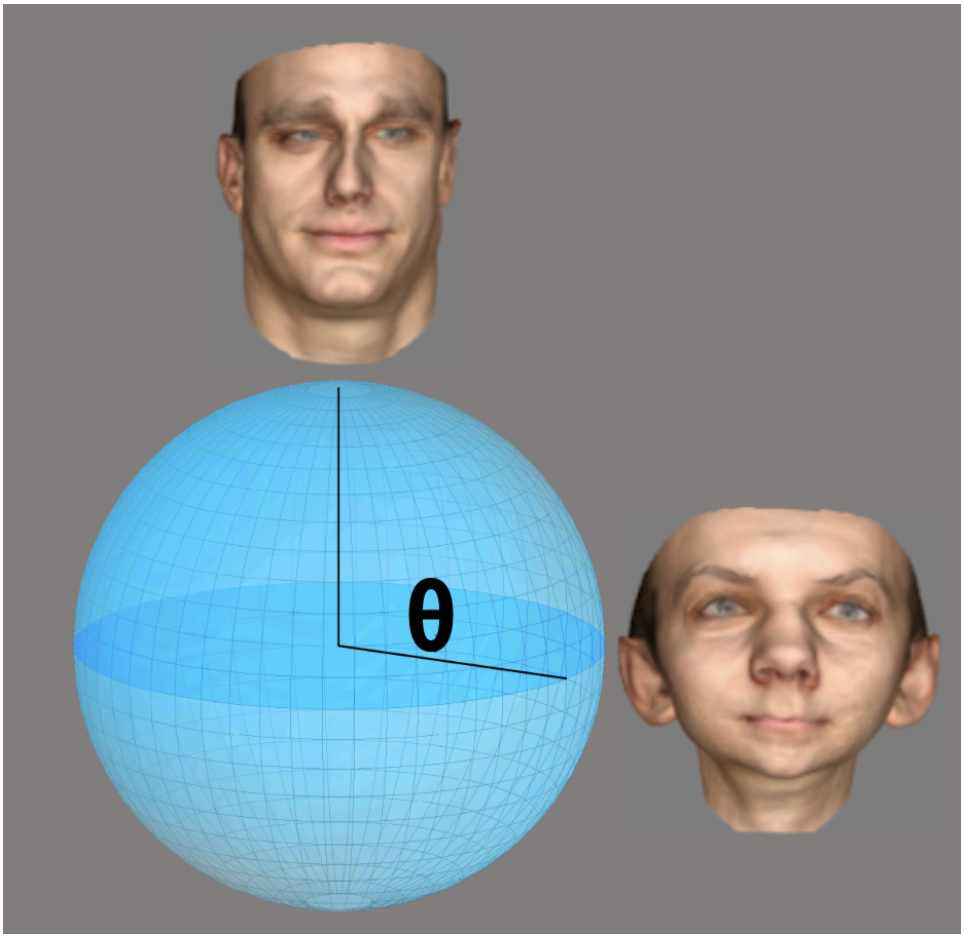

Figure 17. Schematic illustration of different presentations in face space. The two faces demonstrated are variations of one centroid face with manipulations of texture and shape. The threshold difference between the faces are determined by the cosine angle, or euclidean, separation within face space.

3.3 Results

A two tailed t-test was performed prior to the Bland Altman revealing no statistical difference in performance (p= 0.5566) (Figure 18). A Shapiro-Wilk Test confirmed normal distribution of the data. A Bland Altman analysis revealed limited bias (-0.0569) and narrow limits of agreement (-0.621 to 0.734). The coefficient of variation was acceptable at 46%. Testing took an average of an average of 167 seconds, or approximately 2.5 minutes. A Bland Altman of test and retest times yielded bias of 64.49 and limits of agreement were wide (-48.62 to 177.59) (Figure 19).

Table 17. Demographics of control study participants

Demographics	Participants
Age (mean)	20.0 ± 3.3
ETDRS Visual Acuity (logMAR)	-0.22 ± 0.08
Randot 3 Stereoacuity (Arcseconds)	78.78 ± 11.78
Sex, n=48 (%)	
Male	17 (35.4)
Female	31 (64.6)

Table 18. Race and ethnicity demographics for control participants

	Race/ethnicity, n (%)
White	22 (45.8)
Black or African American	6 (12.5)
Asian	14 (29.2)
Hispanic or Latino	7 (14.6)
More than one race	5 (10.4)
Prefer not to say	1 (2.1)

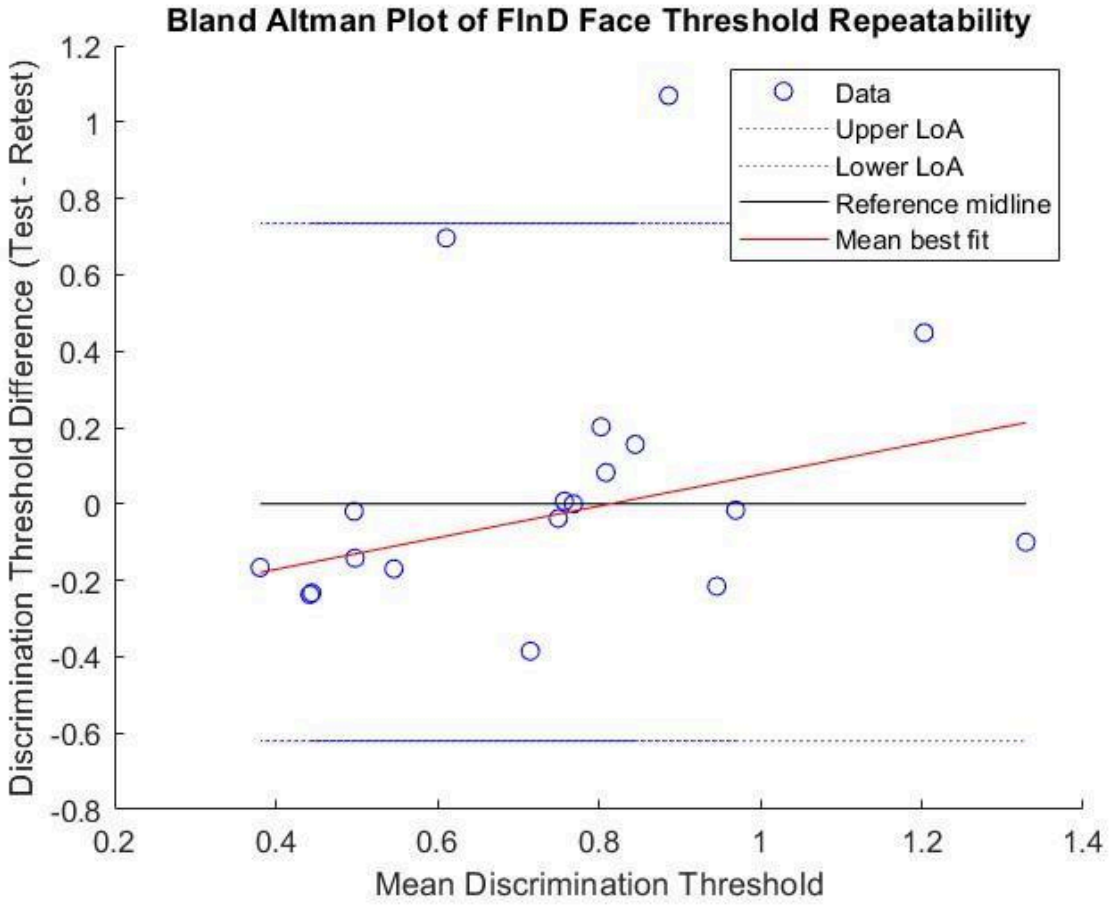

Figure 18. Bland Altman analysis for upright presenting faces in the FInD Faces paradigm. This plot demonstrates the mean euclidean difference threshold function of the threshold difference between test and retest runs. The limits of agreement were defined as -0.621 to 0.734 degrees with a coefficient of variation (COV) of 46%. Bias was limited at 6%.

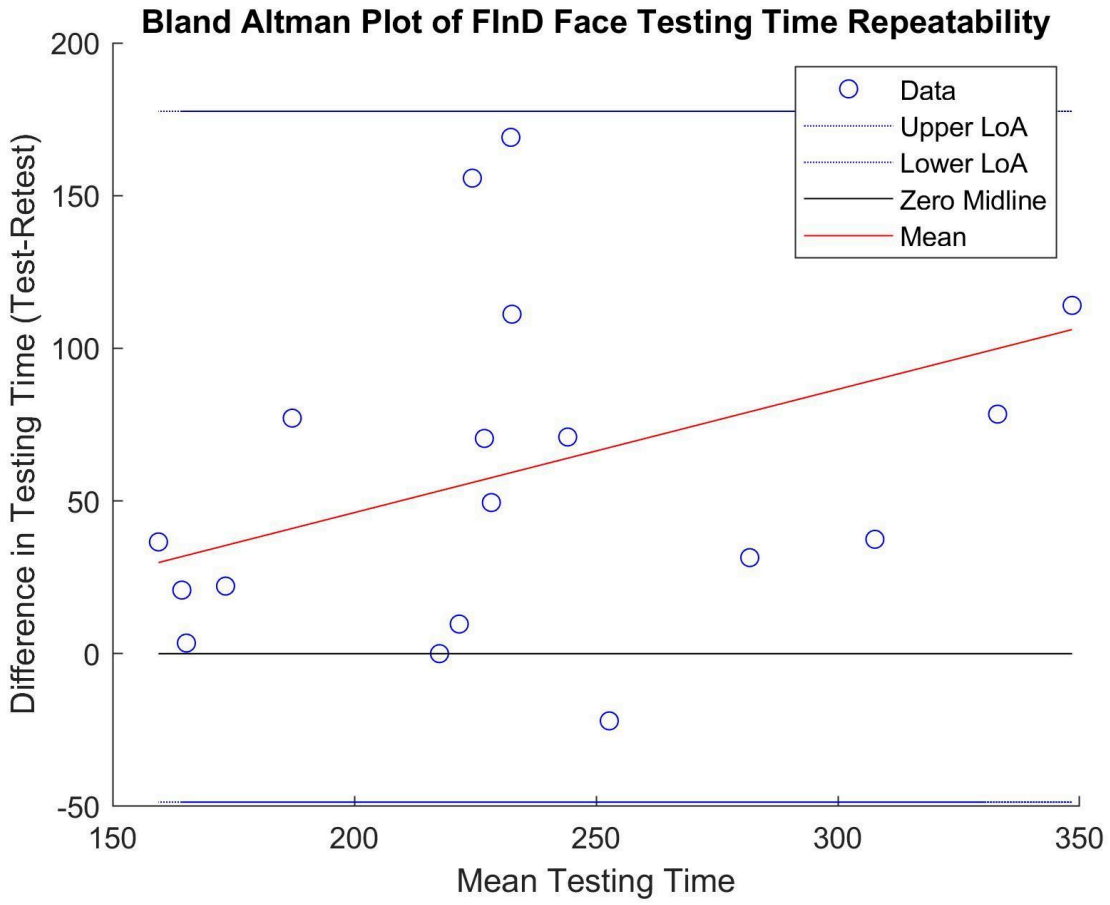

Figure 19. Bland Altman plot of FInD Face testing time. This plot demonstrates the mean testing time and difference between test and retest runs. The limits of agreement were defined as -48.62 to 177.59s with a coefficient of variation (COV) of 24%. Bias was limited at 64%.

3.4 Discussion & Conclusion

The FInD Face method provides a repeatable assessment of face discrimination while using easily manipulated face stimuli. The Bland Altman analysis suggested some variability in performance amongst patients. This reflects positively on the FInD Face model, as previous face discrimination methods have struggled with ceiling effects in individuals with normal discrimination. In fact, the variability seen in the data could be due to biases toward certain

features. For example, harsher eyebrows may be associated with masculine features. However, the Basel Face Model attempts to control for face bias by eliminating variations in race and removing hair to eliminate gender cues. Regardless, bias may be unavoidable due to cultural experiences. Anecdotally, some control participants and later PwA remarked certain faces were easier to distinguish than others due to specified features. Otherwise, the limits of agreement remain narrow suggesting this variation is minimal within the 3D face space. Additionally, the bias between test and retest is limited with no apparent learning bias.

Opposed to previously outlined methods, the stimuli used here are not bound by limited photographs with variable quality. The integration of the Basal Face Model (Walker M et al, 2018) allows original centroid faces to be minutely manipulated in 199 parameters of texture and shape that can not otherwise be achieved with real photographs. The advantage of such ability is that specific features of face discrimination can be tested. For example, sensitivity to changes of the lips, eyebrows, or nose can be isolated and correlated with holistic processing of faces. Therefore, we may better understand what features influence compensatory methods of individuals with decreased face discrimination. The version presented in this paper provides a simplified output for general face thresholds, but data from all face parameters can be extrapolated (Walter K et al, 2025).

Overall, face discrimination in low vision patients remains important when assessing daily functional vision. The implications of deficits in this area can significantly affect quality of life. Therefore, the implementation of tools like FInD Faces will allow clinicians to precisely measure face discrimination.This can be performed remotely, as the algorithm is self-administered and efficient, requiring minimal testing time.

CHAPTER 4: EXPLORATION OF FACE DISCRIMINATION IN ALBINISM

4.1 Introduction

Face perception is a pivotal part of daily human social interaction (Dalmaso M et al, 2025; Klauke S et al, 2023; Avery SN et al, 2016; Barton JJS et al, 2021). Subtle impairments in face processing can markedly affect an individual's quality of life or mental health (Wang SW et al, 2008; Lane J et al, 2008; Klauke S et al, 2023). Previous evaluations of early cognition have established structural development of face discrimination in the occipital temporal lobe (Bruce & Young, 1986; Dalrymple KA, et al , 2012). This was further established in magnetic resonance imaging (MRI) studies, detailing both the occipital temporal and fusiform face areas (Logan AJ, et al, 2022; Grill-Spector K, 2017). The importance of studying face perception, provides insight into the visual processing of one's environment. The evaluation of face perception in low vision patients has been established as important for holistic approaches to care (Dalmaso M et al, 2025; Lane et al, 2018). However, our understanding of face perception in different subgroups – specifically albinism – of low vision is not well understood (Logan et al, 2020; Tejeria et al, 2002).

In addition to our normally accustomed upright face discrimination, there is the face inversion effect (FIE), which is a naturally occurring disruption of face processing. From infancy, humans are familiarized with faces in an upright position. The effect describes the transition of face recognition from an upright to an inverted face (Tian F, et al, 2022). The visual discrimination is not only related to the integration of noted visual features, but also the organization of the face (Tian F, et al, 2022). For example, a typical facial structure will have the eyes above the nose and

mouth. The face inversion effect suggests disruption of this typical face structure impairs face discrimination (Tian F, et al, 2022 & Gerlach C, et al, 2023). Faces are then processed more similarly to objects outside of the face fusiform area (Tian F, et al, 2022 & Gerlach C, et al, 2023). This effect decreases face discrimination by 15-18% (Gerlach C, et al, 2023). Inversion of objects yield similar results on a lesser scale (Gerlach C, et al, 2023). The current understanding of low vision in face and emotion discrimination is there is a deficit in performance amongst patients with central and peripheral vision loss (Venugopaul D, et al, 2023). However, such research has not been explored in PwA exclusively.

In albinism, structural abnormalities of the ocular structures, along with misrouted retinal fibers at the optic chiasm, interfere with normal visual processing and contribute to poor vision This poses concern for reduced input of visual stimuli and irregular processing of this information. Nystagmus contributes to instability of a targeted stimulus causing a reduction in image quality (Federico et al., 2023, Gurnani et al., 2025; Abadi, 2002; Talsma et al., 2023). Foveal hypoplasia may alter proper low level processing of image detail due to absence of properly differentiated cones (Proudlock, 2024; Summers, 1996; Talsma, et al, 2023). Both high prevalence of hyperopic or astigmatism refractive error and foveal hypoplasia may occur with strabismic (Dobhal et al., 2025; Proudlock et al., 2024) or amblyopic tendencies (Kessel et al., 2023; Thomas et al., 2023). Finally, the irregular misrouting of fibers (Hoffmann et al., 2005; Guillery et al., 1975) could comprise neural mapping to the visual cortex and subsequent temporal lobe (Neveu, et al, 2009; Hupfeld et al, 2006). Although this area of albinism pathology is not well understood, this retinofugal disorganization could impair the higher order visual processing. However, previous evaluations of mid level functional vision found there was no

degradation of processing in PwA (Skerswetat et al, 2023). Therefore suggesting possible compensatory mechanisms.

This study aims to clarify if higher-order face processing remains intact in Persons with Albinism (PwA). Again, despite well documented impaired low level processing (i.e., visual acuity and contrast sensitivity), mid level processing of motion remains intact (Skerswetat et al, 2023). Therefore, we postulated that there may be compensatory mechanisms in place within albinism to assist processing in PwA (Figure 20).

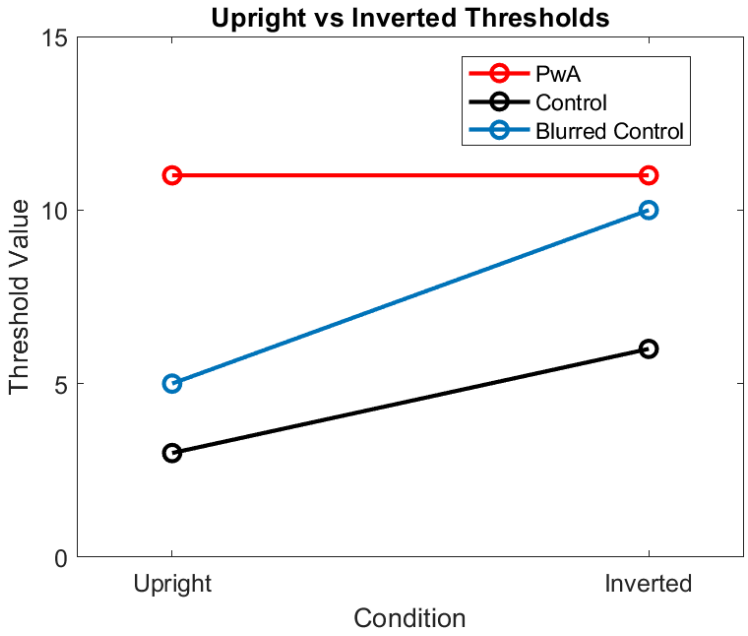

Figure 20. Diagram of study hypothesis, comparison in upright and inverted performance of PwA, controls, and blurred controls. We hypothesized face discrimination would deteriorate from upright to inverted presentations in controls (black line) and blurred controls (blue line). Here thresholds are depicted as lower with best corrected controls to blurred controls to illustrate the influence of visual acuity. In PwA (red line), FIE was hypothesized to also deteriorate.

4.2 Methods

Twenty PwA recruited from the Janet L. LaBreck Center for Low Vision Rehabilitation at the NECO Center for Eye Care were age- and sex-matched with normally sighted control subjects. Included PwA presented with no ocular pathology other than albinism; whereas, controls had no ocular pathology and were correctable to (20/20) 0.0 logMAR. Adequate cognitive status was confirmed with a Mini Mental State Examination after consent was obtained. All participants underwent preliminary testing for which Lighthouse near acuity, distance ETDRS acuity, MNRead, loose lens refraction, cover testing, and Worth-4-dot were recorded.

Both groups completed testing with best correction according to the aforementioned loose lens refraction. The control participants completed testing a second time with plus dioptric blur to match their acuity to that of their matched PwA. The amount of required dioptric blur was determined based on blur tolerance testing from a separate experiment. Acuity was confirmed to be within +/- 0.1logMAR of their matched PwA.

4.2.1 Foraging Interactive D'Prime (FInD) Faces Paradigm

The Foraging Interactive D'Prime (FInD) Faces algorithm was used with integration of the Basel Face Model (Walter & Bex, 2025; Walker et al, 2018). Each face stimuli was composed of 199 shape and texture components manipulated by previous responses (Walter & Bex, 2025). Participants were instructed to select faces that presented as "different people" (Figure 21). Face discrimination thresholds were obtained based on the angular (cosine) difference in face space between texture and shape parameters (Figure 22). FInD Faces was deployed twice for each group, altering face presentation from upright to inverted (Figure 23) in

order to assess integrity of the FIE. Analysis of performance between PwA, controls, and blurred controls was conducted in a Two-Way ANOVA.

Figure 21. Example of Foraging Interactive D'Prime (FInD) Faces chart presentation. Participants were to select face pairs that were different faces, or people. The face pair circled in green (top right) would be considered a correct response; whereas the pair circled in red (top left) would be an incorrect response.

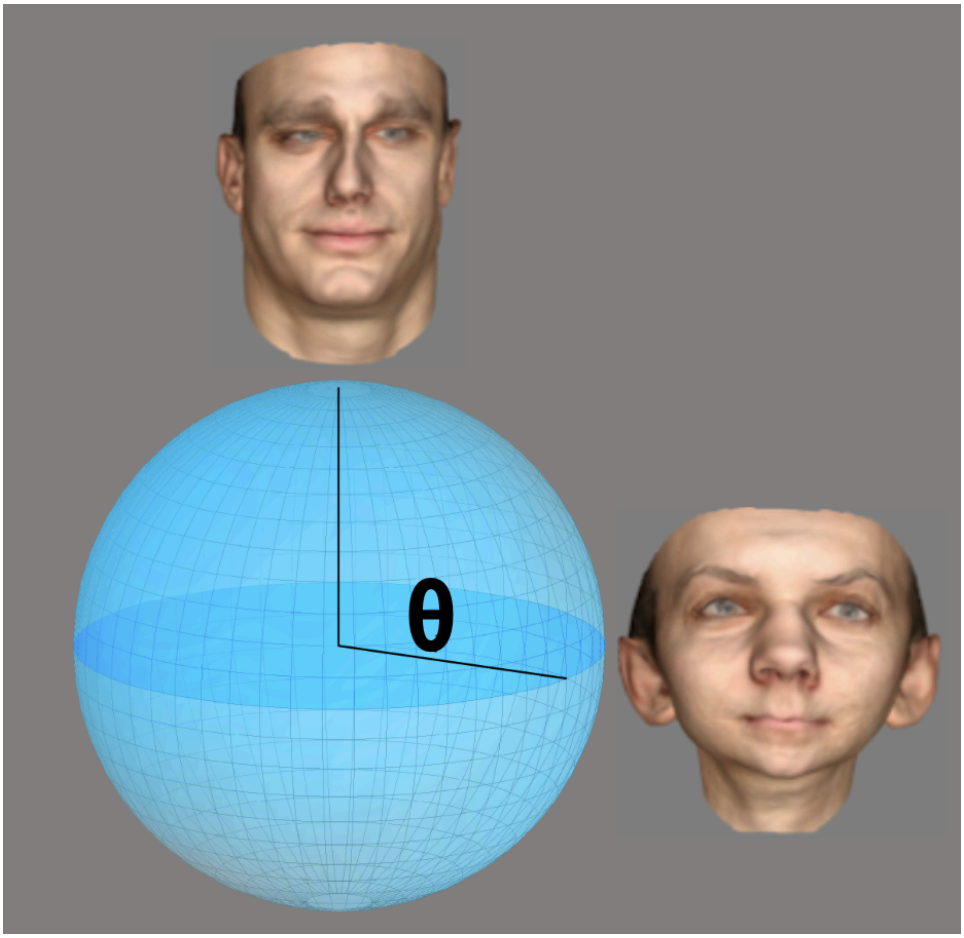

Figure 22. Schematic illustration of different presentations in face space. The two faces demonstrated are variations of one centroid face with manipulations of texture and shape. The threshold difference between the faces are determined by the cosine angle, or euclidean, separation within face space.

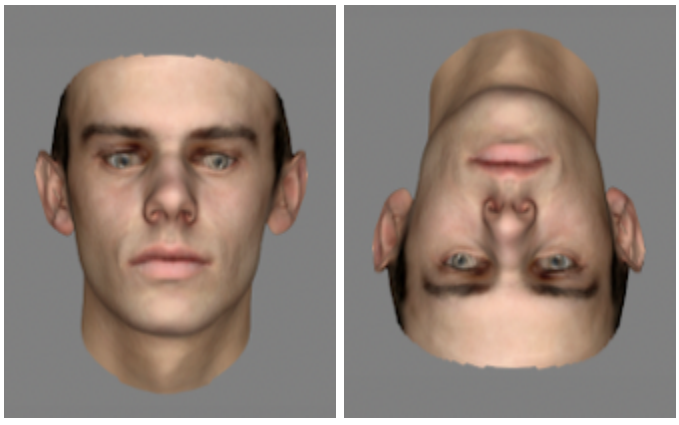

Figure 23. Example of face inversion effect (FIE).

4.3 Results

Table 19. Demographics of participants from the Albinism group and their age matched controls (+/- 5 years).

Demographics	Persons with Albinism (p=20)	Matched Controls
Age (mean)	40.9 (± 21.4)	34.7 (± 19.0)
Sex, n (%)		
Male	7 (35)	7 (35)
Female	13 (65)	13 (65)

Table 20. Comparison of entering clinical measures between the Albinism and Control groups.

	Albinism Group	Control Group	T-test Analysis
Distance ETDRS VA in the better eye (logMAR)	+0.73 (± 0.25)	-0.03 (± 0.15)	p< 0.0001
Near Lighthouse VA in the better eye (logMAR)	+0.62 (± 0.27)	-0.01 (± 0.18)	p<0.0001
Pelli Robson contrast sensitivity in the better eye (logCS)	1.4 (± 0.33)	1.7 (± 0.39)	p= 0.03
MNRead Critical print size (logMAR)	+0.70 (± 0.29)	+0.03 (± 0.18)	p<0.0001

4.3.1 Threshold Comparison Between Albinism and Control Group

A two-way ANOVA and post hoc comparisons were conducted for both upright and inverted threshold comparisons (upright in Figure 24 and inverted in Figure 25). There was no significant difference in performance with upright faces between PwA and controls (p= 0.44, F= 1.51). Between PwA and blurred controls were not significantly different (p= 0.28, F= 2.55). Finally, between controls and the blurred control performance, there was a significant difference

(p= 0.01, F= 6.1).

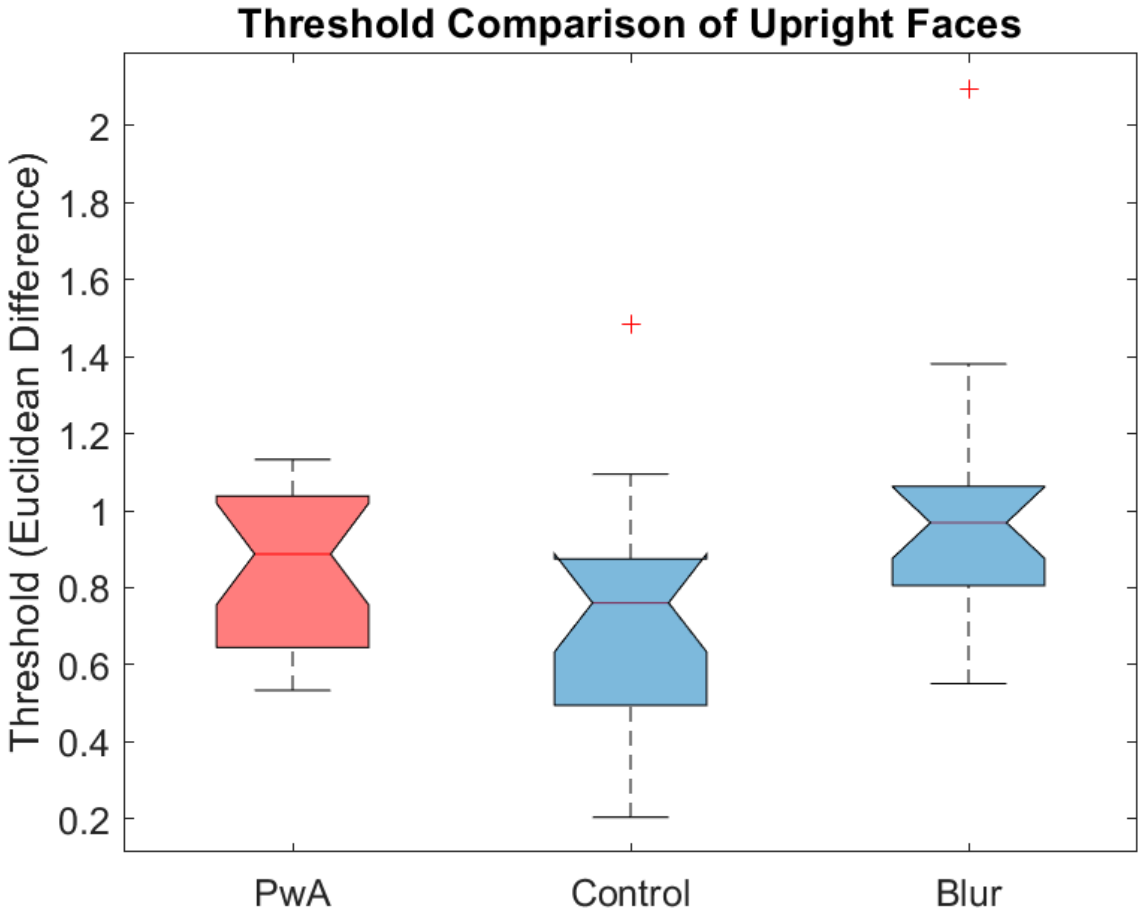

Figure 24. Two-ANOVA comparison of FInD Face thresholds with upright face presentation. The Albinism group was not significantly different from controls (p=0.76) nor the dioptrically blurred controls (p= 0.14). However, there was a difference in blurred or best correct performance in controls (p=0.01).

Similarly, PwA did not perform significantly differently from controls (p= 0.98, F=0.03) or blurred controls (p= 0.76, F= 2.7) with inverted face presentations (Figure 23). Neither did controls perform differently from their blurred counterparts (p= 0.75, F= 0.03). However, participant performance did decrease with inverted performance (ANOVA p= 0.02; p= 0.04 in PwA, p <0.001 in controls). Finally, upright performance in blurred controls did not significantly outperform inverted presentations.

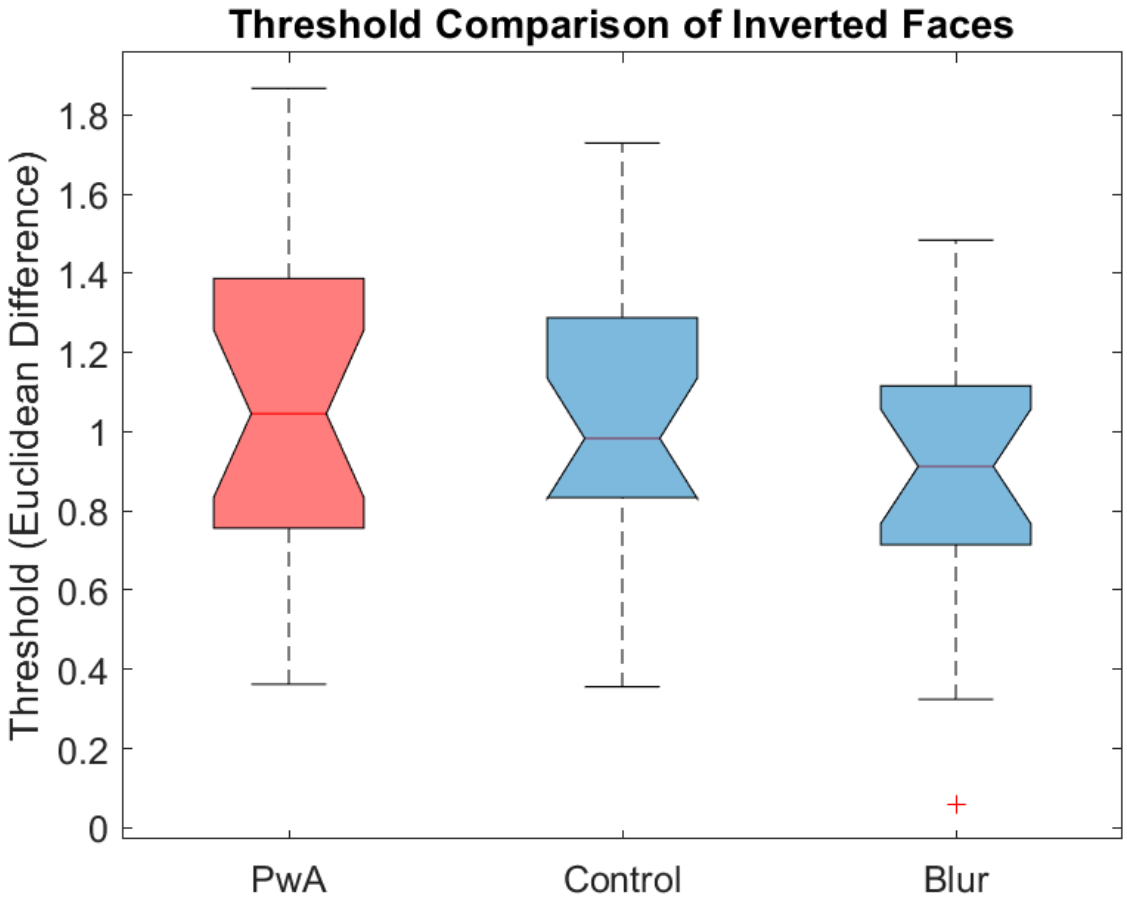

Figure 25. Two-ANOVA comparison of face threshold with inverted faces in FInD face. The Albinism group was not significantly different from controls (p=0.76) or dioptrically blurred controls (p= 0.75). There was also no difference in controls to their blurred counterparts (p= 0.18).

4.3.2 Influence of Dioptric Blur on Threshold Outcomes

A Pearson correlation test was conducted to evaluate the relationship between acuity and threshold performance. In both PwA ($R^2 < 0.001$) and controls ($R^2 < 0.001$) there was a weak correlation between acuity and performance.

3.4 Discussion & Conclusion

The results from this experiment suggest face perception, specifically face discrimination, is preserved in PwA. Face discrimination thresholds were similar in PwA and controls, albeit thresholds were slightly higher in PwA. Interestingly, the upright performance of blurred controls was significantly decreased compared to best correction, but this did not outperform PwA. These comparisons suggest the reduced acuity is not a limiting factor in face discrimination in PwA. Although PwA have slightly increased thresholds their performance is comparable to that of controls.

Face discrimination integrity was also maintained with the FIE. The proportional decrease in performance from upright to inverted presentations agrees with normal disruption in face processing (Tian F, et al, 2022). Opposed to the hypothesized performance, it appears there is comparable change in performance for PwA to controls. In fact, the FIE was not maintained in blurred controls instead citing a breakdown in normal processing. This could be due to compensatory strategies in PwA. Anectodotally, PwA participants confirmed they struggled with face discrimination and developed habits to overcome it. Opposed to acquired prosopagnosia and other low vision patients, PwA may have developed these strategies over the course of their entire lives. Perhaps, participants are relying more on the general shape and size of the faces used. In this study, participants expressed that changes toward the top of the face stimulus were easier to identify. The face stimulus was manipulated in 199 shape parameters., but only the median parameters were reported. Therefore, multiple three-dimensional aspects of the faces were evaluated, but results could have been influenced by particular regions (eg, changes to the forehead region and vertical/horizontal elongation of faces). Future studies can explore what features are most influential in PwA driving presumed compensatory strategies.

This study specifically controlled for the influence of acuity between the groups. Given the mean acuity of +0.73 log MAR in the PwA in the study, there was a presumed advantage of threshold performance in controls. General research in psychophysics alludes to general face perception being similar to that of object form discrimination. Again, the neural mapping and visual processing in the visual cortex and beyond has not been thoroughly investigated in albinism. Previous research from Skerswetat et al, presented preserved mid-level processing (Skerswetat et al, 2023), which remains consistent in these findings. Therefore, low level processing of visual acuity and contrast sensitivity are affected by Albinism pathology, but it does not provide an adequate prediction for face discrimination. This highlights the uniqueness of Albinism as, in general, low vision patients have reduced face discrimination. Thresholds for other vision groups can be evaluated with the FInD Faces paradigm in future studies. Previous studies have shown, face perception in AMD and advanced glaucoma patients has been significantly impacted, but PwA appear to be an anomaly in the low vision population (Venugopaul D, et al, 2023). It is unclear if this preservation of face discrimination is attributable to the congenital nature of pathology and time, opposed to acquired retinal conditions.

CHAPTER 5: A NOVEL METHOD FOR EMOTION DISCRIMINATION TESTING: GENETIC ALGORITHM

5.1 Introduction

Emotion recognition is a fundamental component of face perception and the human social experience (Lane et al, 2018; Khosdelazad et al, 2020). Emotion recognition and facial expressions convey a substantial amount of nonverbal communication (Khosdelazad et al, 2020). Adequate face processing, including emotion recognition, is in turn a significant component of quality of life (Wang SW et al, 2008; Lane J et al, 2008; Klauke S et al, 2023). This area has been thoroughly investigated in autism spectrum disorder and schizophrenia (Macnamara et al, 2022; Fraser et al, 2019). There is now a budding interest in examining emotion recognition deficits in low vision patients.

On a mechanical and neural level, emotion expression has been linked to subtle changes in facial structure caused by a social response (Martinez, 2017; Srinivasan et al, 2016; Neth & Martinez, 2009; Darwin, 1872) . Typically, in research, emotion expressions are separated into action units featuring major facial features such as the eyes, eyebrows, mouth, and nose (Martinez, 2017). The foundation of emotion recognition, however, is the visual input (Franca et al, 2023; Martinez, 2017; Raji et al, 2025). Emotion recognition is processed in the fusiform face region of the temporal sulcus as an extension of retinal projection (Srinivasan et al, 2016; Jehna et al, 2011). Facial expressions rely on the combination of high and low spatial frequency information forming fine-grained facial features (Tian et al, 2018).

Given the connection between emotion recognition and visual input, this is an important area of low vision rehabilitation. It has been generally established that low vision patients, Age-Related Macular Degeneration (AMD) being the large majority, have impaired face

perception (Bullimore & Bailey, 1991). Boucart and colleagues found AMD patients were unable to specify expressions but accurately grouped them happy, angry, or neutral (Boucart, 2008). Due to the central vision loss in many low vision patients, their ability to discern the high spatial frequency characteristics of face stimuli is dampened. Therefore, low spatial frequency (Johnson et al, 2017; Musel et al, 2011) characteristics are favored, losing minute face expression changes (Boucart, 2008). Often, face perception deficits in low vision patients are countered by compensatory strategies, but these methods are not well understood.

The recently proposed adaptive method, Foraging Interactive D'Prime (FInD) Genetic Algorithm, has incorporated dynamic generations of facial expressions (Cui et al, 2023). This paradigm uses the Basel Face Model (Walker M et al, 2018; Gerig T et al, 2018) detailing 199 texture and structure parameters within the face space that can be manipulated. The Genetic Algorithm method here used the signal detection theory (SDT) (Green & Swets, 1966) to evaluate hits, misses, and false alarms for expressions within face space (Valentine, 2016). This method maintains the canonical emotions (i.e., happiness, surprise, anger, sadness, disgust, and fear) (Ekman & Friesen, 1987). However, compared to conventional emotion recognition tasks, the algorithm is able to distinguish sensitivity in different manipulated features. Therefore, analysis is reported as continuous emotion discrimination data opposed to discrete forced-choice tasks. Common methods include the Ekman 60 Faces Test (Ekman & Friesen, 1976), Reading the Mind in the Eyes Test (RMET) (Baron Cohen et al, 2001), and the Penn Emotion Recognition Test (Silver et al, 2002). These methods require participants to label the emotion or categorize a face with one of the canonical expressions. Limitations include a ceiling effect in controls, limited evaluation of deficits, minimal stimulus changes to assess thresholds.

The Genetic Algorithm method in this study was designed to be a quantitative, self administered approach to emotion recognition. The aim of this study was to explore the repeatability of emotion discrimination thresholds, intensity, and emotion effect. Therefore, establishing a repeatable method that can be applied in clinical practice.

5.2 Methods

Thirteen participants from Northeastern University were recruited for a repeatability protocol. Participants were consented and testing was approved by the Northeastern Institutional Review Board (IRB). Demographics, relevant ocular and medical histories were recorded. Inclusion required participants to have vision correctable to 20/20 (0 logMAR). Adequate binocular vision status was confirmed through cover test, stereoacuity, and balanced monocular vision. Additionally, a loose lens refraction was conducted by a proficient optometry student (author OW) to ensure best correction.

Participants completed the genetic algorithm twice with best correction. Testing was performed simultaneously with other psychophysical testing. Testing orders were randomized through the Center for Biostatistics at the Icahn School of Medicine at Mount Sinai's Robust Randomization app and a subsequent excel "random array" configuration.

5.2.1 Visual Stimulus

A 32-inch 60 Hz LG HD 4K monitor system was used and psychophysical testing was conducted 66 cm from the display screen. The FInD algorithm was configured in Matlab (MathWorks, R2021a) using the Psychophysics Toolbox (Pelli et al, 1997; Brainard et al, 1997).

5.2.2 Genetic Algorithm (GA) Paradigm

This GA method incorporates the use of the Basel Face Model (Walker et al, 2018). This model details computerized face stimuli based on real photographs of 40 individuals in standard lighting and neural backgrounds. The faces were used to develop a database of both 2 and 3 dimensional stimuli with morphable features and 199 separate structure and texture components were manipulated along continuous vectors in the face space (Walker et al, 2018; Cui et al, 2023).

The adaptive configuration of each emotion had 6 generations of face presentations (Figures 26 & 27). Participants were required to select faces that displayed a previously announced emotion. The first chart of faces for each emotion presents 12 faces composed of randomized facial parameters. In subsequent generations, parameters – or gene –, are kept and combined with other randomized parameters (Figure 27). Converging on the participants' threshold, the median of all selected parameters are taken to form a final emotional expression. The cosine distance of the final generation face was compared to that of the groups' median parameters (Figure 27). Emotion effect was determined based on systematic comparison of cosine distances between specified emotions (Cui et al, 2023). Finally, participants were required to rate the intensity of emotion in each of the final faces.

Amongst the canonical expressions, anger, sadness, happiness, and amusement were assessed as a balance between positive and negative emotions. The genetic algorithm has the ability to test for all the canonical expressions, however the assessment was condensed keeping visual fatigue in mind. Therefore, in total there were 24 trials (6 generation x 4 emotions) displaying 288 face

stimuli (Cui et al, 2023). The cosine distance from the group medians for each emotion were analyzed in a Bland Altman.

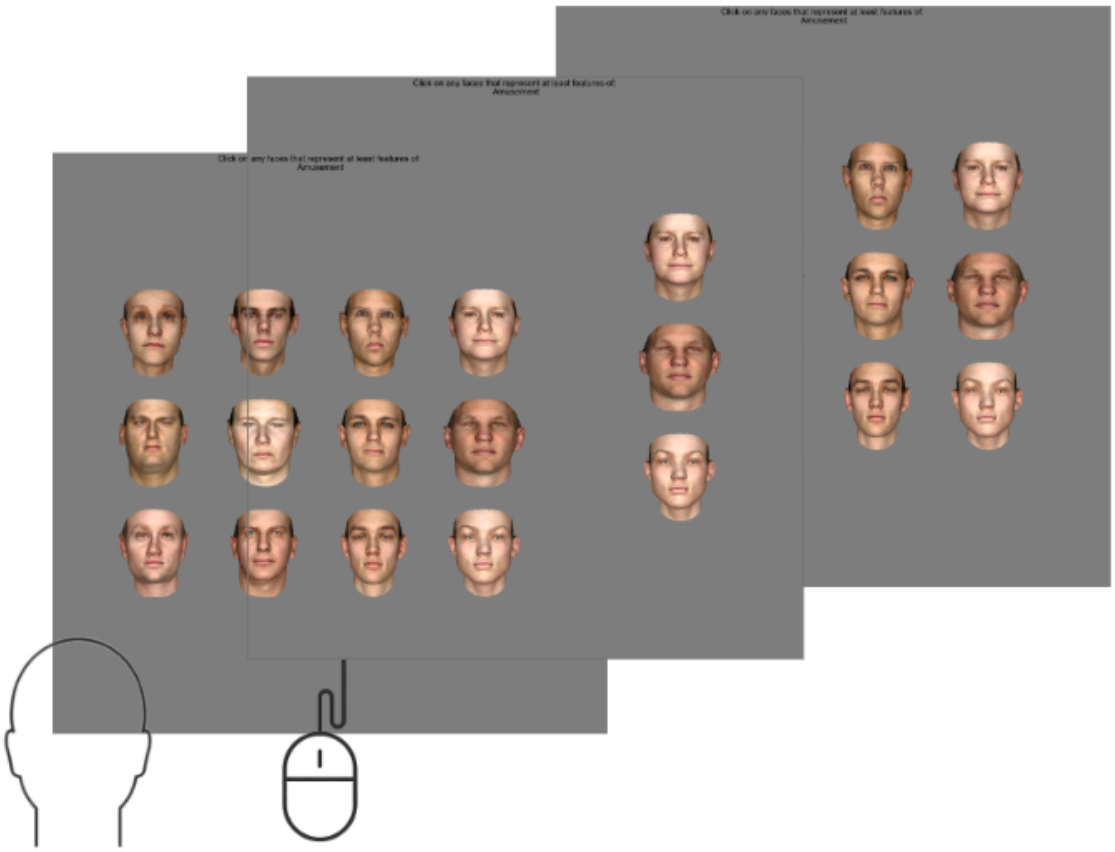

Figure 26. Example of chart presentation for genetic algorithm. The display schematic shows a participant selecting faces resembling amusement. In subsequent charts there is a mix of median parameters, or genes, from previous charts and pseudo randomized genes.

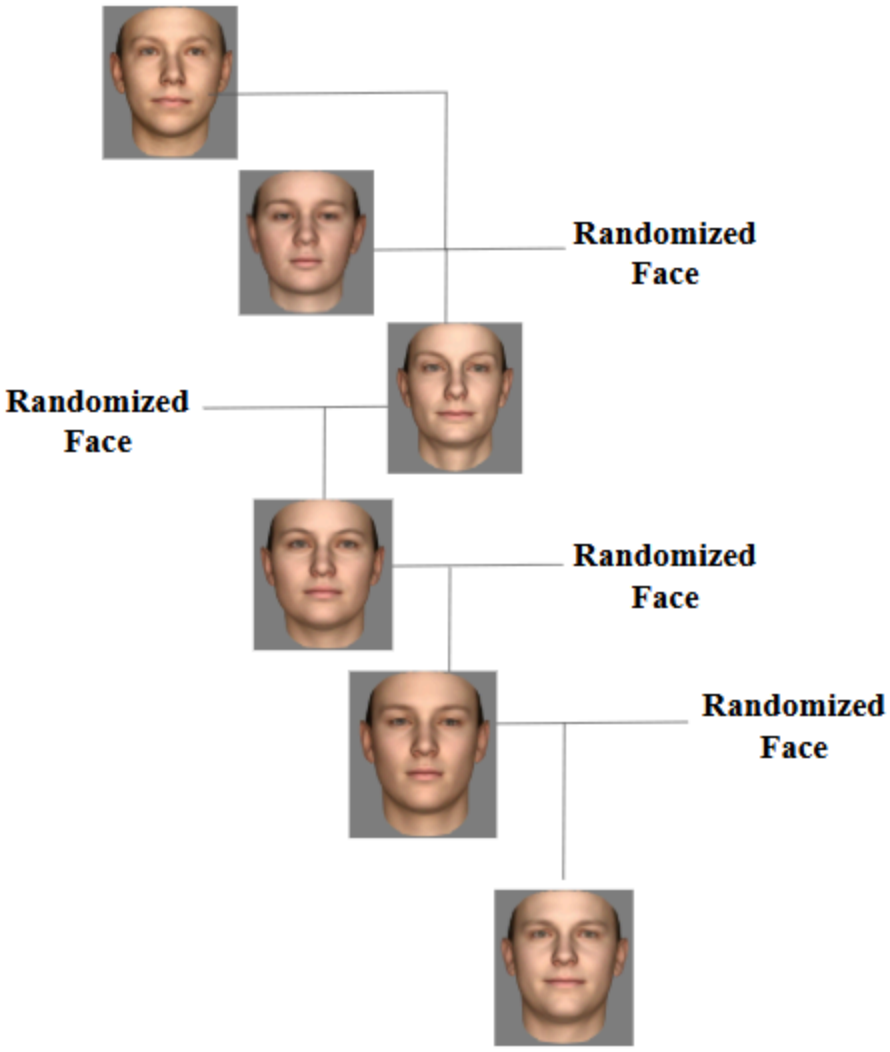

Figure 27. Example of genetic algorithm tree throughout trials. The first face presentation has randomized structural and texture parameters. Subsequent presentations are a combination of previously selected and randomized parameters. After 6 generations, a final face for the specified emotion is created. The median parameters for the final face are used for analysis.

5.3 Results

Participants were confirmed to have adequate vision with the Early Treatment Diabetic Retinopathy Study (ETDRS) Chart (Table 20).

Table 22. Age demographics and entering visual measures for GA emotion repeatability protocol participants.

	Mean ± standard deviation
Age	19.91 ± 1.88
ETDRS Acuity BCVA in the better eye	-0.2 ± 0.05
Stereoacuity	89.17 ± 111.4

A sample two tailed t-test was performed for each emotion comparing the cosine distance output between test and retests. Cosine distance performance for happiness yielded no significant difference (p=0.11), similarly coefficient of variation (CoV) was relatively low at 11% . Bias was also minimal at 8% and the difference in test-retest performance was greater with smaller cosine distances (slope= +1.01) (Figure 28).

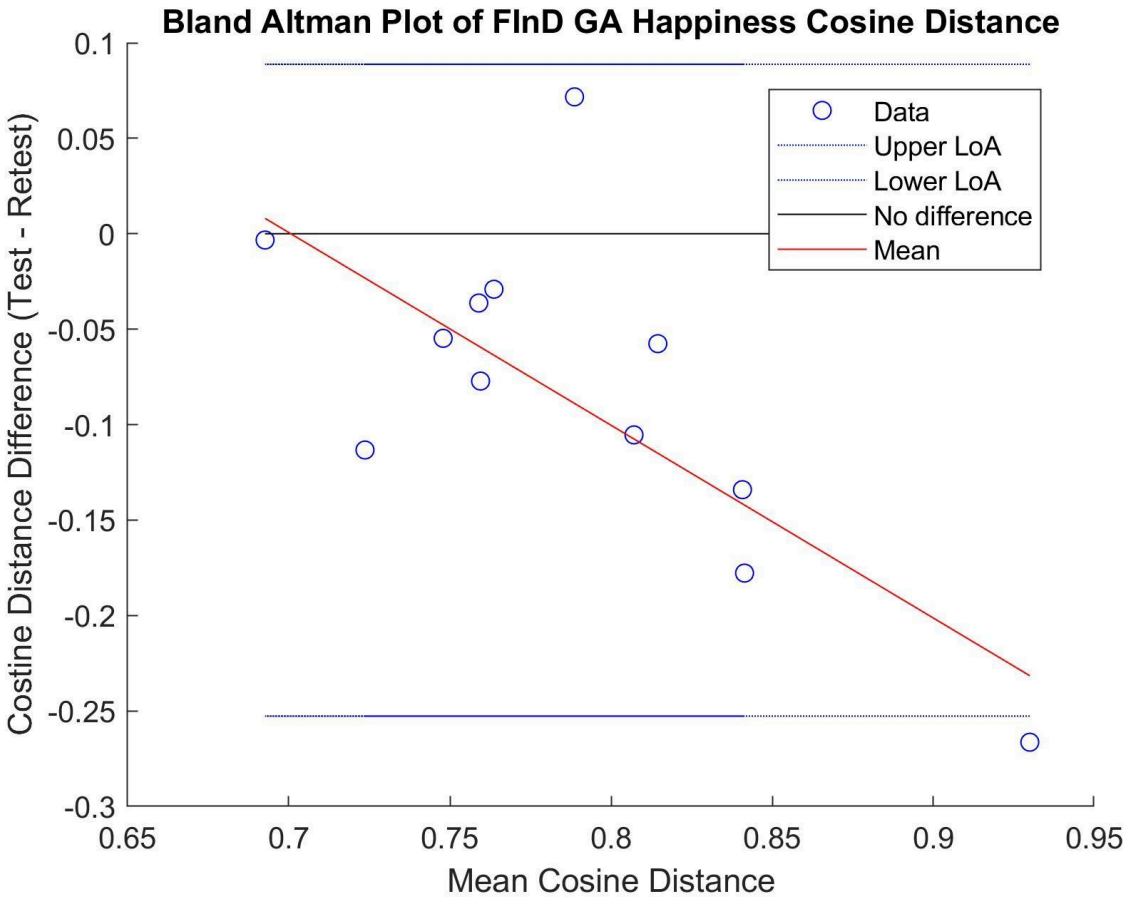

Figure 28. Bland Altman plot for median parameter cosine distance in happiness performance. Bias, coefficient of variation and coefficient of repeatability were calculated to be 0.08, 11%, and 24% respectively. The slope cosine distance to difference in parameters between test and retest was -1.01.

Repeatability for amused faces yielded a non-significant difference between test and retest (p= 0.15). The Bland Altman analysis reported a CoV of 10% and limited bias (6%). In contrast to happiness performance, the slope of the Bland Altman plot indicated minimal differences

between test and retest with smaller cosine distances (+0.47) (Figure 29).

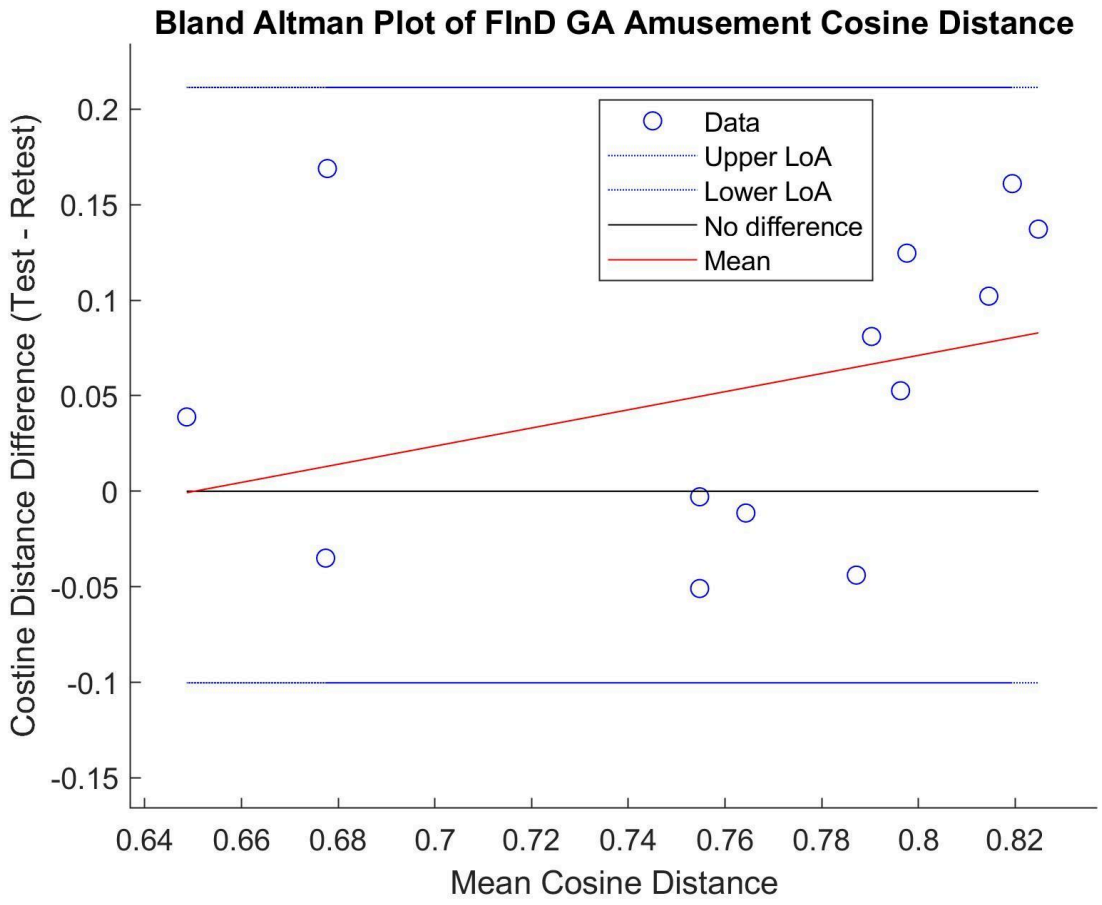

Figure 29. Bland Altman plot for median parameter cosine distance in amusement performance. Bias, correlation of variation and coefficient of repeatability were calculated to be 0.06, 10%, and 19% respectively. The slope cosine distance to difference in parameters between test and retest was +0.47.

Performance for angry expressions, again, yielded no significant difference between test and retest (p= 0.61). The Bland Altman analysis reported a CoV of 9% with <0.000 bias. Slope was similar to that of happiness (+0.49) (Figure 30).

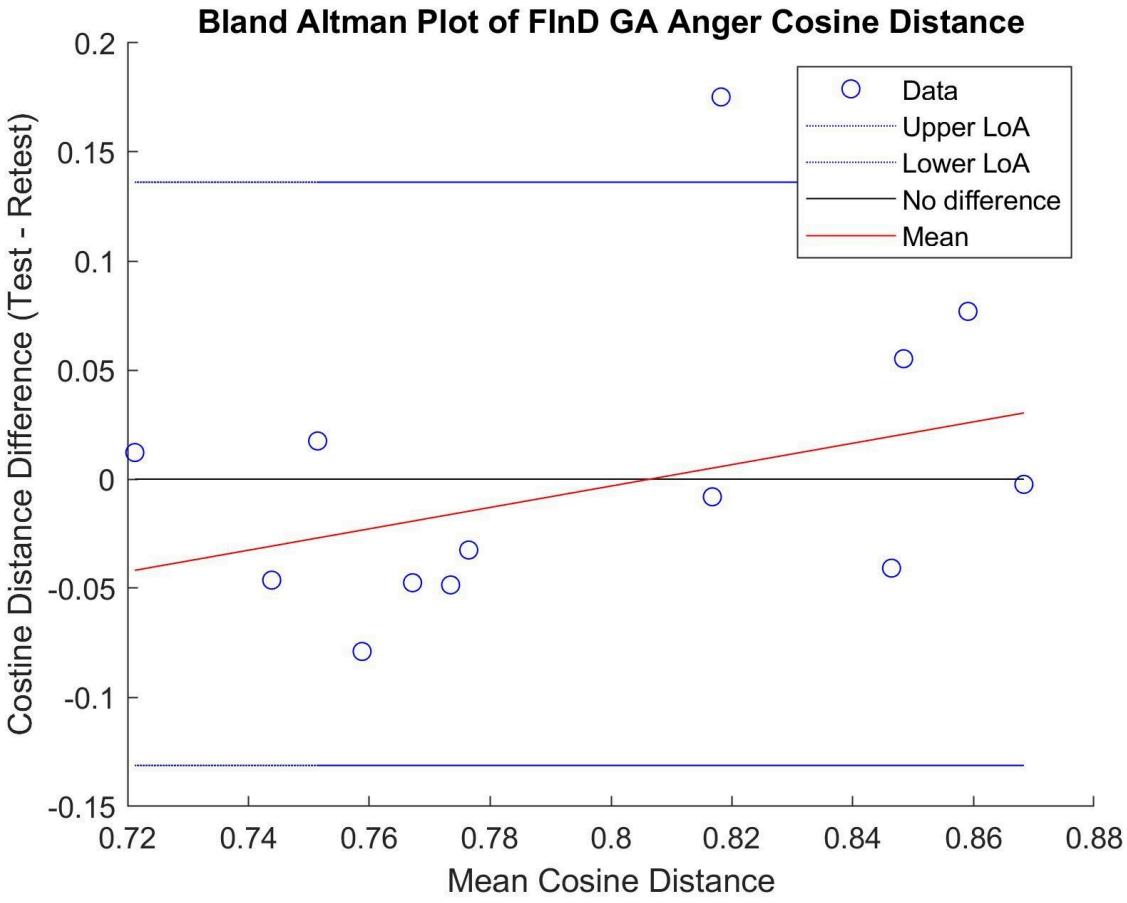

Figure 30. Bland Altman plot for median parameter cosine distance in anger performance. Bias, correlation of variation and coefficient of repeatability were calculated to be <0.000, 9%, and 13% respectively. The slope cosine distance to difference in parameters between test and retest was +0.49.

Finally, performance for disgust yielded no significant difference in performance (p= 0.19). The Bland Altman analysis revealed a CoV of 11% and limited bias (4%). The slope of the plot was similar to amusement at -1.04 (Figure 31).

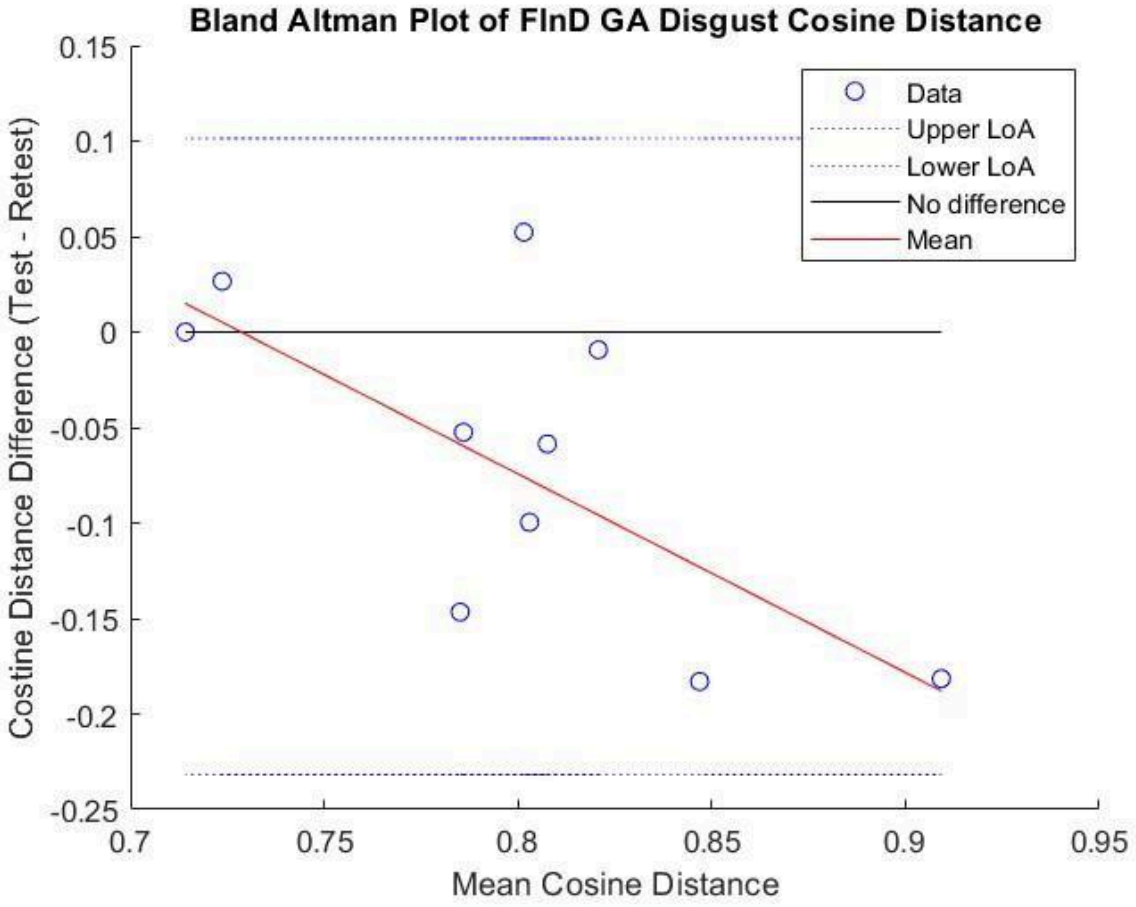

Figure 31. Bland Altman plot for median parameter cosine distance in disgust performance. Bias, correlation of variation and coefficient of repeatability were calculated to be 0.04, 11%, and 21% respectively. The slope cosine distance to difference in parameters between test and retest was -1.04.

5.4 Discussion & Conclusion

This novel genetic algorithm reports repeatable results that offer a self-administered assessment of emotion discrimination. As opposed to traditional emotion discrimination tasks, this algorithm offers a quantitative assessment of facial features. Although the current consensus of face perception research agrees the action units of the face (i.e., eyebrows, eyes, nose, and mouth) (Martinez, 2017) are most influential to emotion recognition, there is little information

about this on a quantitative level. Therefore, compensatory methods in patients with agnosia or visual acuity deficits can go undetected (Cui et al., 2023). Often, the traditional forced-choice methods identify large face processing deficits.

Historically, we see emotion discrimination assessments used in patients on the Autism spectrum and in those suffering with schizophrenia (Macnamara et al., 2022; Fraser et al., 2019). However, the importance of emotion perception has been understated in low vision patients. The previously identified deficits in high spatial frequency facial characteristics perception can be expanded upon with this genetic algorithm. This assertion is in agreement with the application of the genetic algorithm by Cui et al. in patients with central vision loss (Cui et al., 2023). In the future, this emotion discrimination task can be used to simulate daily visual task deficits opposed to the standard visual and contrast acuity. Therefore, clinicians may gain a better understanding of everyday functional vision. Deficits in emotion discrimination have been linked to decrease in quality of life, leading to increased risk for depression and anxiety. Implementing the genetic algorithm in routine clinical practice can heighten our sensitivity to necessary mental health referrals.

Overall, the results from this study serve as a basis for normative data to compare emotions within face space. Comparisons of emotion effects, especially positive versus negative emotions, in performance can be used. In future applications, the test may help differentiate types of emotion recognition deficits arising from normal aging (Barnes CS et al, 2011), cognitive decline, or altered visual acuity (Macnamara et al., 2022).

CHAPTER 6: GENERAL CONCLUSION

5.1 Exploration of Blur Tolerance in Albinism

Considering blur tolerance in clinical care of PwA could perhaps change our approach to refractive correction. Subjectively, if there is no visual gain with glasses, patients may forgo wearing glasses or contacts. However, we must consider objective acuity on a case by case basis. For example, refractive correction may limit driving abilities if acuity is objectively improved. Entering acuity does not appear to be predictive of visual gain, but there should be a discussion of the patient's goals for their vision.

Additionally, refraction procedures have been generalized to include all pathology that constitutes low vision. This does not consider the etiology of vision loss, acquired or congenital. Lens presentation is only influenced by visual acuity. No current studies have explored using larger bracketing lenses than traditionally suggested in low vision procedures, however this method has been proposed in several publications (Bailey, 1978) . The shallow, yet decreasing, visual acuity performance demonstrates one line of acuity loss per diopter. If this were to occur with visual gain, which was not assessed here, we may be blunting visual potential. As an aside, controls did not follow the visual pattern expected with Egger's chart. This group has a loss of two lines per diopter; whereas Egger's presumes a three line reduction per diopter. It should also be acknowledged that Egger's chart does not account for defocus beyond 2.5 diopters.

In future studies, other groups within the low vision population can be assessed for their tolerance of dioptric blur. To name a few conditions, Stargardt's macular disease, AMD and advanced glaucoma can be explored to establish possible delineations for PwA. This study highlighted the blur tolerance in PwA, but why this is the case is still not well understood. Further investigation can elaborate the connection with amplitude nystagmus, the degree of

foveal hypoplasia, and the amount of misrouted fibers at the optic chiasm. Finally, AIM Low Vision can be used as a repeatable visual acuity measurement in all future directions.

5.2 Exploration of Face Discrimination in Albinism

Much of higher-order visual processing in albinism has not been studied. The most studied aspect of albinism pathology has been visual acuity and contrast sensitivity. As these are reduced, like many low vision patients, it has been presumed to decrease face discrimination. Nystagmus and foveal hypoplasia certainly point to reduction of low level processing, but the addition of chiasmal misrouting is not well understood in downstream processing. This thesis presents results showing that face discrimination is preserved in patients with albinism. More importantly, thresholds are comparable to controls both in upright and inverted presentations. This suggests there are visual adaptations PwA use from a young age. Also, these results somewhat disillude us of possible visual disorganization results from chiasmal misrouting.

In future directions, face discrimination in albinism could be compared to other low vision groups. It has been well documented that face discrimination is impaired in low vision groups without specificity. This has not been quantifiable as it is now available with the FInD Faces paradigm. Additionally, strong compensatory strategies may be better understood with the analysis of individual face parameters offered with FInD Faces. Finally, this type of high level visual processing can be further explored in emotion and object recognition.

5.3 Exploration of A Novel Emotion Recognition Model

The Genetic Algorithm explored in this thesis, demonstrated repeatable results of face

processing in face space. Similar to that of the FInD Faces paradigm, using morphological three-dimensional models allow clinicians to assess emotion recognition from all sides. This provides us with continuous data that quantify influential components of facial structures. It was the intention of this thesis to establish the GA Emotion model to be a viable, self administered assessment of how individuals define emotion. Ongoing analysis is exploring emotion perception in PwA and low vision patients with central vision loss. Much like face discrimination, this exploration is with the intention to understand the integrity of face processing and if albinism pathology impacts this system.

REFERENCES

Abadi, R.V. (2002). Mechanisms underlying nystagmus. J R Soc Med, 95 (5), 231–234.

Anderson, J., Lavoie, J., Merrill, K., King, R.A., & Summers, C.G. (2004). Efficacy of spectacles in persons with albinism. J AAPOS, 8 (6), 515–520.

Ather, S., Proudlock, F.A., Welton, T., Morgan, P.S., Sheth, V., Gottlob, I., & Dineen, R.A. (2019). Aberrant visual pathway development in albinism: From retina to cortex. Hum Brain Mapp, 40 (3), 777–788.

Avery, S.N., VanDerKlok, R.M., Heckers, S., & Blackford, J.U. (2016). Impaired face recognition is associated with social inhibition. Psychiatry Res, 236, 53–57.

Bailey, I.L. (2012). Perspective: visual acuity-keeping it clear. Optom Vis Sci, 89 (9), 1247–1248.

Bailey, I.L., & Lovie, J.E. (1976). New design principles for visual acuity letter charts. Am J Optom Physiol Opt, 53 (11), 740–745.

Bailey IL. (1978). Refracting low vision patients. Optometric Monthly 69, 131-135.

Balas, B., Gable, J., & Pearson, H. (2019). The Effects of Blur and Inversion on the Recognition of Ambient Face Images. Perception, 48 (1), 58–71.

Barnes, C.S., De L'Aune, W., & Schuchard, R.A. (2011). A test of face discrimination ability in aging and vision loss. Optom Vis Sci, 88 (2), 188–199.

Baron-Cohen, S., Wheelwright, S., Hill, J., Raste, Y., & Plumb, I. (2001). The "Reading the Mind in the Eyes" Test revised version: a study with normal adults, and adults with Asperger syndrome or high-functioning autism. J Child Psychol Psychiatry, 42 (2), 241–251.

Barton, J.J.S. (2022). Cerebral Visual Loss. Ann Indian Acad Neurol, 25 (Suppl 2), S106–s112.

Barton, J.J.S., Davies-Thompson, J., & Corrow, S.L. (2021). Prosopagnosia and disorders of face

processing. Handb Clin Neurol, 178, 175–193.

Bex PJ, Skerswetat S, Ross N. 2021. FIND – Foraging Interactive d-prime, a method for visual function measurement. *J Vis* 21(9):2817. doi:10.1167/jov.21.9.2817

Binetti, N., Roubtsova, N., Carlisi, C., Cosker, D., Viding, E., & Mareschal, I. (2022). Genetic algorithms reveal profound individual differences in emotion recognition. Proc Natl Acad Sci U S A, 119 (45), e2201380119.

Binetti, N., Roubtsova, N., Carlisi, C., Cosker, D., Viding, E., & Mareschal, I. (2022). Genetic algorithms reveal profound individual differences in emotion recognition. Proc Natl Acad Sci U S A, 119 (45), e2201380119.

Bodamer, J. (1947). [Prosop's agnosia; the agnosia of cognition]. Arch Psychiatr Nervenkr Z Gesamte Neurol Psychiatr, 118 (1-2), 6–53.

Borish , Benjamin, W.J., 2006. Borish's Clinical Refraction-E-Book: Borish's Clinical Refraction-E-Book. Elsevier Health Sciences.

Boucart, M., Dinon, J.F., Despretz, P., Desmettre, T., Hladiuk, K., & Oliva, A. (2008). Recognition of facial emotion in low vision: a flexible usage of facial features. Vis Neurosci, 25 (4), 603–609.

Brainard, D.H. (1997). The Psychophysics Toolbox. Spat Vis, 10 (4), 433–436.

Brucher, V.C., Heiduschka, P., Grenzebach, U., Eter, N., & Biermann, J. (2019). Distribution of macular ganglion cell layer thickness in foveal hypoplasia: A new diagnostic criterion for ocular albinism. PLoS One, 14 (11), e0224410.

Bullimore, M.A., Bailey, I.L., & Wacker, R.T. (1991). Face recognition in age-related maculopathy. Invest Ophthalmol Vis Sci, 32 (7), 2020–2029.

Burton, A.M., White, D., & McNeill, A. (2010). The Glasgow Face Matching Test. Behav Res

Methods, 42 (1), 286–291.

Camparini, M., Cassinari, P., Ferrigno, L., & Macaluso, C. (2001). ETDRS-fast: implementing psychophysical adaptive methods to standardized visual acuity measurement with ETDRS charts. Invest Ophthalmol Vis Sci, 42 (6), 1226–1231.

Cao, R., Qian, C., Ren, S., He, Z., He, S., & Zhang, P. (2021). Visual adaptation and 7T fMRI reveal facial identity processing in the human brain under shallow interocular suppression. Neuroimage, 244, 118622.

Carlisi, C.O., Reed, K., Helmink, F.G.L., Lachlan, R., Cosker, D.P., Viding, E., & Mareschal, I. (2021). Using genetic algorithms to uncover individual differences in how humans represent facial emotion. R Soc Open Sci, 8 (10), 202251.

Chong, G.T., Farsiu, S., Freedman, S.F., Sarin, N., Koreishi, A.F., Izatt, J.A., & Toth, C.A. (2009). Abnormal foveal morphology in ocular albinism imaged with spectral-domain optical coherence tomography. Arch Ophthalmol, 127 (1), 37–44.

Collewijn, H., Apkarian, P., & Spekreijse, H. (1985). The oculomotor behaviour of human albinos. Brain, 108 (Pt 1), 1–28.

Cui B, Bex P, Ross N. 2023. Effects of central vision loss on emotion perception. *Invest Ophthalmol Vis Sci* 64:1468.

Cui, B., & Bex, P. (2025). Facing distortion: Impact of spatial distortions on upright and inverted face identification. PLoS One, 20 (9), e0308675.

Dalmaso, M., Pileggi, S., Murgia, M., & Vicovaro, M. (2026). Explicit and implicit spatial mapping of face age. Psychol Res, 90 (2)

Dalrymple, K.A., Corrow, S., Yonas, A., & Duchaine, B. (2012). Developmental prosopagnosia in childhood. Cogn Neuropsychol, 29 (5-6), 393–418.

De Renzi, E., Faglioni, P., Grossi, D., & Nichelli, P. (1991). Apperceptive and associative forms of prosopagnosia. Cortex, 27 (2), 213–221.

DeGutis, J., Wilmer, J., Mercado, R.J., & Cohan, S. (2013). Using regression to measure holistic face processing reveals a strong link with face recognition ability. Cognition, 126 (1), 87–100.

Dobhal, V., Kumar, A., Garg, I., Kumar, A., & Goel, F. (2025). Strabismus and nystagmus in oculocutaneous albinism: clinical perspectives, diagnosis, and role of neurotransmitters. Neurogenetics, 26 (1), 50.

Duchaine, B., & Nakayama, K. (2006). The Cambridge Face Memory Test: results for neurologically intact individuals and an investigation of its validity using inverted face stimuli and prosopagnosic participants. Neuropsychologia, 44 (4), 576–585.

Dysli, M., & Abegg, M. (2016). Nystagmus Does Not Limit Reading Ability in Albinism. PLoS One, 11 (7), e0158815.

Ekman P, Friesen WV. (1976). Pictures of Facial Affect.

Ekman P, Friesen WV. (1978). Facial Action Coding System.

Federico, J.R., & Krishnamurthy, K. (2025). Albinism. In: StatPearls (Treasure Island (FL): StatPearls Publishing, Copyright © 2025, StatPearls Publishing LLC.

Fox E, Bindemann M. (2020). Visual acuity and face matching. *Appl Cogn Psychol* 34:1034–1046.

Franca, M., Bolognini, N., & Brysbaert, M. (2023). Seeing emotions in the eyes: a validated test to study individual differences in the perception of basic emotions. Cogn Res Princ Implic, 8 (1), 67.

Fraser, S., Beeman, I., Southall, K., & Wittich, W. (2019). Stereotyping as a barrier to the social

participation of older adults with low vision: a qualitative focus group study. BMJ Open, 9 (9), e029940.

Fysh, M.C. (2018). Individual differences in the detection, matching and memory of faces. Cogn Res Princ Implic, 3, 20.

Gerig T, Morel-Forster A, Blumer C, et al. (2018). Morphable face models: An Open Frame Model. *FG 2018* 75–82. doi:10.1109/FG.2018.00021

Gerlach, C., Kühn, C.D., Mathiassen, A.B., Kristensen, C.L., & Starrfelt, R. (2023). The face inversion effect or the face upright effect? Cognition, 232, 105335.

Gillespie, S.M., Rotshtein, P., Satherley, R.M., Beech, A.R., & Mitchell, I.J. (2015). Emotional expression recognition and attribution bias among sexual and violent offenders: a signal detection analysis. Front Psychol, 6, 595.

Goffaux, V., Poncin, A., & Schiltz, C. (2015). Selectivity of Face Perception to Horizontal Information over Lifespan (from 6 to 74 Year Old). PLoS One, 10 (9), e0138812.

Green DM, Swets JA. (1966). Signal Detection Theory and Psychophysics.

Gronskov, K., Ek, J., & Brondum-Nielsen, K. (2007). Oculocutaneous albinism. Orphanet J Rare Dis, 2, 43.

Guillery, R.W., Okoro, A.N., & Witkop, C.J., Jr. (1975). Abnormal visual pathways in the brain of a human albino. Brain Res, 96 (2), 373–377.

Guo, X., Swenor, B.K., & Goldstein, J.E. (2020). Association of Visual Acuity Improvement With Uncorrected Refractive Error in Patients New to Low Vision Clinics. JAMA Ophthalmol, 138 (7), 765–771.

Haque, S., Vaphiades, M.S., & Lueck, C.J. (2018). The Visual Agnosias and Related Disorders. J Neuroophthalmol, 38 (3), 379–392.

Hepler, L.E., Martin, S.J., Fuglseth, K., Cuddihee, L., Giannulis, P., & Arnold, R.W. (2023). Acuity Comparison Methods via Timed Test-Retest Precision of Matching-Card e-ETDRS Compared to PDI Check in Treated Amblyopes and Superb Normals. Clin Optom (Auckl), 15, 81–95.

Hertle, R.W. (2013). Albinism: particular attention to the ocular motor system. Middle East Afr J Ophthalmol, 20 (3), 248–255.

Hoffmann, K.P., Garipis, N., & Distler, C. (2004). Optokinetic deficits in albino ferrets (Mustela putorius furo): a behavioral and electrophysiological study. J Neurosci, 24 (16), 4061–4069.

Hoosen T, Mitha F, Narothan C, et al. (2020). Effect of induced blur on vision. Afr Vision Eye Health 79:575.

Hupfeld, D., Distler, C., & Hoffmann, K.P. (2007). Deficits of visual motion perception and optokinetic nystagmus after posterior suprasylvian lesions in the ferret (Mustela putorius furo). Exp Brain Res, 182 (4), 509–523.

Istrate, M., Vlaicu, B., Poenaru, M., Hasbei-Popa, M., Salavat, M.C., & Iliescu, D.A. (2020). Photoprotection role of melanin in the human retinal pigment epithelium. Imaging techniques for retinal melanin. Rom J Ophthalmol, 64 (2), 100–104.

Istrate, M., Vlaicu, B., Poenaru, M., Hasbei-Popa, M., Salavat, M.C., & Iliescu, D.A. (2020). Photoprotection role of melanin in the human retinal pigment epithelium. Imaging techniques for retinal melanin. Rom J Ophthalmol, 64 (2), 100–104.

Jacobs, R.J., Smith, G., & Chan, C.D. (1989). Effect of defocus on blur thresholds and on thresholds of perceived change in blur: comparison of source and observer methods. Optom Vis Sci, 66 (8), 545–553.

Jeantet, C., Caharel, S., Schwan, R., Lighezzolo-Alnot, J., & Laprevote, V. (2018). Factors influencing spatial frequency extraction in faces: A review. Neurosci Biobehav Rev, 93, 123–138.

Jehna, M., Neuper, C., Ischebeck, A., Loitfelder, M., Ropele, S., Langkammer, C., Ebner, F., Fuchs, S., Schmidt, R., Fazekas, F., & Enzinger, C. (2011). The functional correlates of face perception and recognition of emotional facial expressions as evidenced by fMRI. Brain Res, 1393, 73–83.

Johnson, A.P., Woods-Fry, H., & Wittich, W. (2017). Effects of Magnification on Emotion Perception in Patients With Age-Related Macular Degeneration. Invest Ophthalmol Vis Sci, 58 (5), 2520–2526.

Kasmann-Kellner, B., & Seitz, B. (2007). [Phenotype of the visual system in oculocutaneous and ocular albinism]. Ophthalmologe, 104 (8), 648–661.

Kessel, L., Kjolholm, C.D.B., & Jordana, J.T. (2023). Does Foveal Hypoplasia Affect Emmetropization in Patients with Albinism? Children (Basel), 10 (12)

King, R.A., Pietsch, J., Fryer, J.P., Savage, S., Brott, M.J., Russell-Eggitt, I., Summers, C.G., & Oetting, W.S. (2003). Tyrosinase gene mutations in oculocutaneous albinism 1 (OCA1): definition of the phenotype. Hum Genet, 113 (6), 502–513.

Kirkwood, B.J. (2009). Albinism and its implications with vision. Insight, 34 (2), 13–16.

Klauke, S., Sondocie, C., & Fine, I. (2023). The impact of low vision on social function: The potential importance of lost visual social cues. J Optom, 16 (1), 3–11.

Krautheim, J.T., Steines, M., Dannlowski, U., Neziroğlu, G., Acosta, H., Sommer, J., Straube, B., & Kircher, T. (2020). Emotion specific neural activation for the production and perception of facial expressions. Cortex, 127, 17–28.

Lanca, M., Jerskey, B.A., & O'Connor, M.G. (2003). Neuropsychologic assessment of visual disorders. Neurol Clin, 21 (2), 387–416.

Lane, J., Rohan, E.M.F., Sabeti, F., Essex, R.W., Maddess, T., Barnes, N., He, X., Robbins, R.A., Gradden, T., & McKone, E. (2018). Improving face identity perception in age-related macular degeneration via caricaturing. Sci Rep, 8 (1), 15205.

Lee, D.J., Woertz, E.N., Visotcky, A., Wilk, M.A., Heitkotter, H., Linderman, R.E., Tarima, S., Summers, C.G., Brooks, B.P., Brilliant, M.H., Antony, B.J., Lujan, B.J., & Carroll, J. (2018). The Henle Fiber Layer in Albinism: Comparison to Normal and Relationship to Outer Nuclear Layer Thickness and Foveal Cone Density. Invest Ophthalmol Vis Sci, 59 (13), 5336–5348.

Leibowitz, H.M., Krueger, D.E., Maunder, L.R., Milton, R.C., Kini, M.M., Kahn, H.A., Nickerson, R.J., Pool, J., Colton, T.L., Ganley, J.P., Loewenstein, J.I., & Dawber, T.R. (1980). The Framingham Eye Study monograph: An ophthalmological and epidemiological study of cataract, glaucoma, diabetic retinopathy, macular degeneration, and visual acuity in a general population of 2631 adults, 1973-1975. Surv Ophthalmol, 24 (Suppl), 335–610.

Logan, A.J., Gordon, G.E., & Loffler, G. (2017). Contributions of individual face features to face discrimination. Vision Res, 137, 29–39.

Logan, A.J., Gordon, G.E., & Loffler, G. (2022). Healthy aging impairs face discrimination ability. J Vis, 22 (9), 1.

Loshin, D.S., & Browning, R.A. (1983). Contrast sensitivity in albinotic patients. Am J Optom Physiol Opt, 60 (3), 158–166.

Macnamara, A., Coussens, S., Chen, C., Schinazi, V.R., & Loetscher, T. (2022). The

psychological impact of instrumental activities of daily living on people with simulated age-related macular degeneration. BJPsych Open, 8 (5), e152.

Martinez, A.M. (2017). Computational Models of Face Perception. Curr Dir Psychol Sci, 26 (3), 263–269.

Massof, R.W. (2002). A model of the prevalence and incidence of low vision and blindness among adults in the U.S. Optom Vis Sci, 79 (1), 31–38.

McAllister, J.T., Dubis, A.M., Tait, D.M., Ostler, S., Rha, J., Stepien, K.E., Summers, C.G., & Carroll, J. (2010). Arrested development: high-resolution imaging of foveal morphology in albinism. Vision Res, 50 (8), 810–817.

McAnany, J.J., Shahidi, M., Applegate, R.A., Zelkha, R., & Alexander, K.R. (2011). Contributions of optical and non-optical blur to variation in visual acuity. Optom Vis Sci, 88 (6), 716–723.

McHam, M.L., & Fulton, A. (1992). Albinism. Int Ophthalmol Clin, 32 (1), 185–200.

Neveu, M.M., Jeffery, G., Moore, A.T., & Dakin, S.C. (2009). Deficits in local and global motion perception arising from abnormal eye movements. J Vis, 9 (4), 9.1–15.

Nishida, S., Kawabe, T., Sawayama, M., & Fukiage, T. (2018). Motion Perception: From Detection to Interpretation. Annu Rev Vis Sci, 4, 501–523.

Pang, Y., Sparschu, L., Nylin, E., & Wang, J. (2020). Validation of an Automated Early Treatment Diabetic Retinopathy Study Low-contrast Letter Acuity Test. Optom Vis Sci, 97 (5), 370–376.

Pelli, D.G. (1997). The VideoToolbox software for visual psychophysics: transforming numbers into movies. Spat Vis, 10 (4), 437–442.

Raji, S., Thirunavukarasu, A.J., Taylor, L.J., & MacLaren, R.E. (2025). Functional vision tests as

clinical trial outcome measures in ophthalmology: a scoping review. BMJ Open, 15 (5), e097970.

Rossion, B. (2018). Humans Are Visual Experts at Unfamiliar Face Recognition. Trends Cogn Sci, 22 (6), 471–472.

Rossion, B., Delvenne, J.F., Debatisse, D., Goffaux, V., Bruyer, R., Crommelinck, M., & Guerit, J.M. (1999). Spatio-temporal localization of the face inversion effect: an event-related potentials study. Biol Psychol, 50 (3), 173–189.

Rossion, B., & Michel, C. (2018). Normative accuracy and response time data for the computerized Benton Facial Recognition Test (BFRT-c). Behav Res Methods, 50 (6), 2442–2460.

Schmitz, B., Kasmann-Kellner, B., Schafer, T., Krick, C.M., Gron, G., Backens, M., & Reith, W. (2004). Monocular visual activation patterns in albinism as revealed by functional magnetic resonance imaging. Hum Brain Mapp, 23 (1), 40–52.

Seguy, P.H., Korobelnik, J.F., Delyfer, M.N., Michaud, V., Arveiler, B., Lasseaux, E., Gattoussi, S., Rougier, M.B., Trin, K., Morice-Picard, F., Ghomashchi, N., & Coste, V. (2023). Ophthalmologic Phenotype-Genotype Correlations in Patients With Oculocutaneous Albinism Followed in a Reference Center. Invest Ophthalmol Vis Sci, 64 (12), 26.

Seo, J.H., Yu, Y.S., Kim, J.H., Choung, H.K., Heo, J.W., & Kim, S.J. (2007). Correlation of visual acuity with foveal hypoplasia grading by optical coherence tomography in albinism. Ophthalmology, 114 (8), 1547–1551.

Silver, H., Shlomo, N., Schwartz, M., & Hocherman, S. (2002). Impaired visuomotor function in schizophrenic patients compared with control subjects. J Neuropsychiatry Clin Neurosci, 14 (1), 72–76.

Skerswetat, J., He, J., Shah, J.B., Aycardi, N., & Bex, P.J. (2023). AIM (Angular Indication Measurement) paradigm: Adaptive, self-administered, and generalizable vision assessment used to measure visual acuity. bioRxiv, 2023.2002.2025.529586.

Skerswetat, J., Ross, N.C., Idman-Rait, C., Sun, K., Wynn, O., & Bex, P.J. (2024). Visual Performance of People With Albinism Assessed With Generalizable and Adaptive AIM and FInD Methods. Invest Ophthalmol Vis Sci, 65 (11), 34.

Srinivasan R, Golomb JD, Martinez AM. 2016. Facial action recognition. J Neurosci 36:4434–4442.

Summers, C.G. (1996). Vision in albinism. Trans Am Ophthalmol Soc, 94, 1095–1155.

Summers, C.G. (2009). Albinism: classification, clinical characteristics, and recent findings. Optom Vis Sci, 86 (6), 659–662.

Sunness, J.S., & El Annan, J. (2010). Improvement of visual acuity by refraction in a low-vision population. Ophthalmology, 117 (7), 1442–1446.

Talsma, H.E., Kruijt, C.C., de Wit, G.C., Zwerver, S.H.L., & van Genderen, M.M. (2023). Nystagmus Characteristics in Albinism: Unveiling the Link to Foveal Hypoplasia and Visual Acuity. Invest Ophthalmol Vis Sci, 64 (15), 30.

Taneri, S., Arba-Mosquera, S., Rost, A., Kiessler, S., & Dick, H.B. (2020). Repeatability and reproducibility of manifest refraction. J Cataract Refract Surg, 46 (12), 1659–1666.

Taubert, J., Apthorp, D., Aagten-Murphy, D., & Alais, D. (2011). The role of holistic processing in face perception: evidence from the face inversion effect. Vision Res, 51 (11), 1273–1278.

Tejeria, L., Harper, R.A., Artes, P.H., & Dickinson, C.M. (2002). Face recognition in age related

macular degeneration: perceived disability, measured disability, and performance with a bioptic device. Br J Ophthalmol, 86 (9), 1019–1026.

Thomas, M.G., Kumar, A., Mohammad, S., Proudlock, F.A., Engle, E.C., Andrews, C., Chan, W.M., Thomas, S., & Gottlob, I. (2011). Structural grading of foveal hypoplasia using spectral-domain optical coherence tomography a predictor of visual acuity? Ophthalmology, 118 (8), 1653–1660.

Thomas, M.G., Zippin, J., & Brooks, B.P. (1993). Oculocutaneous Albinism and Ocular Albinism Overview. In: M.P. Adam, S. Bick, G.M. Mirzaa, R.A. Pagon, S.E. Wallace, & A. Amemiya (Eds.), GeneReviews((R)) (Seattle (WA).

Tian, F., Xie, H., Song, Y., Hu, S., & Liu, J. (2022). The Face Inversion Effect in Deep Convolutional Neural Networks. Front Comput Neurosci, 16, 854218.

Tian, J., Wang, J., Xia, T., Zhao, W., Xu, Q., & He, W. (2018). The influence of spatial frequency content on facial expression processing: An ERP study using rapid serial visual presentation. Sci Rep, 8 (1), 2383.

Tsao, D.Y., & Livingstone, M.S. (2008). Mechanisms of face perception. Annu Rev Neurosci, 31, 411–437.

Valentine, T., Lewis, M.B., & Hills, P.J. (2016). Face-space: A unifying concept in face recognition research. Q J Exp Psychol (Hove), 69 (10), 1996–2019.

Venugopal, D., Wood, J.M., Black, A.A., & Bentley, S.A. (2023). Effect of low luminance on face recognition in adults with central and peripheral vision loss. Ophthalmic Physiol Opt, 43 (6), 1344–1355.

Vera-Diaz, F.A., Woods, R.L., & Peli, E. (2017). Blur Adaptation to Central Retinal Disease. Invest Ophthalmol Vis Sci, 58 (9), 3646–3655.

Walter, K., & Bex, P. (2024). A novel, rapid, quantitative method for face discrimination. PLoS One, 19 (12), e0315998.

Walter, K., Manley, C.E., Merabet, L.B., & Bex, P.J. (2025). Impaired face identity discrimination in individuals with cerebral visual impairment: a pilot study. Ann Transl Med, 13 (4), 41.

Wang, S.W., & Boerner, K. (2008). Staying connected: re-establishing social relationships following vision loss. Clin Rehabil, 22 (9), 816–824.

Wildsoet, C.F., Oswald, P.J., & Clark, S. (2000). Albinism: its implications for refractive development. Invest Ophthalmol Vis Sci, 41 (1), 1–7.

Wilmer, J.B., Germine, L., Chabris, C.F., Chatterjee, G., Williams, M., Loken, E., Nakayama, K., & Duchaine, B. (2010). Human face recognition ability is specific and highly heritable. Proc Natl Acad Sci U S A, 107 (11), 5238–5241.

Yahalom, C., Tzur, V., Blumenfeld, A., Greifner, G., Eli, D., Rosenmann, A., Glanzer, S., & Anteby, I. (2012). Refractive profile in oculocutaneous albinism and its correlation with final visual outcome. Br J Ophthalmol, 96 (4), 537–539.

APPENDIX

Appendix A. Albinism Group Participant AIM Performance Linear Regression Trends

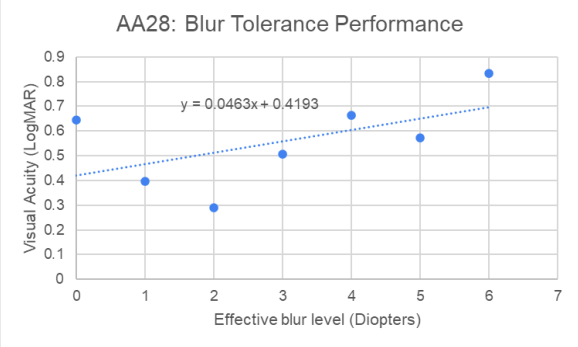

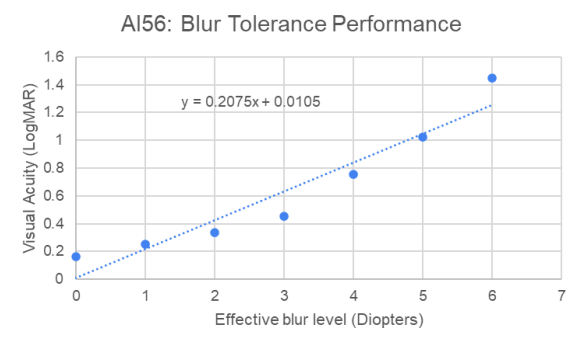

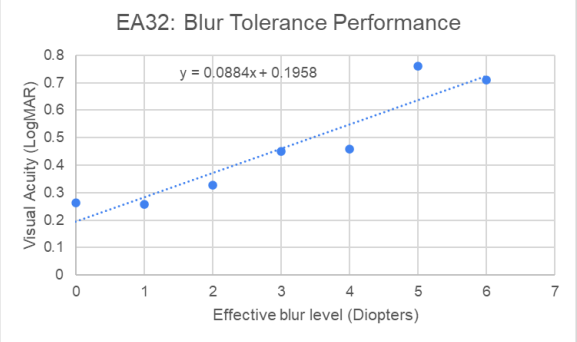

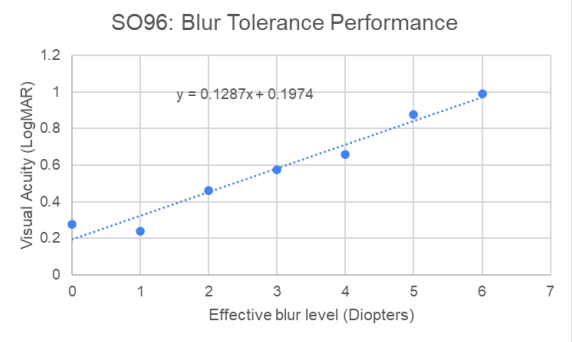

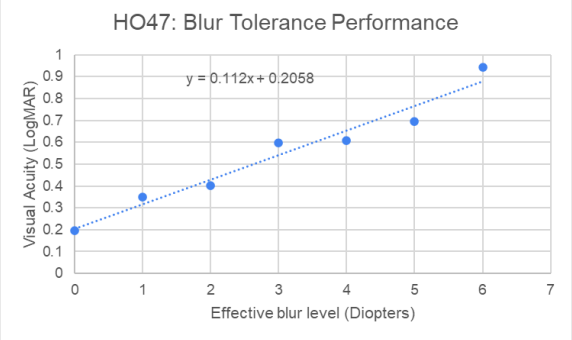

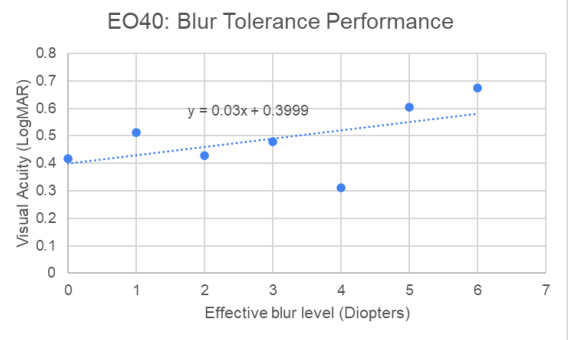

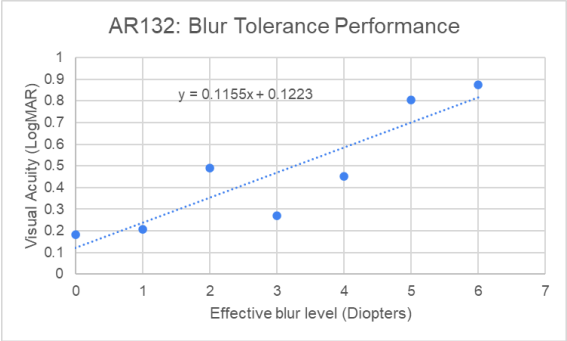
AR132: Blur Tolerance Performance
y = 0.1155x + 0.1223
Visual Acuity (LogMAR)
Effective blur level (Diopters)

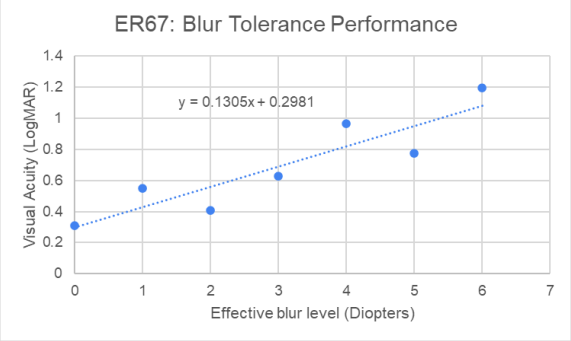
ER67: Blur Tolerance Performance
y = 0.1305x + 0.2981
Visual Acuity (LogMAR)
Effective blur level (Diopters)

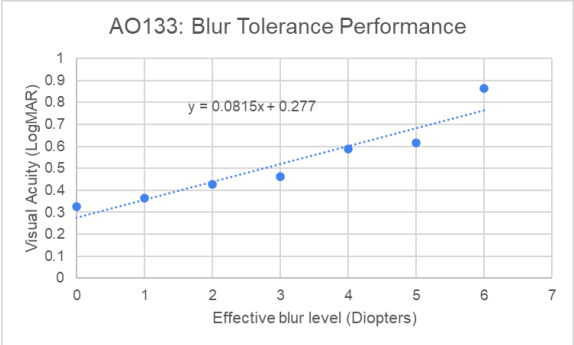
AO133: Blur Tolerance Performance
y = 0.0815x + 0.277
Visual Acuity (LogMAR)
Effective blur level (Diopters)

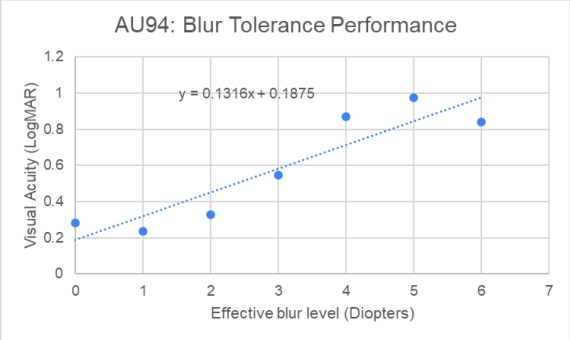
AU94: Blur Tolerance Performance
y = 0.1316x + 0.1875
Visual Acuity (LogMAR)
Effective blur level (Diopters)

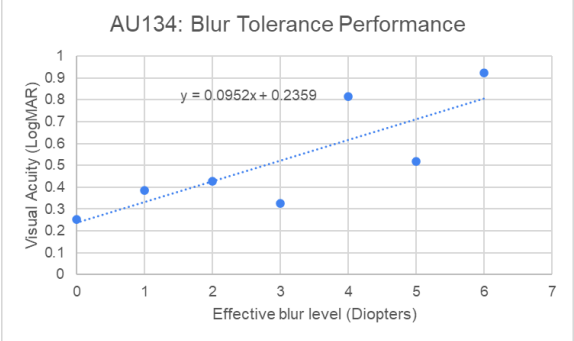
AU134: Blur Tolerance Performance
y = 0.0952x + 0.2359
Visual Acuity (LogMAR)
Effective blur level (Diopters)

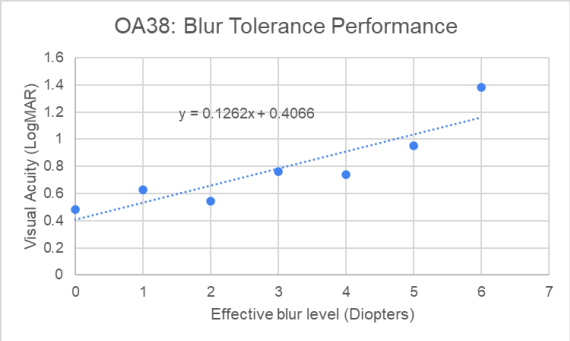
OA38: Blur Tolerance Performance
y = 0.1262x + 0.4066
Visual Acuity (LogMAR)
Effective blur level (Diopters)

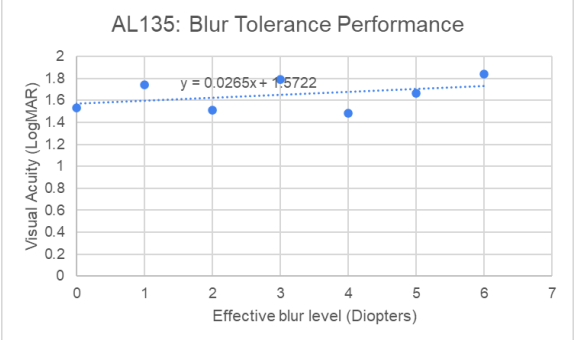
AL135: Blur Tolerance Performance
y = 0.0265x + 1.5722
Visual Acuity (LogMAR)
Effective blur level (Diopters)

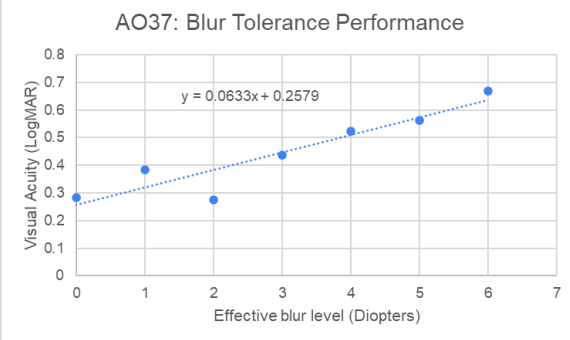
AO37: Blur Tolerance Performance
y = 0.0633x + 0.2579
Visual Acuity (LogMAR)
Effective blur level (Diopters)

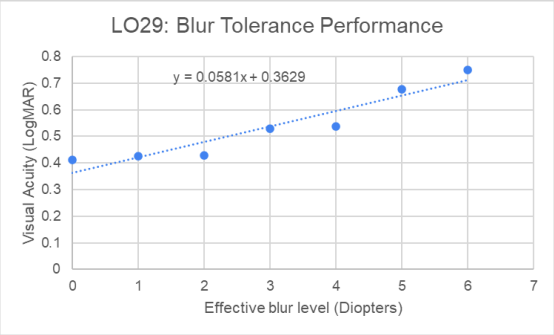

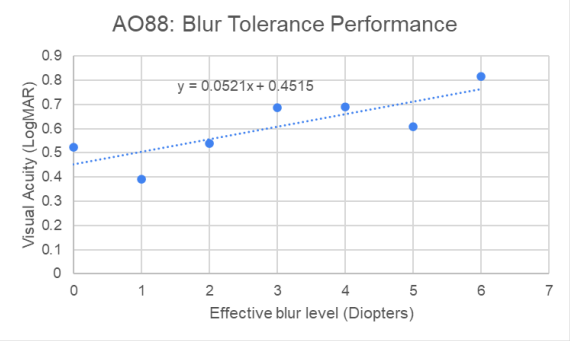

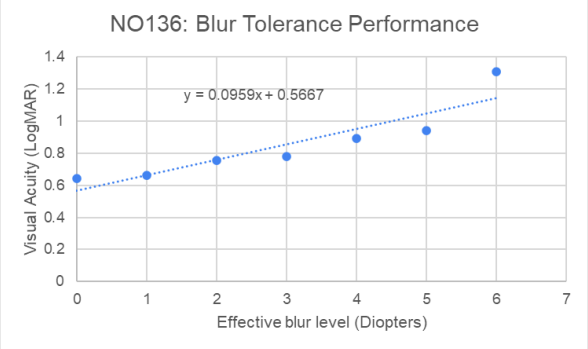

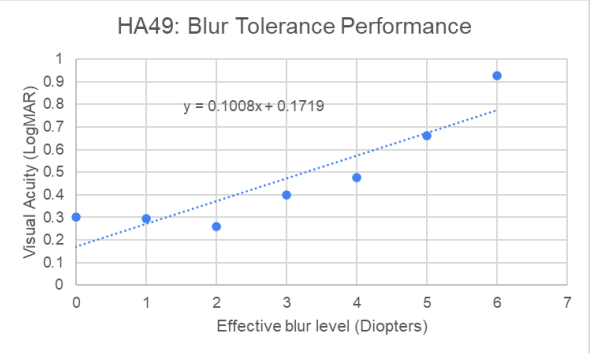

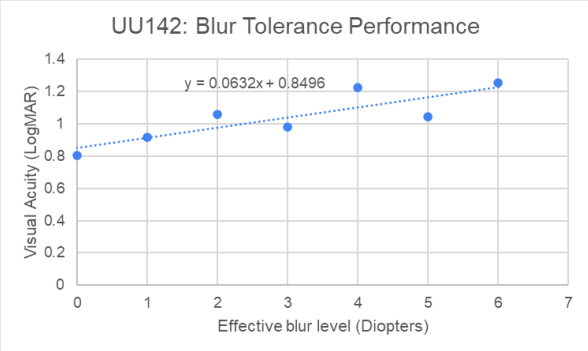

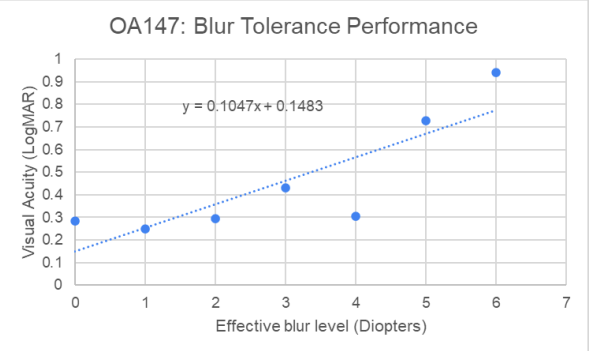

Control Participants

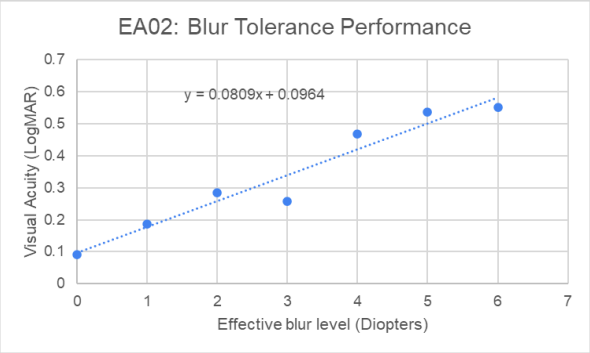
EA02: Blur Tolerance Performance
y = 0.0809x + 0.0964
Visual Acuity (LogMAR)
Effective blur level (Diopters)

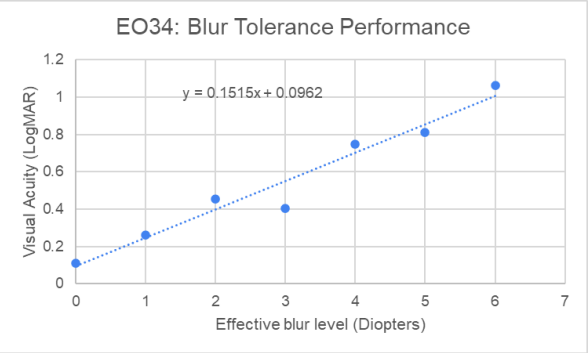
EO34: Blur Tolerance Performance
y = 0.1515x + 0.0962
Visual Acuity (LogMAR)
Effective blur level (Diopters)

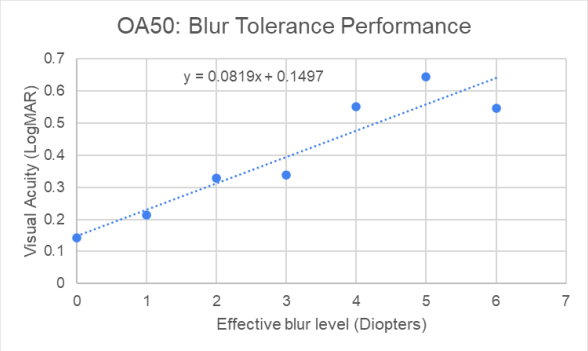
OA50: Blur Tolerance Performance
y = 0.0819x + 0.1497
Visual Acuity (LogMAR)
Effective blur level (Diopters)

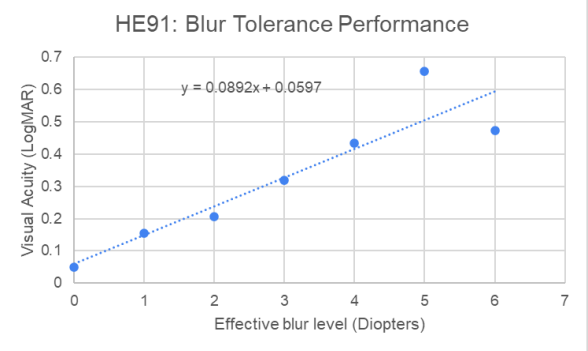
HE91: Blur Tolerance Performance
y = 0.0892x + 0.0597
Visual Acuity (LogMAR)
Effective blur level (Diopters)

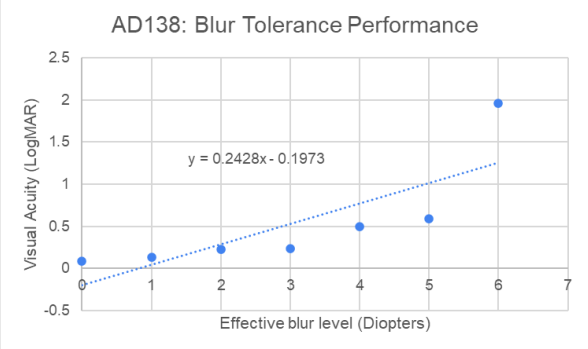
AD138: Blur Tolerance Performance
y = 0.2428x - 0.1973
Visual Acuity (LogMAR)
Effective blur level (Diopters)

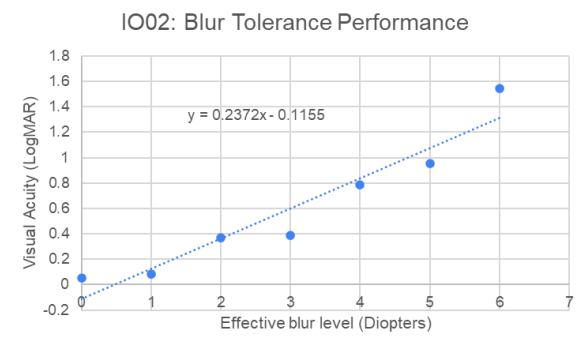
IO02: Blur Tolerance Performance
y = 0.2372x - 0.1155
Visual Acuity (LogMAR)
Effective blur level (Diopters)

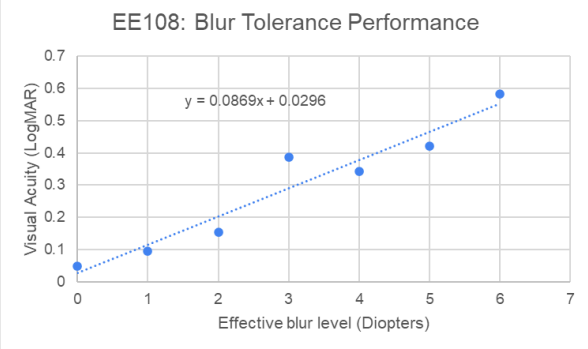
EE108: Blur Tolerance Performance
y = 0.0869x + 0.0296
Visual Acuity (LogMAR)
Effective blur level (Diopters)

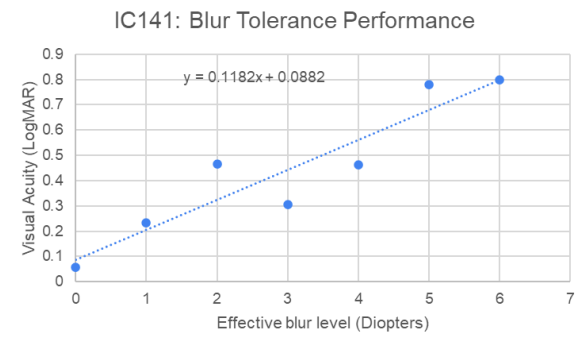
IC141: Blur Tolerance Performance
y = 0.1182x + 0.0882
Visual Acuity (LogMAR)
Effective blur level (Diopters)

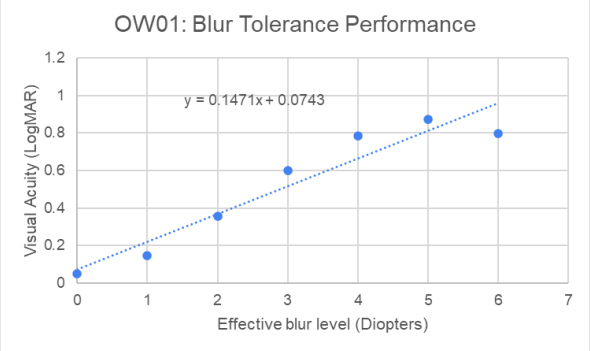
OW01: Blur Tolerance Performance
y = 0.1471x + 0.0743
Visual Acuity (LogMAR)
Effective blur level (Diopters)

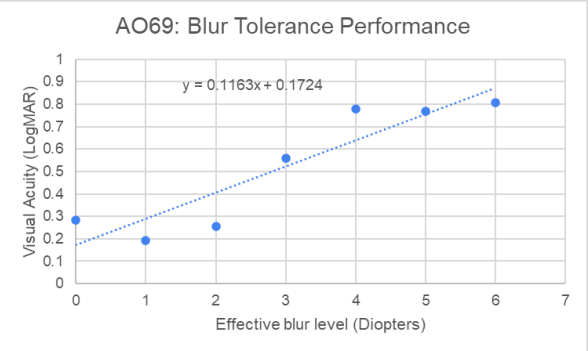
AO69: Blur Tolerance Performance
y = 0.1163x + 0.1724
Visual Acuity (LogMAR)
Effective blur level (Diopters)

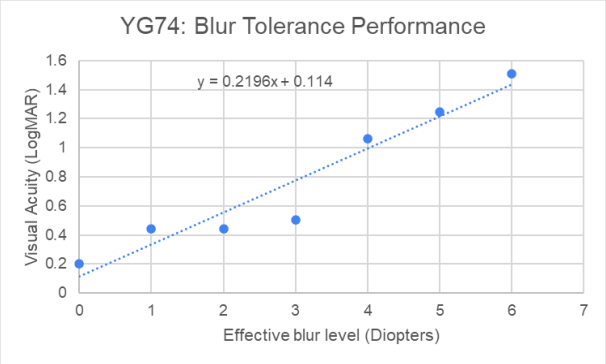
YG74: Blur Tolerance Performance
y = 0.2196x + 0.114
Visual Acuity (LogMAR)
Effective blur level (Diopters)

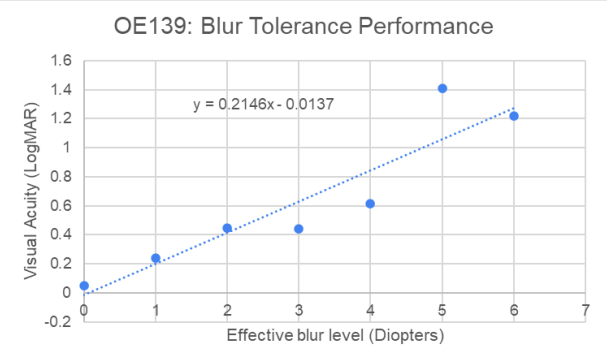
OE139: Blur Tolerance Performance
y = 0.2146x - 0.0137
Visual Acuity (LogMAR)
Effective blur level (Diopters)

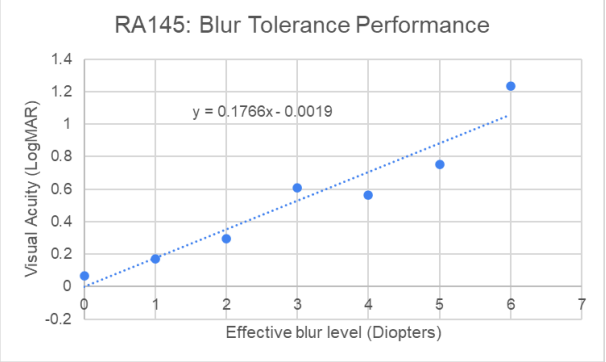
RA145: Blur Tolerance Performance
y = 0.1766x - 0.0019
Visual Acuity (LogMAR)
Effective blur level (Diopters)

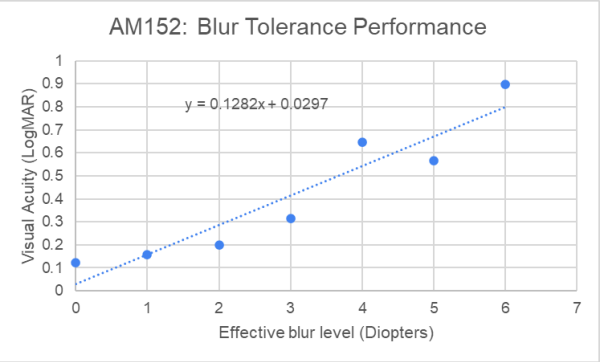
AM152: Blur Tolerance Performance
y = 0.1282x + 0.0297
Visual Acuity (LogMAR)
Effective blur level (Diopters)

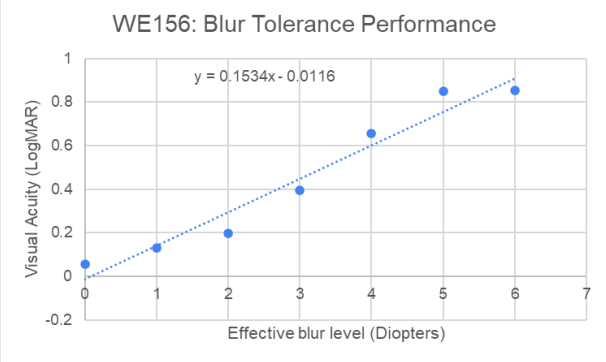
WE156: Blur Tolerance Performance
y = 0.1534x - 0.0116
Visual Acuity (LogMAR)
Effective blur level (Diopters)

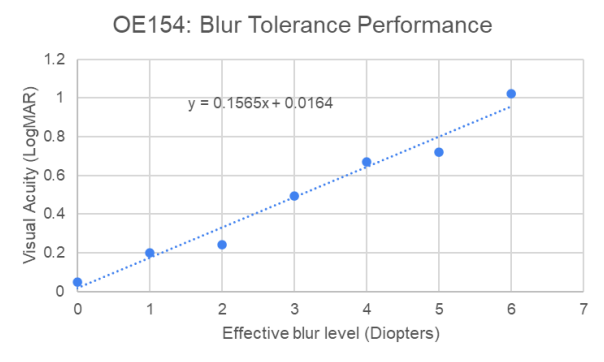
OE154: Blur Tolerance Performance
y = 0.1565x + 0.0164
Visual Acuity (LogMAR)
Effective blur level (Diopters)

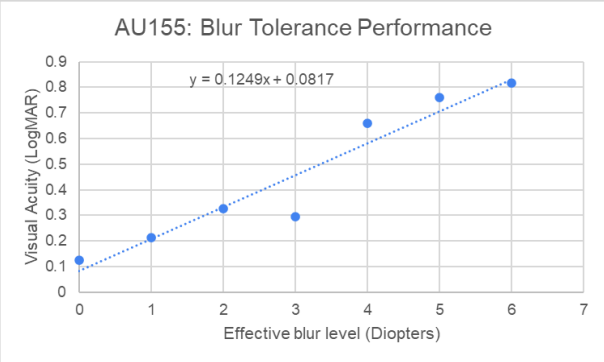

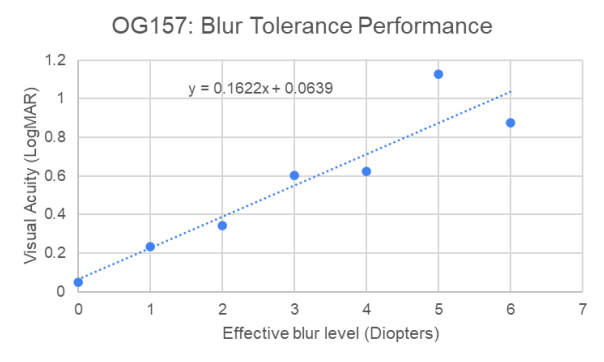

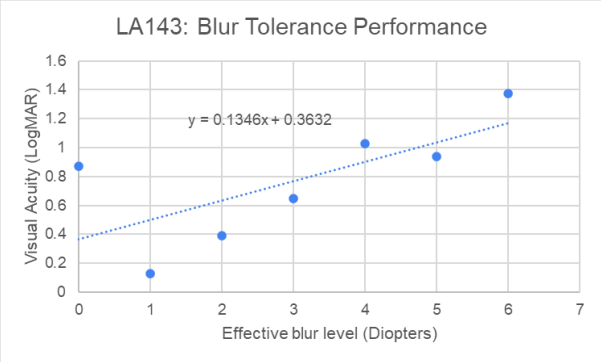

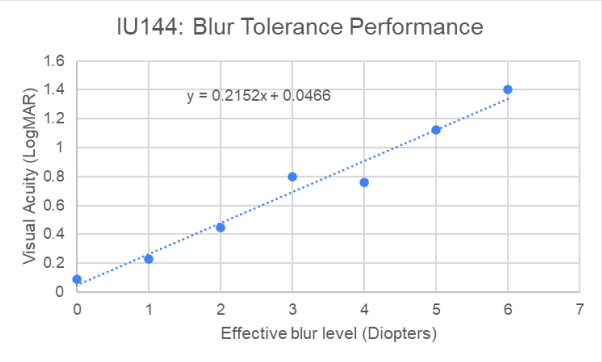

Appendix B: Additional Bland Altman Analysis from AIM Low Vision Repeatability

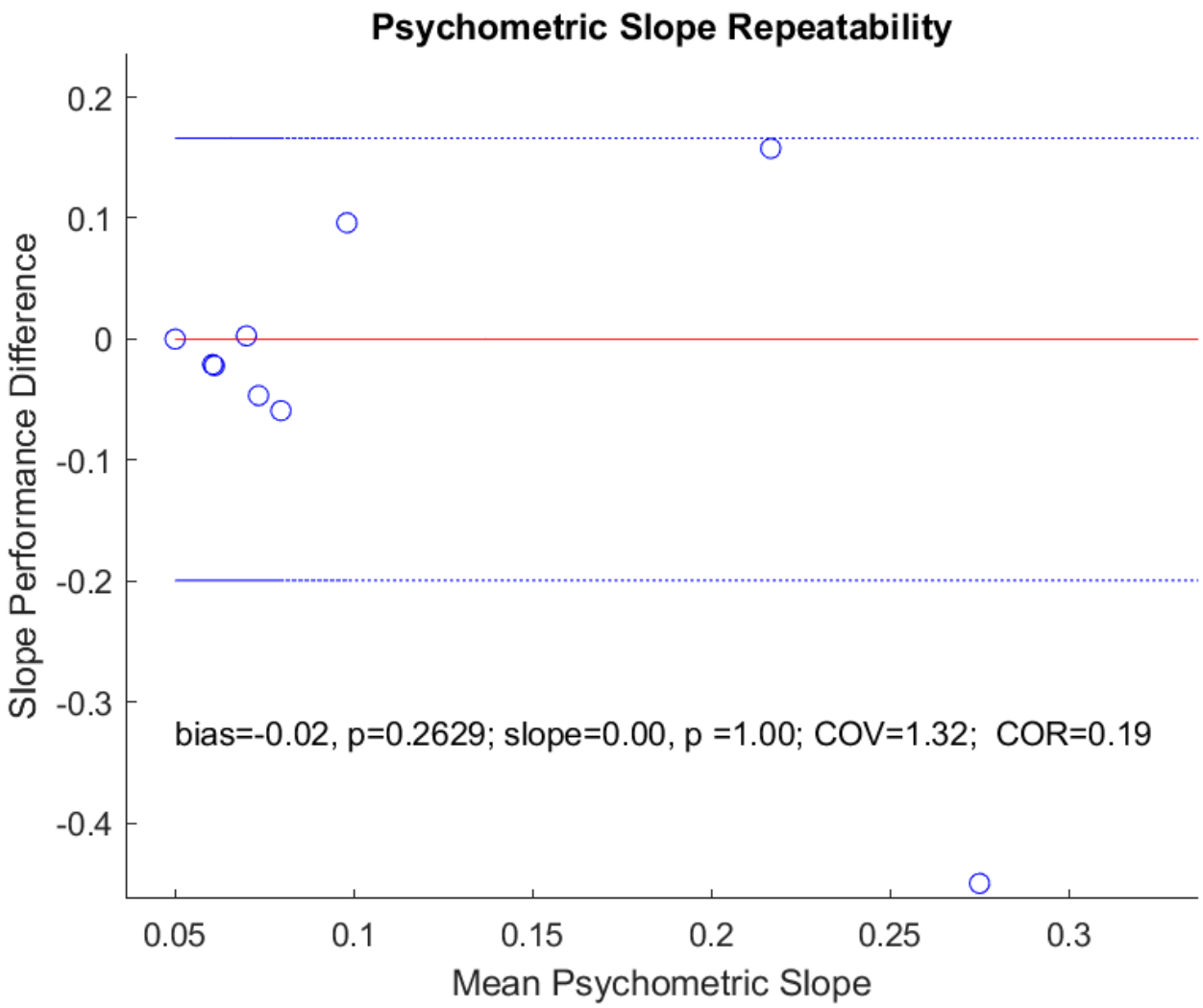

Figure B1. Bland Altman of AIM Low Vision Psychometric Slope in Best Corrected Controls

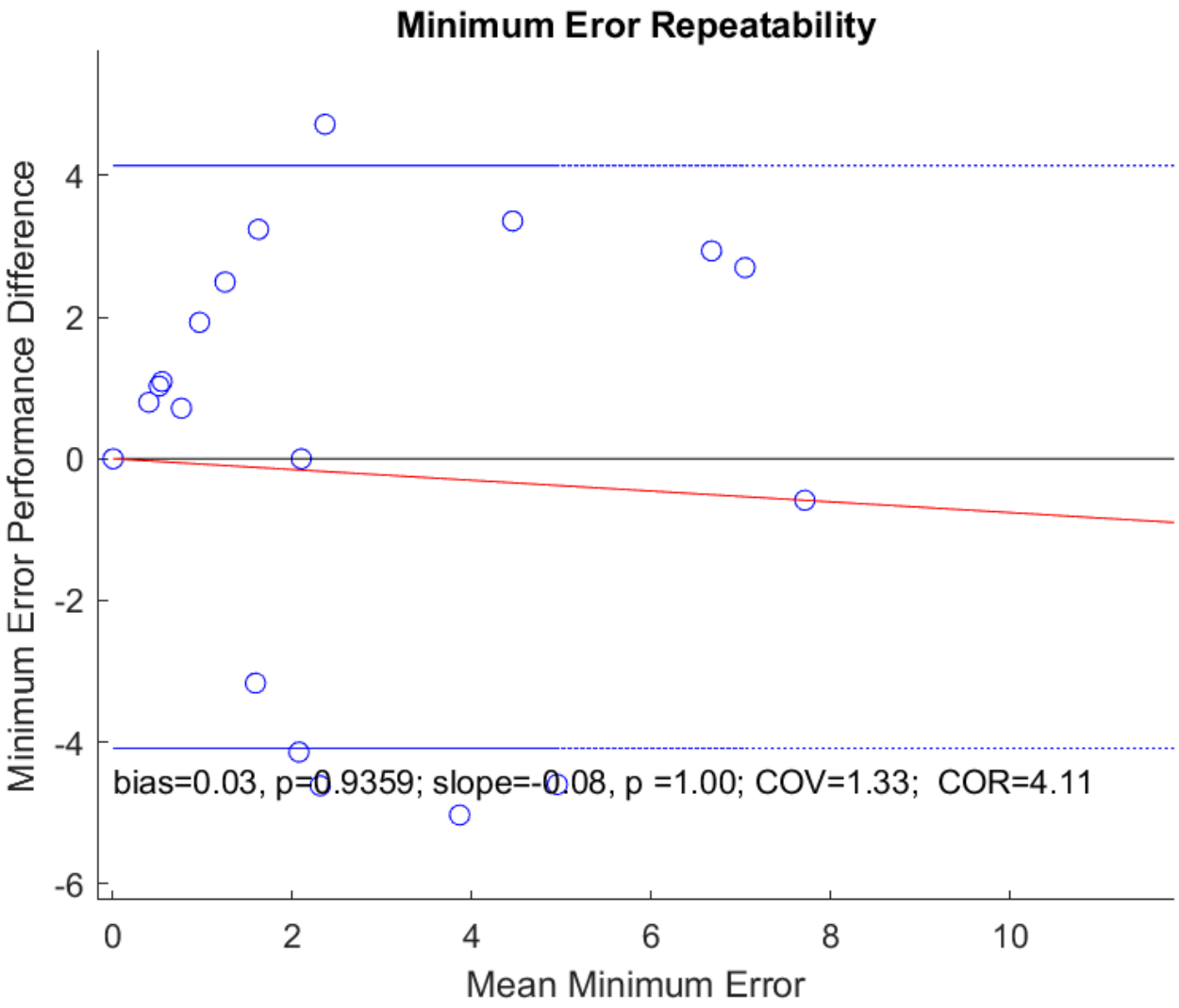

Figure B2. Bland Altman of AIM Low Vision Minimum Error Report in Best Corrected Controls

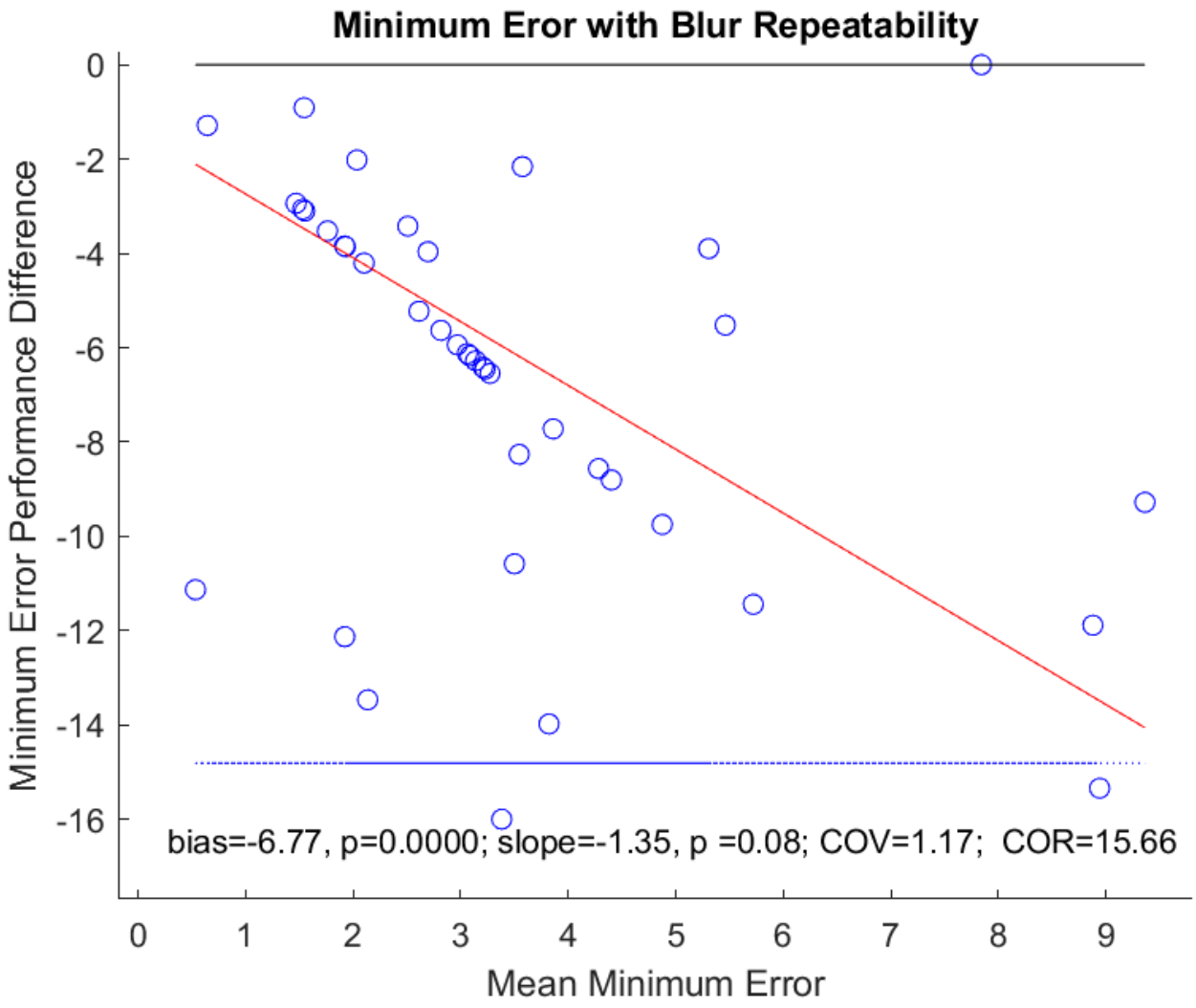
Minimum Eror with Blur Repeatability
Minimum Error Performance Difference
Mean Minimum Error
bias=-6.77, p=0.0000; slope=-1.35, p =0.08; COV=1.17; COR=15.66
0
-2
-4
-6
-8
-10
-12
-14
-16
0
1
2
3
4
5
6
7
8
9